

# Program on Technology Innovation: Study on the Integration of High Temperature Superconducting DC Cables within the Eastern and Western North American Power Grids





# **Program on Technology Innovation: Study on the Integration of High Temperature Superconducting DC Cables within the Eastern and Western North American Power Grids**

**1020330**

Final Report, November 2009

EPRI Project Manager  
S. Eckroad

## **DISCLAIMER OF WARRANTIES AND LIMITATION OF LIABILITIES**

THIS DOCUMENT WAS PREPARED BY THE ORGANIZATION(S) NAMED BELOW AS AN ACCOUNT OF WORK SPONSORED OR COSPONSORED BY THE ELECTRIC POWER RESEARCH INSTITUTE, INC. (EPRI). NEITHER EPRI, ANY MEMBER OF EPRI, ANY COSPONSOR, THE ORGANIZATION(S) BELOW, NOR ANY PERSON ACTING ON BEHALF OF ANY OF THEM:

(A) MAKES ANY WARRANTY OR REPRESENTATION WHATSOEVER, EXPRESS OR IMPLIED, (I) WITH RESPECT TO THE USE OF ANY INFORMATION, APPARATUS, METHOD, PROCESS, OR SIMILAR ITEM DISCLOSED IN THIS DOCUMENT, INCLUDING MERCHANTABILITY AND FITNESS FOR A PARTICULAR PURPOSE, OR (II) THAT SUCH USE DOES NOT INFRINGE ON OR INTERFERE WITH PRIVATELY OWNED RIGHTS, INCLUDING ANY PARTY'S INTELLECTUAL PROPERTY, OR (III) THAT THIS DOCUMENT IS SUITABLE TO ANY PARTICULAR USER'S CIRCUMSTANCE; OR

(B) ASSUMES RESPONSIBILITY FOR ANY DAMAGES OR OTHER LIABILITY WHATSOEVER (INCLUDING ANY CONSEQUENTIAL DAMAGES, EVEN IF EPRI OR ANY EPRI REPRESENTATIVE HAS BEEN ADVISED OF THE POSSIBILITY OF SUCH DAMAGES) RESULTING FROM YOUR SELECTION OR USE OF THIS DOCUMENT OR ANY INFORMATION, APPARATUS, METHOD, PROCESS, OR SIMILAR ITEM DISCLOSED IN THIS DOCUMENT.

ORGANIZATION(S) THAT PREPARED THIS DOCUMENT

**PowerWorld Corporation**

## **NOTE**

For further information about EPRI, call the EPRI Customer Assistance Center at 800.313.3774 or e-mail [askepri@epri.com](mailto:askepri@epri.com).

Electric Power Research Institute, EPRI, and TOGETHER...SHAPING THE FUTURE OF ELECTRICITY are registered service marks of the Electric Power Research Institute, Inc.

Copyright © 2009 Electric Power Research Institute, Inc. All rights reserved.

# CITATIONS

---

This document was prepared by

PowerWorld Corporation  
2001 South First Street  
Champaign, IL 61820

Principal Investigators

T. Overbye  
P. Ribeiro  
T. Baldwin

This document describes research sponsored by the Electric Power Research Institute (EPRI).

This publication is a corporate document that should be cited in the literature in the following manner:

*Program on Technology Innovation: Study on the Integration of High Temperature Superconducting DC Cables within the Eastern and Western North American Power Grids.*  
EPRI, Palo Alto, CA: 2009. 1020330.



# PRODUCT DESCRIPTION

---

The study described in this report examined the power flow and transient stability issues associated with the integration of a superconducting direct current (dc) cable system within the existing eastern and western North American power grids. The study assumed a multi-tap superconducting dc cable system capable of carrying up to 10 GW over a distance of 1000 mi (1609 km). Another objective was to perform preliminary analyses and develop possible topologies for a superconducting dc cable multi-terminal system, while determining the parameters necessary for subsequent dynamic electromechanical stability study.

## Results and Findings

The Eastern Interconnect study considered a 10-GW system supplying power from asynchronous generation located in the southern Great Plains to loads near Oklahoma City, Oklahoma; Kansas City, Missouri; St. Louis, Missouri; and Chicago, Illinois (two taps). No attempt was made to perform the system studies necessary to ensure that the resultant system is n-1 secure. Nonetheless, the conclusion from the power flow portion of this study was that the integration of the superconducting dc cable within the existing system will require modifications to the transmission grid similar to those needed to accommodate a new generator of similar size at each terminal of the cable system. From the perspectives of transient stability and short-term voltage stability, such a system is plausible. Maximum frequency deviations for the loss of 5 GW are approximately 0.2 Hz. Voltage recovery following the fault was adequate.

The Western Electricity Coordinating Council study considered an 8.5-GW system supplying power from asynchronous generation located in the southern Great Plains to loads near Denver, Colorado; Albuquerque, New Mexico; Phoenix, Arizona; San Diego, California; and Los Angeles, California. Again, no attempt was made to perform the system studies necessary to ensure that the resultant system is n-1 secure, and the same power flow conclusion applied as from the Eastern Interconnect study. From the perspectives of transient stability and short-term voltage stability, 8.5 GW is near the upper limit for acceptable system integration. Maximum frequency deviations for the loss of 4.25 GW are in the range of 0.4–0.5 Hz. Voltage recovery following the fault was slower than for the Eastern Interconnect but adequate. Several small loads experienced motor stalls—conditions that would require further investigation.

Two basic topologies with six and seven nodes/stations were configured for stability system studies. The studies, from a stability point of view, show the viability and sustainable power flow and transient performance of a long-distance, high-power superconducting dc transmission line.

## Challenges and Objectives

Superconducting dc cables are an advanced transmission technology in the conceptual development stage. Although such a transmission line can be built with today's technology,

significant engineering optimization and system studies must be completed before the concept will become a commercial reality. The analyses undertaken in this project break new ground in taking a first look at some of the most prominent issues that must be addressed as the technology matures.

### **Applications, Value, and Use**

Superconducting dc cable systems have the potential to dramatically change the transmission landscape in North America. Renewable and other energy resources that will be tapped by future generations are typically remote from load centers. The cable system assessed in this report can satisfy a number of concerns in bringing this power to market, including environmental, aesthetics, and reliability issues. This report is intended for engineers and managers considering the construction of superconducting dc cable systems; for systems built in the future, the report will be an excellent starting point for investigation into the topic and the ways in which superconducting dc cables could impact the larger grid. By covering the impact of superconducting dc cables on large interconnected power systems, the report can guide the development of such systems.

### **EPRI Perspective**

Very few studies have examined a superconducting dc cable system within the context of large North American power grids. The studies that are the subject of this report will provide a unique resource to researchers and engineers interested in studying, and perhaps building, superconducting dc cables. The report should be used in conjunction with the following companion Electric Power Research Institute (EPRI) reports produced in the same project: *A Superconducting DC Cable* (1020458) and *Transient Response of a Superconducting DC, Long Length Cable System Using Voltage Source Converters* (1020339).

### **Approach**

For the load flow and transient system response component of the project, the system modeled contained about a half-dozen converter stations at which the system was connected into the existing alternating current (ac) power grid at a transmission system voltage (230–765 kV). The rated power for the converter stations was between 1.5 GW and 2.5 GW. Each converter station was also assumed to be redundant; in the event of a fault, full power could be transferred from the faulted cable to the unfaulted cable in several seconds. The most severe contingency considered was the failure of one cable with no transfer of power to the unfaulted cable, hence a sustained loss of 50% of the pre-fault power.

For the electromagnetic transient study component, researchers reviewed results of a detailed two-terminal system modeling effort by another EPRI contractor and performed additional simulations in order to substantiate findings, investigate multi-terminal operational and control issues, and develop a functional specification for the voltage source converters proposed for use in the superconducting dc cable system.

### **Keywords**

Green transmission  
Power flow studies  
Superconducting dc cables  
Transient stability studies  
Voltage source converters

# ABSTRACT

---

For power grids, the need for greatly enhanced transmission system capacity is a rapidly emerging challenge. Several transmission technologies exist to meet this need, including overhead alternating current (ac), overhead direct current (dc), superconducting underground ac, and superconducting underground dc. The last of these transmission technologies—superconducting dc cable systems—is still in the conceptual development stage but has the potential to dramatically change the transmission landscape in North America.

The project described in this report considered the power flow and transient stability issues associated with integrating superconducting dc cables within the existing eastern and western North American power grids. Another objective was to perform preliminary analyses and develop possible topologies for a superconducting dc cable multi-terminal system, while determining the parameters necessary for subsequent dynamic electromechanical stability study. Prior to this report, very few studies have examined a superconducting dc cable system within the context of large North American power grids.

In the study, a multi-tap superconducting dc cable system capable of carrying up to 10 GW over a distance of 1000 mi (1609 km) was used. In order to achieve good reliability, the system was assumed to be completely redundant, with two parallel superconducting dc cables, each capable of carrying the entire loading. Two actual North American systems—the Eastern Interconnect and Western Interconnect models—were chosen as study subjects over artificial equivalent systems.

The results presented herein are an initial assessment of concept feasibility, and the particular cable routes were chosen for illustrative purposes only. Nonetheless, the report will be a unique and valuable resource to researchers and engineers considering the construction of superconducting dc cable systems.



## **ACKNOWLEDGMENTS**

---

The authors would like to gratefully acknowledge the support of EPRI and PowerWorld Corporation.



# CONTENTS

---

- 1 INTRODUCTION ..... 1-1**
  
- 2 BASIC CASE DEFINITIONS AND SYSTEM PARAMETERS FOR STABILITY STUDIES ..... 2-1**
  - Proposed Cases for Evaluation of Superconducting DC Cable Performance..... 2-1
  - Cases for the Seven-Node Test System ..... 2-4
  - Cases for the Six-Node Test System ..... 2-6
  
- 3 EASTERN INTERCONNECT STUDIES ..... 3-1**
  - Power Flow Results and System Modifications..... 3-2
  - Transient Stability Setup ..... 3-4
  - Transient Stability Load Model ..... 3-5
  - Transient Stability Results – Frequency Response..... 3-6
  - Transient Stability Results – Voltage Response ..... 3-18
  
- 4 WESTERN ELECTRICITY COORDINATING COUNCIL STUDIES ..... 4-1**
  - Power Flow Results and System Modifications..... 4-2
  - Transient Stability Results – Frequency Response..... 4-3
  - Transient Stability Results – Voltage Response ..... 4-9
  
- 5 CONSIDERATIONS ON THE OPERATION OF SUPERCONDUCTING DC CABLES FED BY MULTIPLE VOLTAGE SOURCE CONVERTERS ..... 5-1**
  - Voltage Source Converter Superconducting DC Cable Topology..... 5-1
  - Multi-Terminal Voltage Source Converter Design Issues..... 5-3
  - Ramp Rate Limits for Long Cables ..... 5-4
  - Impact of Cable Length ..... 5-4

---

<b>6 ELECTROMAGNETIC TRANSIENT STUDIES FOR A SUPERCONDUCTING DC CABLE SYSTEM.....</b>	<b>6-1</b>
Typical HVDC System Results – Single Line-to-Ground Fault with Two Voltage Source Converters .....	6-1
Superconducting DC System Results – DC Fault with Two Voltage Source Converters.....	6-10
Superconducting DC System Results – AC Fault with Two Voltage Source Converters....	6-19
Superconducting DC System Results – DC Fault with Three Voltage Source Converters.....	6-28
Superconducting DC System Results – AC Fault with Three Voltage Source Converters.....	6-36
<b>7 VOLTAGE SOURCE CONVERTER – HIGH VOLTAGE DC CONTROLS.....</b>	<b>7-1</b>
Dynamic Model of the VSC-HVDC Converter Station.....	7-2
Model of VSC-HVDC Control System .....	7-3
Transient Damping Control .....	7-5
Operation Modes.....	7-6
<b>A VOLTAGE SOURCE CONVERTER FUNCTIONAL SPECIFICATIONS.....</b>	<b>A-1</b>
Voltage Source Converter Functional Specifications for Superconducting DC Multi-Terminal Operation.....	A-1
Sample Document.....	A-1
<b>B BIBLIOGRAPHY.....</b>	<b>B-1</b>
<b>C REFERENCES.....</b>	<b>C-1</b>

## LIST OF FIGURES

---

Figure 2-1 Seven-node test system .....	2-2
Figure 2-2 One-line seven-node test system topology .....	2-2
Figure 2-3 Six-node test system .....	2-3
Figure 2-4 One-line six-node test system topology.....	2-3
Figure 2-5 Model of a terminal station .....	2-6
Figure 3-1 Eastern Interconnect Route for a 10 GW, six station system .....	3-2
Figure 3-2 Original Kansas City Area Flows and Voltages .....	3-3
Figure 3-3 Kansas City Area Flows and Voltage with Superconducting DC Cable .....	3-4
Figure 3-4 Large machine torque-speed characteristics.....	3-5
Figure 3-5 Small machine torque-speed characteristics (P=1 slip= 0.0217) .....	3-6
Figure 3-6 Frequency response for all generators with no ramping.....	3-7
Figure 3-7 Frequency response for twelve large generators with no ramping .....	3-7
Figure 3-8 Governor response for a coal generator (at Bus 32461) .....	3-8
Figure 3-9 Frequency response for all generators with no ramping and 200 GVA of governor response disabled .....	3-9
Figure 3-10 Frequency response for all generators with no ramping and 400 GVA of governor response disabled .....	3-9
Figure 3-11 Frequency response for all generators with no ramping and 600 GVA of governor response disabled .....	3-10
Figure 3-12 Spatial frequency response for no ramping case, at time = 0.5 seconds .....	3-11
Figure 3-13 Spatial frequency response for no ramping case, at time = 1.0 second.....	3-11
Figure 3-14 Spatial frequency response for no ramping case, at time = 1.5 seconds .....	3-12
Figure 3-15 Frequency response for all generators with ten second ramping .....	3-13
Figure 3-16 Frequency response for twelve large generators with ten second ramping .....	3-13
Figure 3-17 Governor response at generator 32461 with ten second ramping.....	3-14
Figure 3-18 Frequency response for all generators with five second ramping .....	3-15
Figure 3-19 Frequency response for twelve large generators with five second ramping.....	3-15
Figure 3-20 Frequency response for all generators with three second ramping.....	3-16
Figure 3-21 Frequency response for twelve large generators with three second ramping .....	3-16
Figure 3-22 Frequency response for all generators with one second ramping .....	3-17
Figure 3-23 Frequency response for twelve large generators with one second ramping .....	3-17
Figure 3-24 Voltage response versus load model comparison .....	3-18
Figure 3-25 Pre-fault voltage contour .....	3-19
Figure 3-26 Voltage contour for no ramp case at 0.1 seconds .....	3-19
Figure 3-27 Voltage contour for no ramp case at 0.5 seconds .....	3-20
Figure 3-28 Voltage contour for no ramp case at 1.0 second.....	3-20

Figure 3-29 Voltage response at selected buses for no ramp case for the first two seconds.....	3-21
Figure 3-30 Voltage response at selected buses for three second ramp case for the first two seconds .....	3-22
Figure 4-1 WECC route for a 8.5 GW, six station system.....	4-2
Figure 4-2 WECC voltage contour and transmission flows with superconducting dc cable system.....	4-3
Figure 4-3 Frequency response for all generators with no ramping.....	4-4
Figure 4-4 Frequency response for ten large generators with no ramping .....	4-4
Figure 4-5 Frequency response for all generators with ten second ramping.....	4-5
Figure 4-6 Frequency response for ten large generators with ten second ramping.....	4-6
Figure 4-7 Frequency response for all generators with five second ramping .....	4-6
Figure 4-8 Frequency response for ten large generators with five second ramping.....	4-7
Figure 4-9 Frequency response for all generators with three second ramping.....	4-7
Figure 4-10 Frequency response for ten large generators with three second ramping .....	4-8
Figure 4-11 Frequency response for all generators with one second ramping.....	4-8
Figure 4-12 Frequency response for ten large generators with one second ramping.....	4-9
Figure 4-13 WECC case pre-fault substation PU voltage contour.....	4-10
Figure 4-14 WECC no ramp case at 0.1 seconds .....	4-10
Figure 4-15 WECC no ramp case at 0.5 seconds .....	4-11
Figure 4-16 WECC no ramp case at 1.0 seconds .....	4-11
Figure 4-17 WECC no ramp case at 2.0 seconds .....	4-12
Figure 4-18 Voltage response at selected buses for no ramp case for the first five seconds.....	4-13
Figure 4-19 Voltage response at selected buses for no ramp case for the first fifteen seconds.....	4-14
Figure 5-1 Switching arrangement to transfer Converter A from a failed to a healthy cable; similar switches are required on Converter B.....	5-2
Figure 5-2 Converters are connected at the same substation point and transients caused by switching of cables need to be investigated in detail.....	5-2
Figure 5-3 Superconducting DC general topology.....	5-3
Figure 5-4 1000-mile cable voltage ripple.....	5-5
Figure 5-5 2000-mile cable voltage ripple.....	5-5
Figure 5-6 4000-mile cable voltage ripple.....	5-6
Figure 6-1 PSCAD <sup>®</sup> voltage source converter topology.....	6-1
Figure 6-2 1000km HVDC real power .....	6-2
Figure 6-3 1000km HVDC reactive power .....	6-2
Figure 6-4 1000km HVDC AC voltage .....	6-3
Figure 6-5 1000km HVDC DC voltage.....	6-3
Figure 6-6 1000km HVDC DC current .....	6-4
Figure 6-7 2000km HVDC real power.....	6-5
Figure 6-8 2000km HVDC reactive power .....	6-5
Figure 6-9 2000km HVDC AC voltage .....	6-6
Figure 6-10 2000km HVDC DC voltage.....	6-6
Figure 6-11 2000km HVDC DC current .....	6-7

---

Figure 6-12 4000km HVDC real power .....	6-8
Figure 6-13 4000km HVDC reactive power .....	6-8
Figure 6-14 4000km HVDC AC voltage .....	6-9
Figure 6-15 4000km HVDC DC voltage .....	6-9
Figure 6-16 4000km HVDC DC current .....	6-10
Figure 6-17 1000km cable DC fault two voltage source converters, real power.....	6-11
Figure 6-18 1000km cable DC fault two voltage source converters, reactive power .....	6-11
Figure 6-19 1000km cable DC fault two voltage source converters, AC voltage .....	6-12
Figure 6-20 1000km cable DC fault two voltage source converters, DC voltage.....	6-12
Figure 6-21 1000km cable DC fault two voltage source converters, DC current .....	6-13
Figure 6-22 2000km cable DC fault two voltage source converters, real power.....	6-13
Figure 6-23 2000km cable DC fault two voltage source converters, reactive power .....	6-14
Figure 6-24 2000km cable DC fault two voltage source converters, AC voltage .....	6-14
Figure 6-25 2000km cable DC fault two voltage source converters, DC voltage.....	6-15
Figure 6-26 2000km cable DC fault two voltage source converters, DC current .....	6-15
Figure 6-27 4000km cable DC fault two voltage source converters, real power.....	6-16
Figure 6-28 4000km cable DC fault two voltage source converters, reactive power .....	6-17
Figure 6-29 4000km cable DC fault two voltage source converters, AC voltage .....	6-17
Figure 6-30 4000km cable DC fault two voltage source converters, DC voltage.....	6-18
Figure 6-31 4000km cable DC fault two voltage source converters, DC current .....	6-18
Figure 6-32 1000km cable AC fault two voltage source converters, real power.....	6-19
Figure 6-33 1000km cable AC fault two voltage source converters, reactive power .....	6-20
Figure 6-34 1000km cable AC fault two voltage source converters, AC voltage .....	6-20
Figure 6-35 1000km cable AC fault two voltage source converters, DC voltage.....	6-21
Figure 6-36 1000km cable AC fault two voltage source converters, DC current .....	6-21
Figure 6-37 2000km cable AC fault two voltage source converters, real power .....	6-22
Figure 6-38 2000km cable AC fault two voltage source converters, reactive power .....	6-23
Figure 6-39 2000km cable AC fault two voltage source converters, AC voltage .....	6-23
Figure 6-40 2000km cable AC fault two voltage source converters, DC voltage.....	6-24
Figure 6-41 2000km cable AC fault two voltage source converters, DC current .....	6-24
Figure 6-42 4000km cable AC fault two voltage source converters, real power.....	6-25
Figure 6-43 4000km cable AC fault two voltage source converters, reactive power .....	6-26
Figure 6-44 4000km cable AC fault two voltage source converters, AC voltage .....	6-26
Figure 6-45 4000km cable AC fault two voltage source converters, DC voltage.....	6-27
Figure 6-46 4000km cable AC fault two voltage source converters, DC current .....	6-27
Figure 6-47 1000km cable DC fault three voltage source converters, real power .....	6-28
Figure 6-48 1000km cable DC fault three voltage source converters, reactive power.....	6-29
Figure 6-49 1000km cable DC fault three voltage source converters, AC voltage .....	6-29
Figure 6-50 1000km cable DC fault three voltage source converters, DC voltage .....	6-30
Figure 6-51 1000km cable DC fault three voltage source converters, DC current .....	6-30
Figure 6-52 2000km cable DC fault three voltage source converters, real power .....	6-31
Figure 6-53 2000km cable DC fault three voltage source converters, reactive power.....	6-31
Figure 6-54 2000km cable DC fault three voltage source converters, AC voltage .....	6-32
Figure 6-55 2000km cable DC fault three voltage source converters, DC voltage .....	6-32

---

Figure 6-56 2000km cable DC fault three voltage source converters, DC current .....	6-33
Figure 6-57 4000km cable DC fault three voltage source converters, real power .....	6-33
Figure 6-58 4000km cable DC fault three voltage source converters, reactive power.....	6-34
Figure 6-59 4000km cable DC fault three voltage source converters, AC voltage .....	6-34
Figure 6-60 4000km cable DC fault three voltage source converters, DC voltage .....	6-35
Figure 6-61 4000km cable DC fault three voltage source converters, DC current .....	6-35
Figure 6-62 1000km cable AC fault three voltage source converters, real power .....	6-36
Figure 6-63 1000km cable AC fault three voltage source converters, reactive power.....	6-37
Figure 6-64 1000km cable AC fault three voltage source converters, AC voltage .....	6-37
Figure 6-65 1000km cable AC fault three voltage source converters, DC voltage .....	6-38
Figure 6-66 1000km cable AC fault three voltage source converters, DC current.....	6-38
Figure 6-67 2000km cable AC fault three voltage source converters, real power .....	6-39
Figure 6-68 2000km cable AC fault three voltage source converters, reactive power.....	6-39
Figure 6-69 2000km cable AC fault three voltage source converters, AC voltage .....	6-40
Figure 6-70 2000km cable AC fault three voltage source converters, DC voltage .....	6-40
Figure 6-71 2000km cable AC fault three voltage source converters, DC current.....	6-41
Figure 6-72 4000km cable AC fault three voltage source converters, real power .....	6-41
Figure 6-73 4000km cable AC fault three voltage source converters, reactive power.....	6-42
Figure 6-74 4000km cable AC fault three voltage source converters, AC voltage .....	6-42
Figure 6-75 4000km cable AC fault three voltage source converters, DC voltage .....	6-43
Figure 6-76 4000km cable AC fault three voltage source converters, DC current.....	6-43
Figure 7-1 One-line diagram of a VSC-HVDC converter station.....	7-1
Figure 7-2 Dynamic equivalent circuit of a VSC-HVDC converter station.....	7-2
Figure 7-3 Hierarchical control diagram for the VSC-HVDC converter .....	7-3
Figure 7-4 Transfer-function block diagram of the simplified VSC-HVDC controls.....	7-5

# LIST OF TABLES

---

Table 2-1 Basic cases.....	2-4
Table 2-2 Superconducting DC line data .....	2-4
Table 2-3 Superconducting DC power delivery distribution .....	2-5
Table 2-4 Local load composition/generation characteristics .....	2-5
Table 2-5 Terminal station model parameters .....	2-6
Table 2-6 Basic cases.....	2-7
Table 2-7 Superconducting DC line data .....	2-7
Table 2-8 Superconducting DC power delivery distribution .....	2-8
Table 2-9 Local load composition/generation characteristics .....	2-8
Table 5-1 Sags for the 2000-mile superconducting DC cable .....	5-4
Table 7-1 Active power/DC bus voltage control parameters.....	7-5
Table 7-2 Active power damping control parameters .....	7-6
Table 7-3 Reactive power/AC bus voltage control parameters.....	7-6
Table 7-4 Control modes for the converters stations in the seven-node test system .....	7-7
Table 7-5 Control modes for the converters stations in the six-node test system.....	7-7



# 1

## INTRODUCTION

---

One of the power grid challenges that is rapidly emerging is the need for greatly enhanced transmission system capacity. Several different transmission technologies exist to meet this need, including overhead ac, overhead dc, superconducting underground ac, and superconducting underground dc. The purpose of this project was to consider the power flow and transient stability issues associated with integrating superconducting dc cables, within the existing Eastern and Western North American power grids.

For this project a multi-tap superconducting dc cable system was assumed capable of carrying up to 10 GW over a distant of about 1000 miles. In order to achieve good reliability, the system was assumed to be completely redundant, including two parallel superconducting dc cables, with each capable of carrying the entire loading but nominally operated at half load. The system contained about a half dozen voltage-source converter stations at which the system was connected into the existing ac power grid at a transmission system voltage (230 kV to 765 kV). The rated power for the converters stations was between 1.5 and 2.5 GW.<sup>1</sup> Each converter station was also assumed to be redundant, so that in the event of a fault full power could be transferred from the faulted line to the unfaulted line within several seconds. The system configuration studied was one in which there was a single converter station acting as a generation source, and then five or six converter stations in which the power was injected into the existing ac system. This might model a situation in which an asynchronous ac system feeds a large amount of wind power into the source converter station, and then the superconducting dc cable system is used to transmit the power to the urban load centers at distances of 1000 miles or more.

Of course, to construct this system would require significant engineering studies and likely entail modification of the underlying ac system since each converter station would appear electrically to the system as a major new generation source. (This, by the way, is one of the significant advantages of the long-distance superconducting dc cable: generation located close to load centers without the concomitant issues of fuel delivery, emissions, siting, etc.). The purpose of this study was not to provide this planning. Rather, this study's purpose was to provide an initial assessment of whether the integration of such a system was even possible. Therefore the study focused on the response of the ac system to what was assumed to be the most severe contingency – the failure of one of the two superconducting dc cables when each cable was carrying 50% of rated power, with full power then ramped to the unfaulted cable within time periods ranging

---

<sup>1</sup> In actual practice, a number of smaller Voltage Source Converters, e.g., 250 MW each, may be paralleled at a single converter “station”. Even more attractive may be the distribution of these smaller Voltage Source Converters around the perimeter, for example, of a large urban metroplex. However, for simplicity in modeling in this study, single large Voltage Source Converters were employed at each tap along the 1000-mile route.

from one second to never. From the ac system perspective this was modeled as a simultaneous, balanced three phase fault at each of the converter stations, followed by the fault being cleared after three cycles (0.05 seconds).

Immediately after the fault was cleared, the net power injection at each converter station dropped to 50%, with its value then being linearly ramped back to 100% over several different time period scenarios.

In determining the power systems to use in the study, the decision was made to use the actual North American Eastern Interconnect and Western Interconnect models rather than some artificial equivalent systems. The clear advantage of this approach is it directly addresses the issue of system realism since the real systems were used (with the modeling details provided in the description of each system). Of course, this approach also, of necessity, requires integrating the superconducting dc cable system into the grid at particular bus locations. This could inadvertently lead some to conclude that the selected cable routes are the only, or even the best configurations. The authors would like to emphasize that the results presented here are just an initial assessment to determine concept feasibility. The particular cable routes were chosen for illustrative purposes only. Note, the system studies presented in Sections 3 and 4 were done using PowerWorld Simulator version 14, with the transient stability add-on.

Several technical, reliability, and economic challenges characterize such projects at present. Among them are:

1. Complexity of controls systems for multi-terminal operation
2. Need for high power capacity dc circuit breakers
3. Mitigation of transients associated with faults and system events
4. Improved efficiency of forced commutation converters to avoid offsetting the gains of the superconducting dc system
5. Improved power electronics reliability and system performance during major system events
6. Lower costs of power electronics and superconducting dc systems
7. Deregulated utility structure and emphasis on distributed (renewable) generation and micro-grids for increased system reliability and survivability

The control systems for a multi-terminal voltage source converter based superconducting dc cable system needs to be fully assessed for all possible system conditions and events including ac and dc faults. Although voltage source converters will no doubt have superior performance when compared with current source line-commutated converters, more detailed modeling and simulations with multiple converters at the actual current and power levels proposed for the superconducting dc system need to be carried out. Similarly, dc circuit breakers can be constructed, but for the current levels proposed by the superconducting dc cable project advanced technologies will be required. Superior voltage source converter controls plus active and passive filtering will mitigate the challenging transients associated with superconducting dc cables.

Advances in power electronics will soon allow voltage source converters with ratings within the gigawatt (GW) range by the use of modular-multi-level technologies. However, performance and reliability during major system events as well as associated costs will be a challenge.

Performance and reliability at the high power level required for the superconducting dc application must first be demonstrated over shorter distances before going to transcontinental scales. Furthermore, long distance transmission technologies such as this must be rationalized with the new deregulated utility structure and its emphasis on distributed generation and micro-grids.



# 2

## **BASIC CASE DEFINITIONS AND SYSTEM PARAMETERS FOR STABILITY STUDIES**

---

Based on realistic topologies of the Western Electricity Coordinating Council (WECC) and Midwest areas, two basic test systems were originally proposed to investigate the impact of the superconducting dc cable on the associated and interconnected ac network. These cases are detailed in the following subsections to provide an introduction to the results obtained and presented in sections three and four. Two basic generation conditions (5GW and 10GW) were considered. However, conclusions drawn from the use of these test systems imply modeled rather than actual behaviors on the WECC or Midwest areas.

### **Proposed Cases for Evaluation of Superconducting DC Cable Performance**

Figure 2-1 and Figure 2-2 show the generic test system and corresponding one-line diagram for the WECC case seven-node multi-tap dc test system with seven ac sub-systems. Figure 2-3 and Figure 2-4 show the Midwest alternative with six-node multi-tap dc test system and six ac sub-systems. It should be noted that only the Midwest alternative case was actually used in this study. An alternative six-node test system, outlined in section four, was instead used for the WECC area.

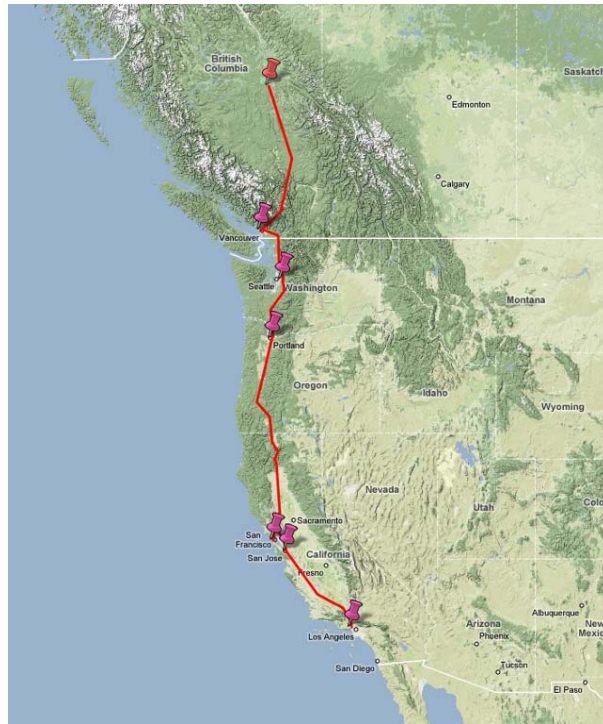


**Figure 2-1**  
**Seven-node test system**

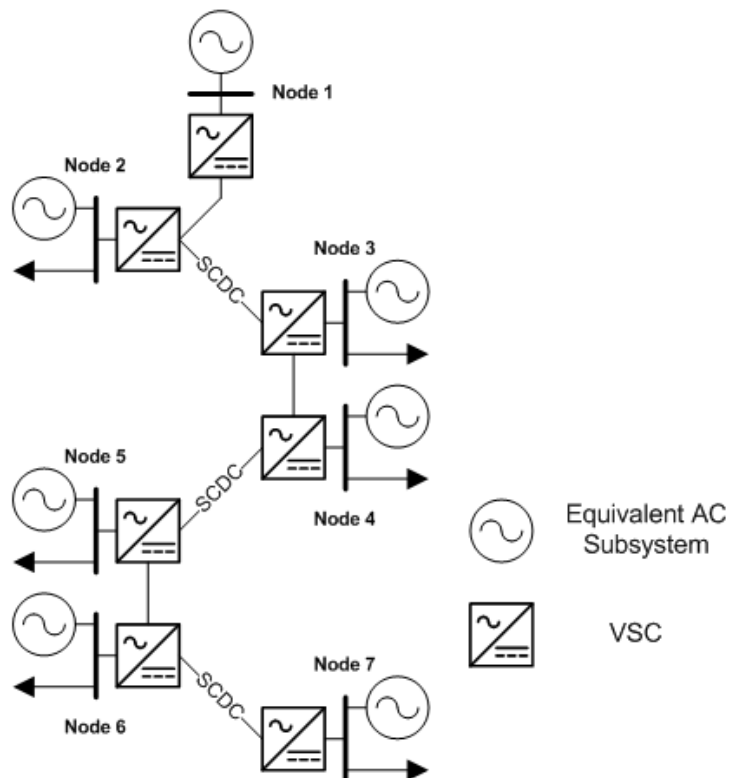


**Figure 2-2**  
**One-line seven-node test system topology**

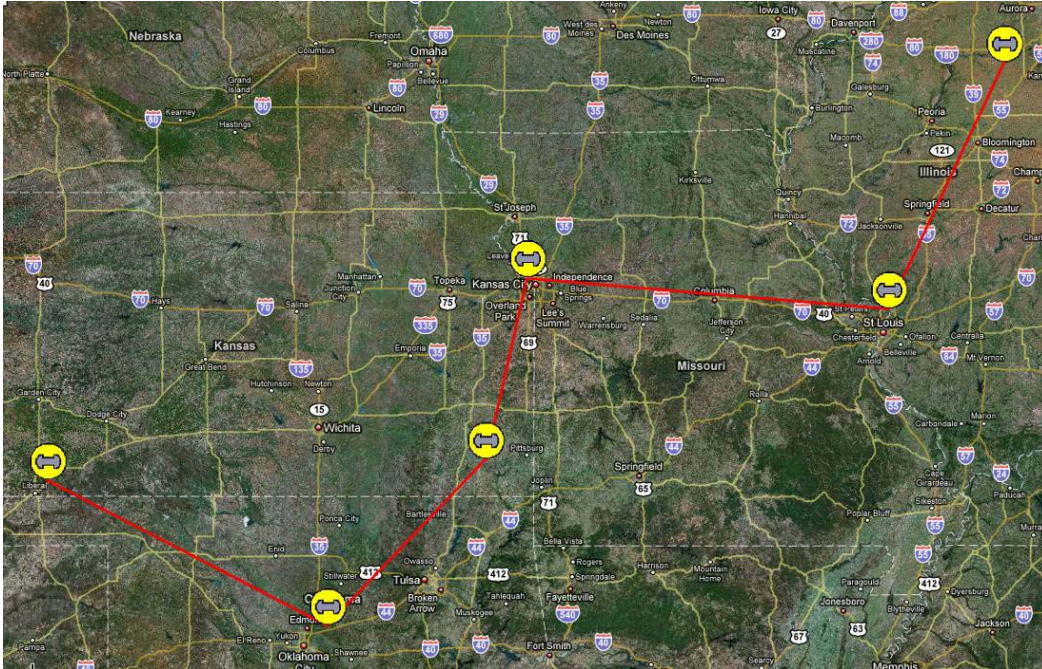


**Figure 2-3**  
Six-node test system

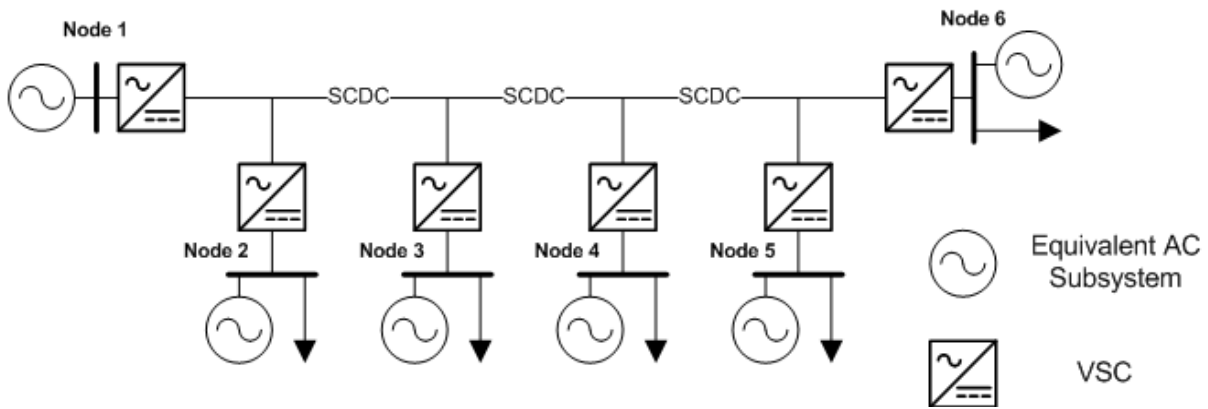


**Figure 2-4**  
One-line six-node test system topology

For both the seven-node and six-node test systems shown, there are several ac sub-systems that can be strongly or weakly interconnected on the ac side. All ac sub-systems are assumed to have local generation and voltage control capability. In order to reduce the complexity and size of the simulation each of the ac sub-systems should be represented by a reduced number of nodes (15 to 20 transmission buses) with an adequate representation of generation dynamics and load characteristics. The initial basic cases shown tabularized in the next subsection involve three phase faults on the ac system and loss of all or half of the inverters at each dc/ac station. In addition, the proportion of generation import and export by each system is indicated with the majority of the dc transmission capacity being delivered to the final delivery point.

## Cases for the Seven-Node Test System

Table 2-1 shows the basic cases proposed. The cases are divided according to transmission capacity (5GW or 10GW), three phase faults on the ac subsystems, and converter substation contingencies.

Table 2-2 shows the line data for the topology selected, Table 2-3 shows the power delivery distribution among the 6 converter stations / ac systems, Table 2-4 lists the local load composition and generation characteristics, and Table 2-5 lists the terminal station model parameters.

**Table 2-1**  
**Basic cases**

Case #	Description	Observations
1	System 1 sending power Systems 2 to 7 receiving or injecting power under normal conditions and with Three Phase Faults	5GW Condition
2	System 1 sending power Systems 2 to 6 receiving or injecting power under normal conditions with Three Phase Faults	10 GW Condition
3	System 1 sending power Systems 2 to 6 receiving or injecting power under normal conditions Case 1 with Loss of Inverter Station	5GW Condition
4	System 1 sending power Systems 2 to 7 receiving or injecting power under normal conditions with Loss of all or fraction of Inverter	10 GW Condition

**Table 2-2**  
**Superconducting DC line data**

Line Identifier	Distance	Inductance	Capacitance	Resistance
1-2	350 miles	70 $\mu$ H	0.136 mF	(0.714 $\times$ f) $\Omega$
2-3	150 miles	30 $\mu$ H	0.058 mF	(0.306 $\times$ f) $\Omega$
3-4	150 miles	30 $\mu$ H	0.058 mF	(0.306 $\times$ f) $\Omega$
4-5	550 miles	110 $\mu$ H	0.213 mF	(1.123 $\times$ f) $\Omega$
5-6	100 miles	20 $\mu$ H	0.039 mF	(0.204 $\times$ f) $\Omega$
6-7	350 miles	70 $\mu$ H	0.136 mF	(0.714 $\times$ f) $\Omega$

**Table 2-3**  
**Superconducting DC power delivery distribution**

Location	Percentage of Total Transmission Capacity Absorption	Generation 5 or 10 GW
System 1 (Local Generation)		80%
System 2 (Local Generation)		20%
System 3 (Local Generation)	10%	
System 4 (Local Generation)	10%	
System 5 (Local Generation)	15%	
System 6 (Local Generation)	15%	
System 7 (Local Generation)	50%	

**Table 2-4**  
**Local load composition/generation characteristics**

Location	Load Composition			Basic Generation Characteristics				
	Induction Motor	Electronic Load	Resistive Load	Inertia	X'd	X''d	Gov Time Constant	Turbine Time Constant
System 1 (Generation)				5-20	0.15-0.25	0.07-0.12	0.2-0.3	0.5-0.6
System 2 (Local Generation)	40%	25%	35%	5-20	0.15-0.25	0.07-0.12	0.2-0.3	0.5-0.6
System 3 (Local Generation)	40%	25%	35%	5-20	0.15-0.25	0.07-0.12	0.2-0.3	0.5-0.6
System 4 (Local Generation)	40%	25%	35%	5-20	0.15-0.25	0.07-0.12	0.2-0.3	0.5-0.6
System 5 (Local Generation)	50%	25%	20%	5-20	0.15-0.25	0.07-0.12	0.2-0.3	0.5-0.6
System 6 (Local Generation)	60%	20%	20%	5-20	0.15-0.25	0.07-0.12	0.2-0.3	0.5-0.6
System 7 (Local Generation)	60%	20%	20%	5-20	0.15-0.25	0.07-0.12	0.2-0.3	0.5-0.6

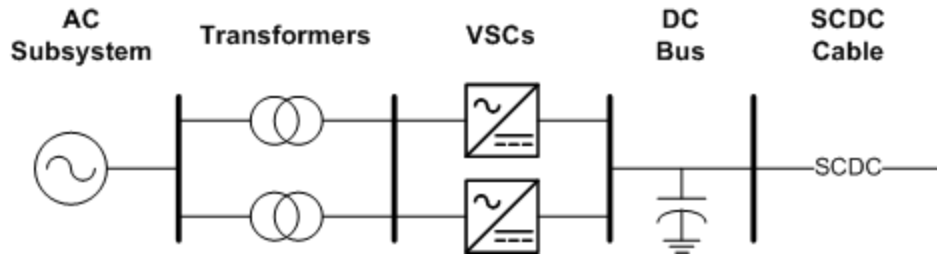


**Figure 2-5**  
Model of a terminal station

**Table 2-5**  
Terminal station model parameters

Parameter	Value
DC Bus Terminal Capacitance (Converter Filter)	2 mF
Inverter Number of Inverters	2
MVA Rating (based on station rating)	100%
Nominal Operating MVA	50%
Transformer MVA Rating (based on station rating)	150%
Resistance	1%
Reactance	7.5% to 10%

## Cases for the Six-Node Test System

Table 2-6 shows the basic cases selected for the six-node system. The cases are divided according to transmission capacity (5GW or 10GW), three phase faults on the ac systems, and converter substation contingencies.

Table 2-7 shows the superconducting dc line data for the topology selected. In computing the values for the table, **the cable model of Hassenzahl has been employed**. The equivalent ac resistance of the superconducting cable is based on the ac power losses in the superconductors and is a function of the frequency. The power loss formula is given as:

$$P(W/m) = \frac{\mu_0}{2\pi} \sum_{\forall n} \omega_n I_n^2 \tag{Equation 1}$$

Table 2-8 shows the superconducting dc power delivery distribution among the 5 converter stations/ac systems, Table 2-9 lists the local load composition and generation characteristics.

**Table 2-6  
Basic cases**

Case #	Description	Observations
1A - E	Systems 1 and 3 sending power Systems 2 & 4 to 6 receiving or injecting power under normal conditions with Three Phase Faults	5GW Condition
2A - E	Systems 1 and 3 sending power Systems 2 & 4 to 6 receiving or injecting power under normal conditions with Three Phase Faults	10GW Condition
3A - E	Systems 1 and 3 sending power Systems 2 & 4 to 6 receiving or injecting power under normal conditions with Loss of Inverter Station	5GW Condition
4A - E	Systems 1 and 3 sending power Systems 2 & 4 to 6 receiving or injecting power under normal conditions with Loss of all or fraction of Inverter Station	10GW Condition

**Table 2-7  
Superconducting DC line data**

Line Identifier	Distance	Inductance	Capacitance	Resistance
1-2	220 miles	44 μH	0.085 mF	(0.449 × f) Ω
2-3	160 miles	32 μH	0.062 mF	(0.327 × f) Ω
3-4	130 miles	26 μH	0.050 mF	(0.265 × f) Ω
4-5	250 miles	50 μH	0.097 mF	(0.510 × f) Ω
5-6	180 miles	36 μH	0.070 mF	(0.367 × f) Ω

**Table 2-8**  
**Superconducting DC power delivery distribution**

Location	Percentage of Total Transmission Capacity Absorption	Generation 5 or 10 GW
System 1 (Local Generation)		60%
System 2 (Local Generation)	20%	
System 3 (Local Generation)		40%
System 4 (Local Generation)	20%	
System 5 (Local Generation)	20%	
System 6 (Local Generation)	40%	

**Table 2-9**  
**Local load composition/generation characteristics**

Location	Load Composition			Basic Generation Characteristics				
	Induction Motor	Electronic	Resistive Load	Inertia	X'd	X''d	Gov Time Constant	Turbine Time Constant
System 1 (Generation)				5-20	0.15-0.25	0.07-0.12	0.2-0.3	0.5-0.6
System 2 (Local Generation)	40%	25%	35%	5-20	0.15-0.25	0.07-0.12	0.2-0.3	0.5-0.6
System 3 (Local Generation)				5-20	0.15-0.25	0.07-0.12	0.2-0.3	0.5-0.6
System 4 (Local Generation)	50%	25%	25%	5-20	0.15-0.25	0.07-0.12	0.2-0.3	0.5-0.6
System 5 (Local Generation)	60%	20%	20%	5-20	0.15-0.25	0.07-0.12	0.2-0.3	0.5-0.6
System 6 (Local Generation)	60%	20%	20%	5-20	0.15-0.25	0.07-0.12	0.2-0.3	0.5-0.6

# 3

## EASTERN INTERCONNECT STUDIES

---

The North American Electric Reliability Corporation (NERC) / Multi-regional Modeling Working Group (MMWG) 2006 series estimated summer 2008 peak loading condition case was used for the Eastern Interconnect study. This case contains more than 48,000 buses and 7400 generators, with a total system load of about 660GW. Of the 7400 generators, around 2100 are modeled as being out-of-service, so the case actually had about 5300 in-service generators (the out-of-service generators were primarily very small units). As is common with the MMWG cases there were many initial line violations, with 330 transmission lines or transformers (lines) loaded at more than 100% of their “limit A” MVA ratings, of which 95 were loaded at above 120% of their limits. However, it should be noted that most of these violations are either on relatively low voltage lines or on generator step-up transformers. To perform the transient stability studies the power flow case data was augmented with the dynamic models from the 2006\_nerc08S\_30.3.1-ds dataset. It should be noted that the dynamic models for several small generators needed to be disabled due to what appeared to be spurious dynamic parameters – an approach the authors believe is common modeling practice.

The superconducting dc cable system scenario assumed 10 GW of asynchronous generation located somewhere in the southwest Great Plains. The design goal was then to supply this power to the load using five taps of about 2GW each with one in the Oklahoma City area, one in the Kansas City area, one near St. Louis and two near Chicago. Figure 3-1 shows the route for this system, superimposed on a map of the existing transmission grid.

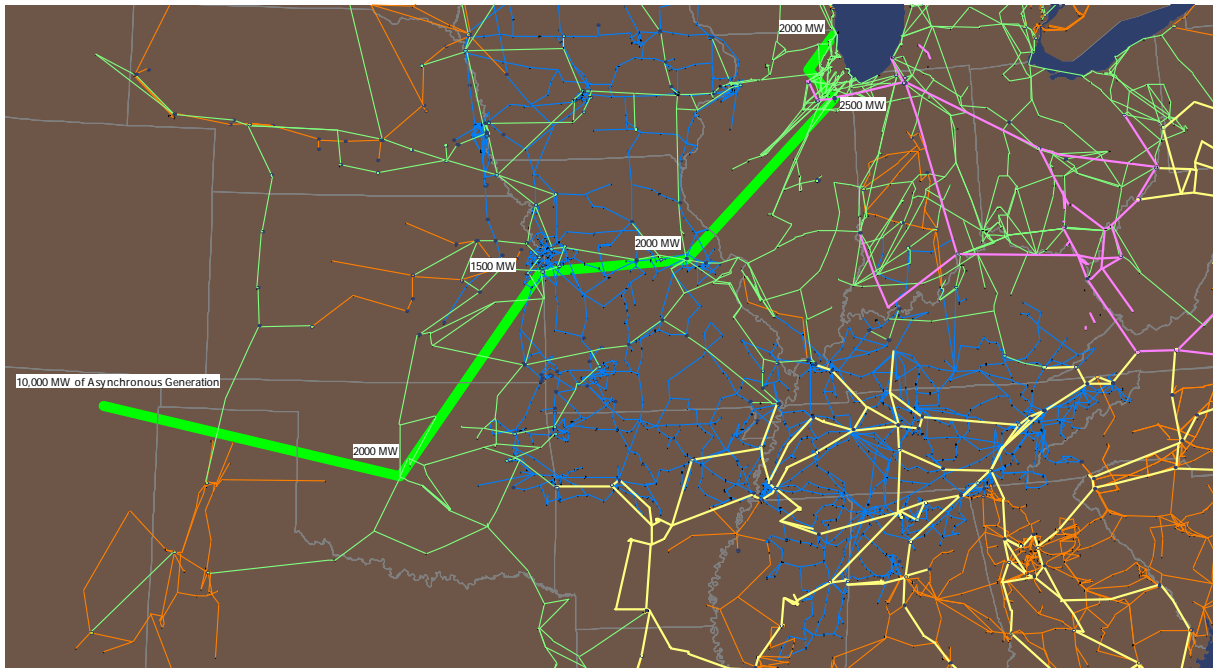


**Figure 3-1**  
**Eastern Interconnect Route for a 10 GW, six station system**

## Power Flow Results and System Modifications

The purpose for the power flow study was to determine locations in the existing grid that could accommodate the power injections from the superconducting dc cable system. Of course, trying to site approximately 2GW of new generation in an existing grid is a significant design challenge that was beyond the scope of this study, let alone doing it in five locations simultaneously. Therefore no attempt was made to do the detailed studies and system additions that would be needed to make sure the system with the superconducting dc cable would be n-1 secure or would satisfy a host of other planning criteria. Rather, a study was done to identify locations in the existing grid that could accommodate the desired power injections with at least no basecase (non-contingent) flow violations and with a reasonable voltage profile. This was possible in all the locations except the Kansas City area, in which two new 345 kV transmission lines were needed. The selected locations were to have 2 GW supplied in the Oklahoma City area (bus 54901 at 345 kV), 1.5 GW by Kansas City (bus 57968 at 345 kV), 2 GW by St. Louis (bus 31230 at 345 kV), 2.5 GW on the south side of Chicago metro area (bus 36260 at 765 kV) and 2.0 GW on the north side (bus 36421 at 345 kV). The new lines were added between buses 57977-57968 and 57868-59200.

The NERC power flow case was modified to include two new generation buses near each of the five connection points. Each generator bus had a generator with a power rating equal to 50% of the cable injection at that location. A short, essentially lossless transmission line joined the new generator to its connection bus. The cable system source generation was not explicitly modeled since it was assumed to be operating asynchronous with the rest of the grid. Then the existing generation in areas with superconducting dc cable injections was reduced to satisfy area control

error (ACE) requirements, maintaining their net interchange at the original values. All the cable injections were assumed to be at unity power factor. As an example of these results, Figure 3-2 shows the flows and voltages in the Kansas City area before the cable addition, while Figure 3-3 shows the results afterward.

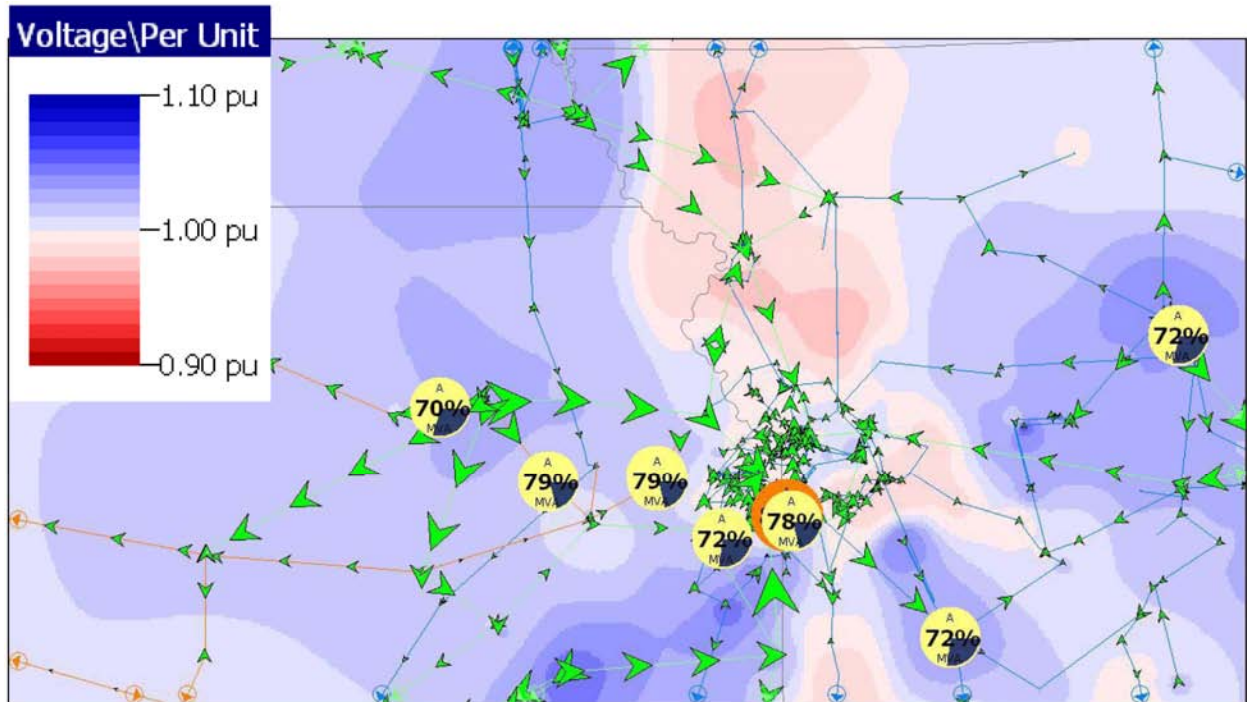


**Figure 3-2**  
**Original Kansas City Area Flows and Voltages**

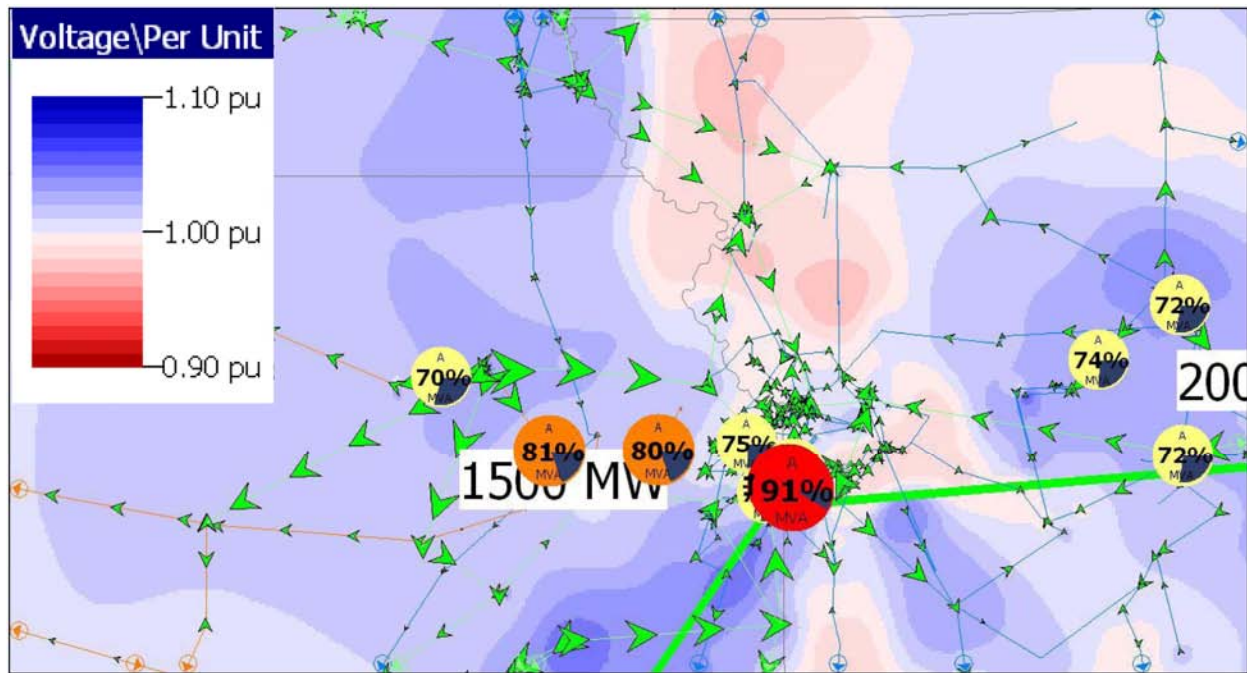


**Figure 3-3**  
**Kansas City Area Flows and Voltage with Superconducting DC Cable**

The conclusion from the power flow portion of this study was that the integration of the superconducting dc cable within the existing system will require modifications to the transmission grid similar to those needed to accommodate a new generator of similar size. During a cable contingency, any flow changes should be rapidly (within seconds) corrected by power transfers to the unfaulted cable. Therefore the key design issues seem to be in the transient stability area.

### Transient Stability Setup

The purpose for a transient stability study is to determine whether the system retains angular and voltage stability following a system disturbance. The disturbance scenario assumed here was the loss of one of the superconducting dc cables at a time when both of the cables were each carrying 50% of the rated power. Then, after the faulted cable is opened (not modeled in detail here), the power level on the unfaulted cable is linearly ramped over a period of seconds from 50% to 100%, so that once the ramping is complete the resultant net power injection at each station is equal to its pre-fault value. From an ac system perspective, the cable fault was modeled by simultaneously applying balanced three phase solid faults at each of the five terminal buses for the faulted cable, with the faults cleared after three cycles by the opening of the line joining that bus to its connection bus. Transient stability solutions were then run for 15 seconds using a ¼ cycle time step for five different scenarios: 1) the no ramping case, in which it was assumed the unfaulted cable continued to operate at 50%, 2) ten second ramping, in which the unfaulted cable's power ramped linearly from 50% to 100% over ten seconds, 3) five second ramping, 4) three second ramping, and 5) one second ramping.

## Transient Stability Load Model

Research over the past decade or two has made it clear that the load models used in a transient stability study can have a significant impact on the results, particularly with respect to voltage stability [1, 2, 3]. Motivated by the recommendations from [2] and [3], the load was modeled using a mix of 15% large induction motors, 45% small induction motors, 20% discharge lighting and the remainder as constant current for the real power and constant impedance for the reactive power. The induction motors were modeled using the parameters and third order models from [2]. For reference, the torque-speed characteristics for the large motor model is shown in Figure 3-4 and for the small motor model in Figure 3-5. The germane issue associated with induction motors is that during a fault, when the voltage is depressed, the induction motor torque decreases as the square of the voltage. This causes the motor to rapidly decelerate increasing its slip and greatly increasing its reactive power consumption, which in turn can impede the voltage recovery.

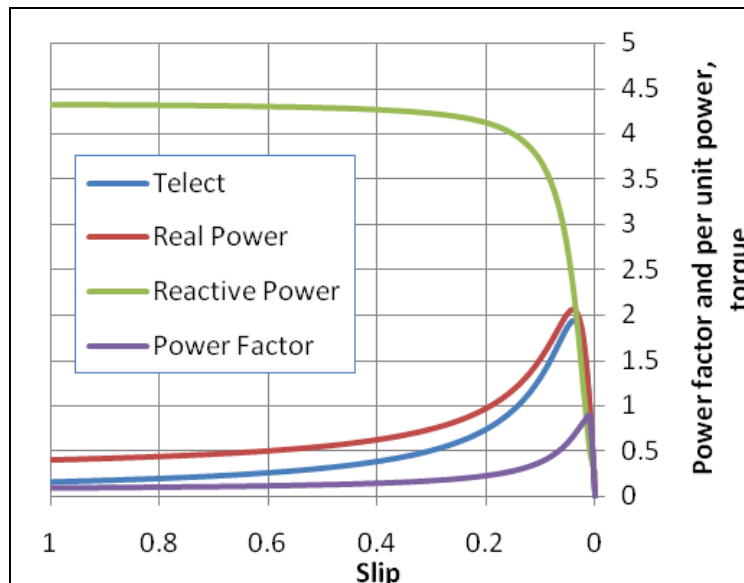


**Figure 3-4**  
Large machine torque-speed characteristics

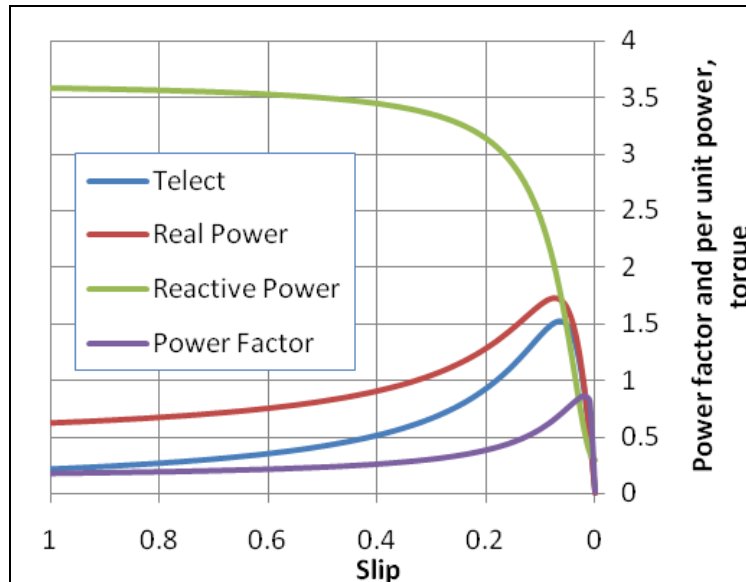


**Figure 3-5**  
Small machine torque-speed characteristics ( $P=1$  slip= 0.0217)

## Transient Stability Results – Frequency Response

Transient stability addresses the issue of whether all the system generators will retain synchronism following a system fault. For the scenarios under consideration here, the initial fault will perturb the system generators away from their equilibrium points. Also, because there is a net loss of generation, at least for the time period before full power is ramped to the unfaulted cable, the overall frequency will also start to decay. How quickly the frequency declines depends the spinning inertia of the system, and the response of the generator governors.

The most severe credible contingency considered here is the case in which one cable is lost, and then (for whatever reason) no power is transferred to the unfaulted cable. Hence there is a net, sustained loss of 5 GW of generation. Figure 3-6 shows a plot of the individual frequencies at all the 5300 in-service generators modeled in the case. Therefore the figure provides a bound on the system frequency response. What is encouraging is that even for this most severe contingency no frequency value falls below 59.7 Hz and none rises above 60.2 Hz. Given that underfrequency loading shedding does not occur unless the frequency goes below 59.3 Hz (for the Eastern Interconnect), this contingency should be manageable.

Figure 3-7 provides a more readable view of the frequency response for a small subset consisting of twelve large, geographically dispersed generators. Notice that at the end of the simulation the system frequency has not been restored to 60 Hz, rather it settles to a value of about 59.973 Hz. This is because of the net drop in total generation. While the lost generation is restored by the generator governor response, the frequency is not fully restored because of the governor droop characteristics (i.e., they are not isochronous governors). In the actual system the frequency would eventually be fully restored to 60 Hz by the action of automatic generation control (AGC).

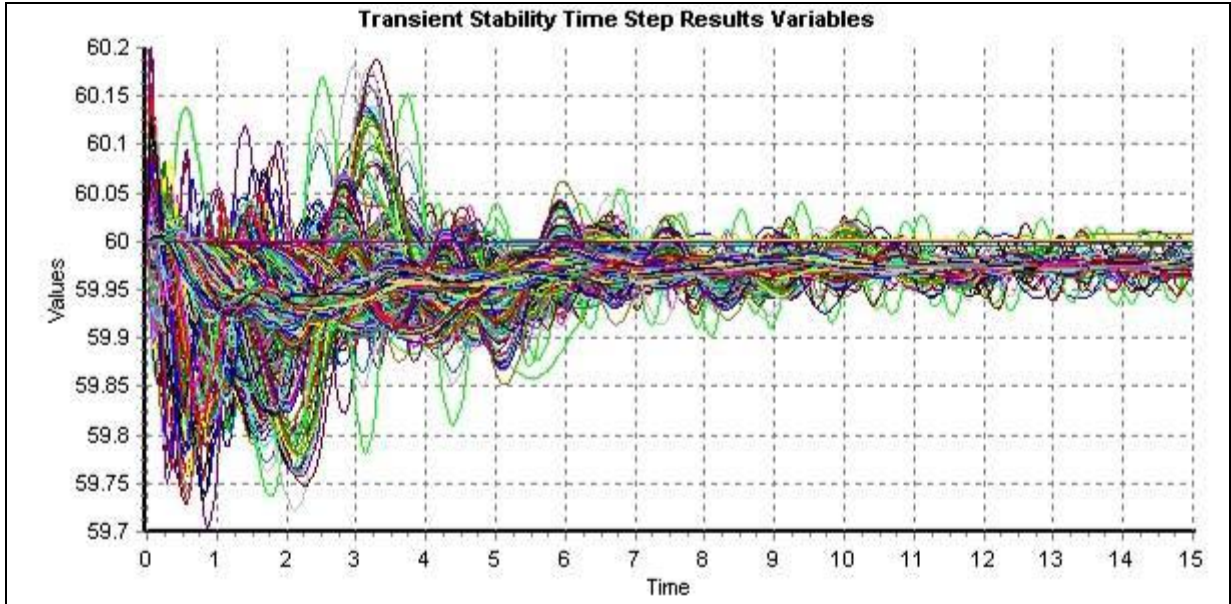


**Figure 3-6**  
Frequency response for all generators with no ramping

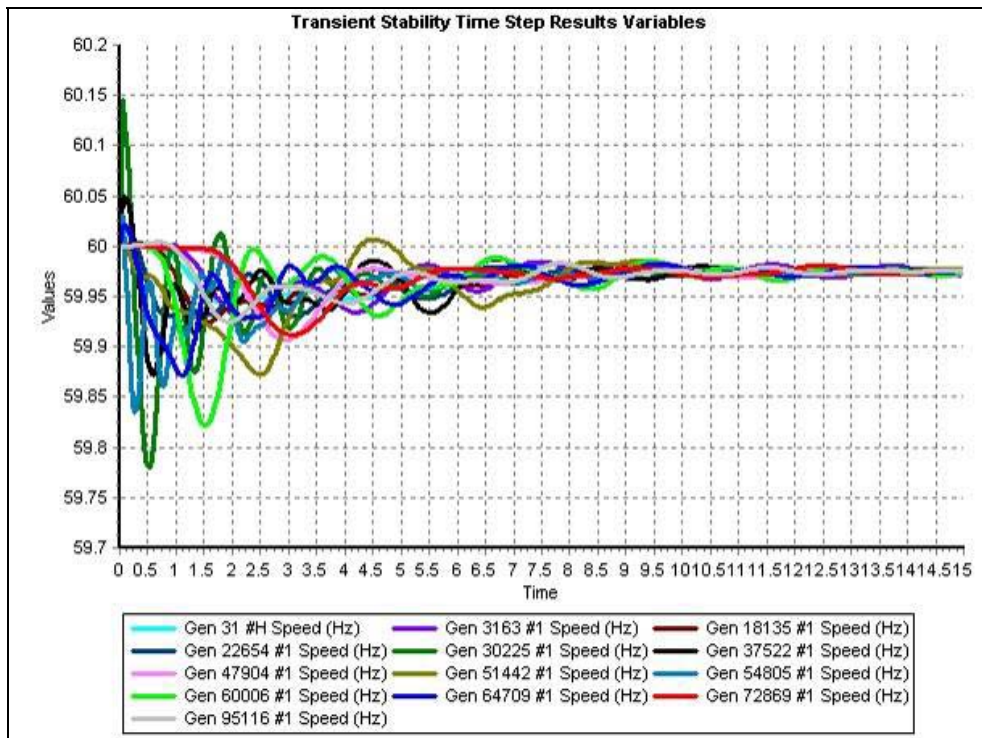


**Figure 3-7**  
Frequency response for twelve large generators with no ramping

Figure 3-8 gives an example of how the generator mechanical power input varies due to the governor response for a generator located close to the fault. Because for this scenario there is a sustained loss of 5 GW, each generator on governor control needs to increase its output (subject to the governor limits). Assuming all generators in the interconnect participate proportionally in this redispatch (at least for the time period of seconds to minutes before the AGC response), in a system with 676 GW of total generation, the response for the 626 MW unit from Figure 3-8 should be about 5 MW.

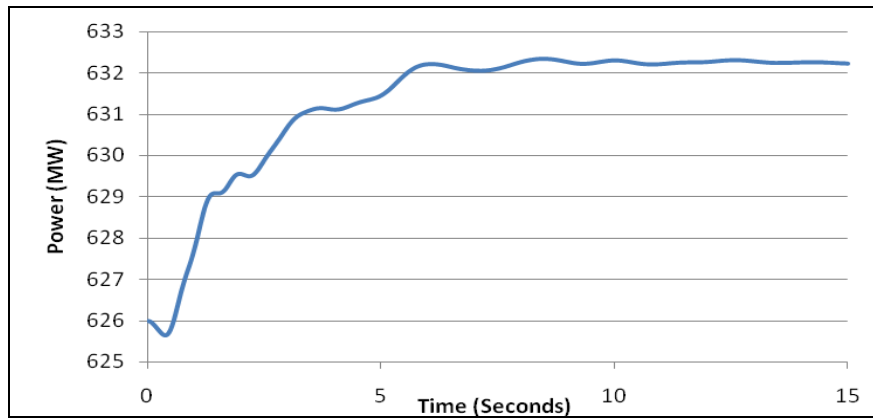


**Figure 3-8**  
**Governor response for a coal generator (at Bus 32461)**

The actual frequency response following a large power system disturbance depends upon how many generator governors are actually set to respond effectively. This issue has recently been addressed in [4] with one of the key concerns being that power plant governing response is often considerably less than expected and planned [5]. This seems to be more of an issue in the Eastern Interconnect than in the Western Electricity Coordinating Council (WECC) or Electric Reliability Council of Texas (ERCOT) systems because the larger size of the Eastern Interconnect makes it so even when a substantial number of the generator governors are disabled there is still an adequate frequency response.

As was mentioned in the introduction to this section, the results presented here were done using a 2006 series MMWG case using the governor models provided with the rest of the dynamics data. While the authors have no way of knowing whether individual governors modeled as being in-service are in fact disabled in practice, the resultant change in system frequency of -0.027 Hz for a sustained 5 GW generator loss is low when compared to historical values. For example, based upon Figures 2-22 and Figure 2-24 of [4] one would expect a frequency response in the Eastern Interconnect of about 2500 MW/0.1 Hz, and hence a drop of about 0.2 Hz for the loss of 5 GW.

In an attempt to duplicate these actual responses the Figure 3-6 results were re-run with various governors deliberately disabled. Figure 3-9 shows the results with 200 GVA of governor response disabled (out of an original total of 722 GVA), Figure 3-10 shows the case with 400 GVA disabled, and 600 GVA. The resultant final frequencies are 59.962 Hz for the 200 GVA case (-0.038 Hz), 59.932 Hz for the 400 GVA case (-0.068 Hz) and 59.823 Hz (-0.177 Hz) (note, the constant values at 60 Hz in the figures are from disabled generators and should be ignored).

In looking at the figures, notice the amount of governor response has very little impact on the magnitude of the first swing frequency decline (i.e., the drop within the first second). Hence even when a large number of governors are disabled or operating at their limits the system should retain adequate frequency margin.

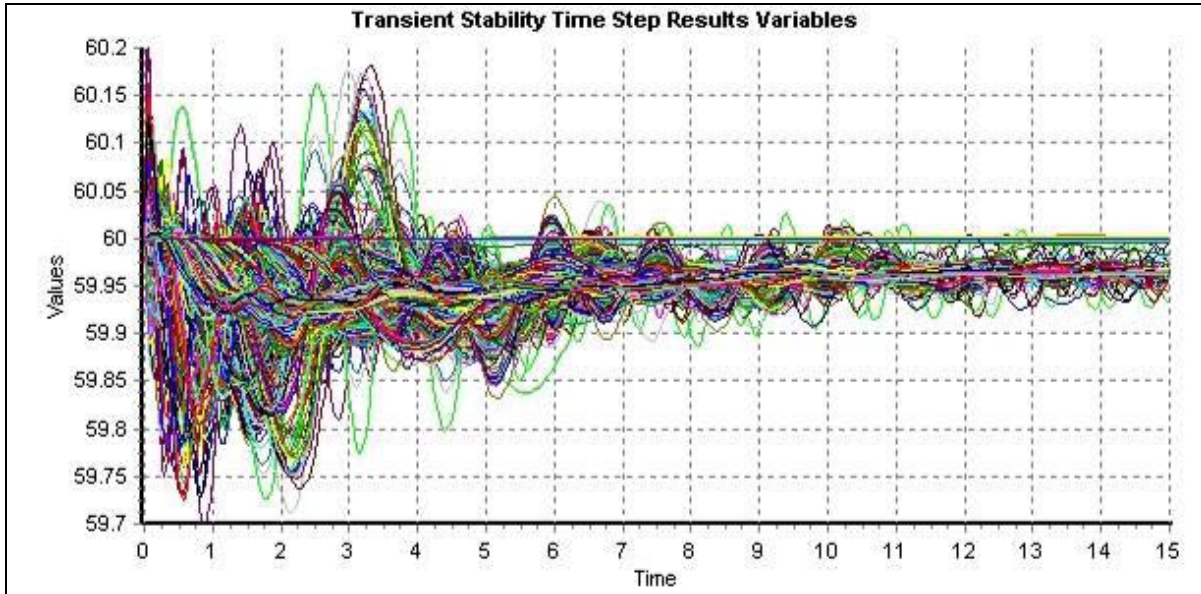


**Figure 3-9**  
Frequency response for all generators with no ramping and 200 GVA of governor response disabled

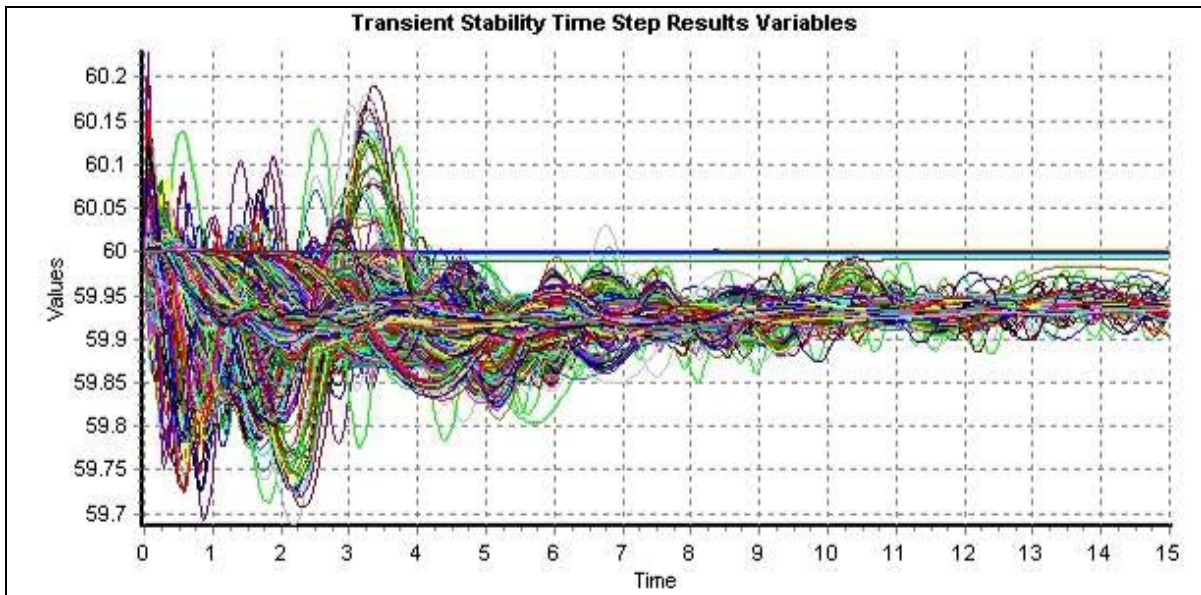


**Figure 3-10**  
Frequency response for all generators with no ramping and 400 GVA of governor response disabled

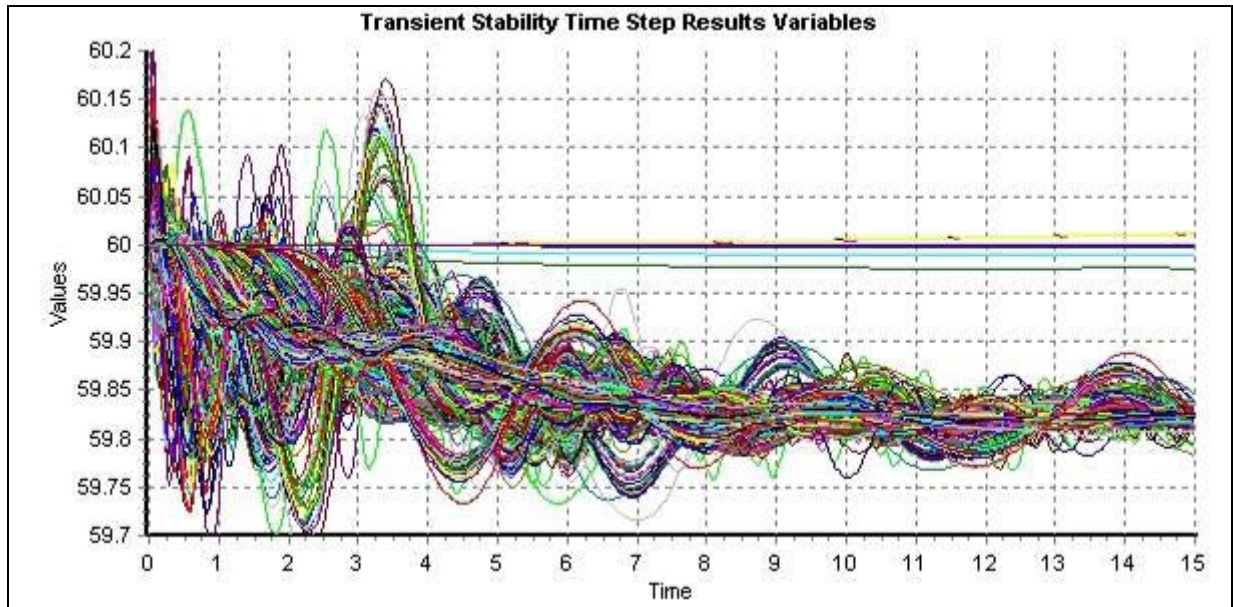


**Figure 3-11**  
**Frequency response for all generators with no ramping and 600 GVA of governor response disabled**

Figure 3-12 through Figure 3-14 provide an alternative, spatially-oriented view of the system frequency information for the Figure 3-6 case. All three figures provide a contour of the individual bus frequencies, with Figure 3-12 showing the values at 0.5 second after the initial fault, Figure 3-13 at 1.0 seconds, and Figure 3-14 at 1.5 seconds. Notice that the frequency disturbance propagates perpendicularly away from the faulted line at a velocity of several hundred miles per second. This spatial frequency response is also indicated in Figure 3-7, particularly by looking at the response of generator 72869 (located in New Hampshire), 3163 (located in Pennsylvania) and 95116 (located in Virginia). When these spatially-oriented frequency contours are shown in an animation sequence, the frequency changes can be seen to propagate through the system in a wavelike manner, reflecting off the system boundaries. As indicated by Figure 3-6, the disturbance damps out after about five seconds.

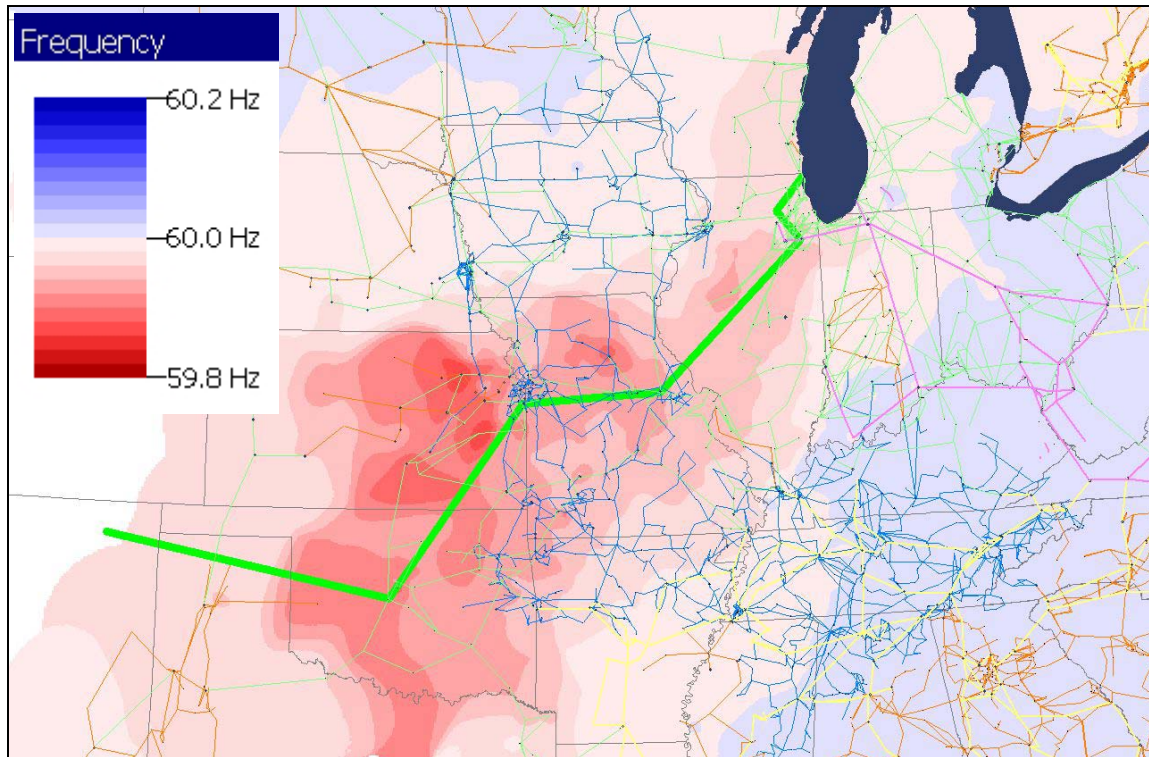


**Figure 3-12**  
Spatial frequency response for no ramping case, at time = 0.5 seconds

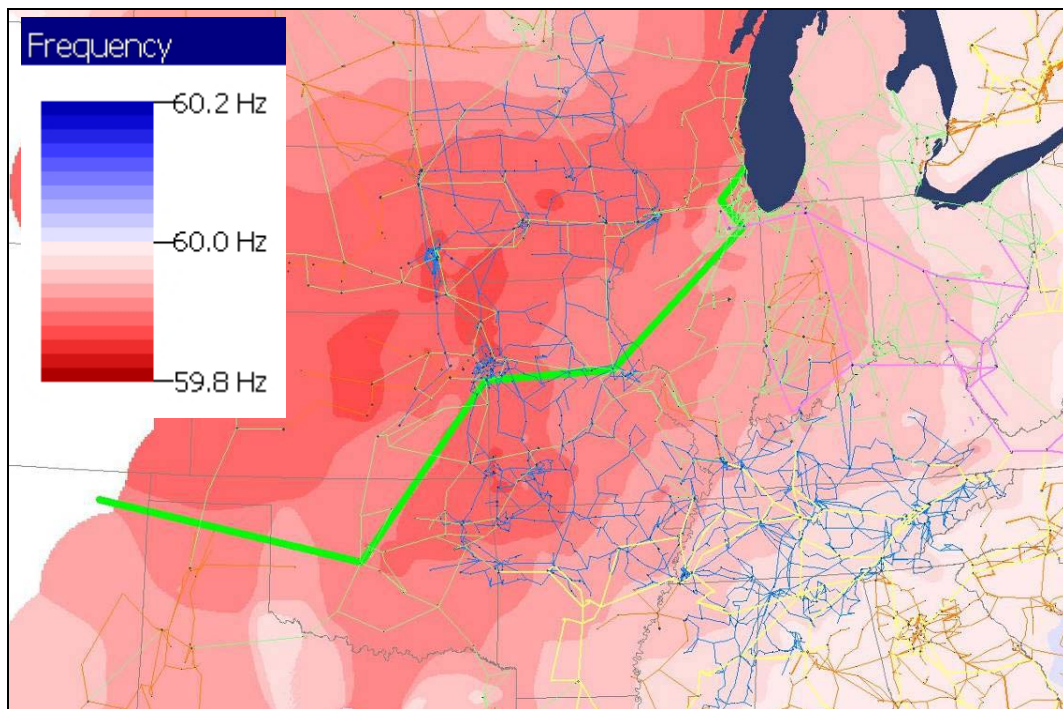


**Figure 3-13**  
Spatial frequency response for no ramping case, at time = 1.0 second

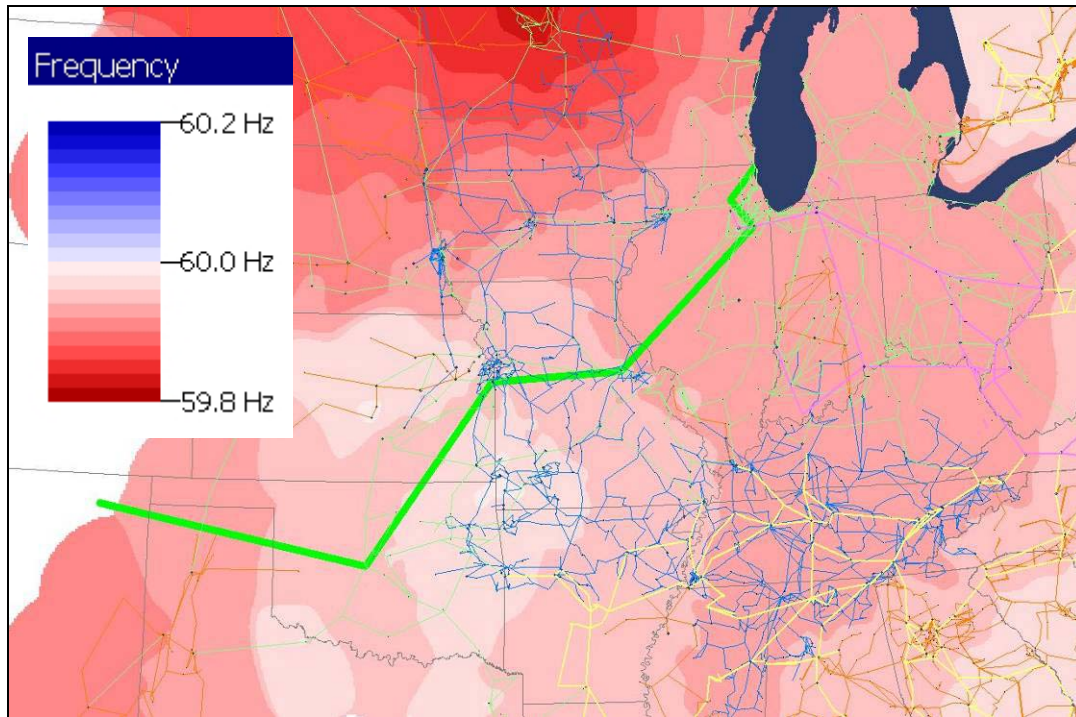


**Figure 3-14**  
**Spatial frequency response for no ramping case, at time = 1.5 seconds**

The conclusion from the previous scenario is that from a system frequency point of view the failure of one cable without any power transfer should be a manageable contingency even when substantial numbers of generator governors are disabled. The remainder of this section presents results for scenarios in which following the fault the power level on the unfaulted cable is linearly ramped to 100% over varying time periods ranging from 10 seconds to one second.

Figure 3-15 and Figure 3-16 show the same values as were shown in Figure 3-6 and Figure 3-7 except for this scenario the power flowing on the unfaulted cable was linearly ramped from 50% to 100% over the course of ten seconds. Notice that the frequency results are almost the same for the first several seconds, again bounded between 59.7 and 60.2 Hz, and damping out after about five or so seconds. The key difference between the scenarios is because the superconducting dc cable system is ramped back to full power, there is no final frequency error. This is easiest to see in Figure 3-16 with the curves all converging back to 60 Hz. The plot of the governor response at Generator 32461 also indicates the cable response – initially moving upwards to make up the generation imbalance, and then settling back to its pre-fault value within 15 seconds. These results help to justify the power flow assumption that as long as the unfaulted cable power flow could be moved to 100% there were essentially no immediate steady-state ramifications to a cable fault.

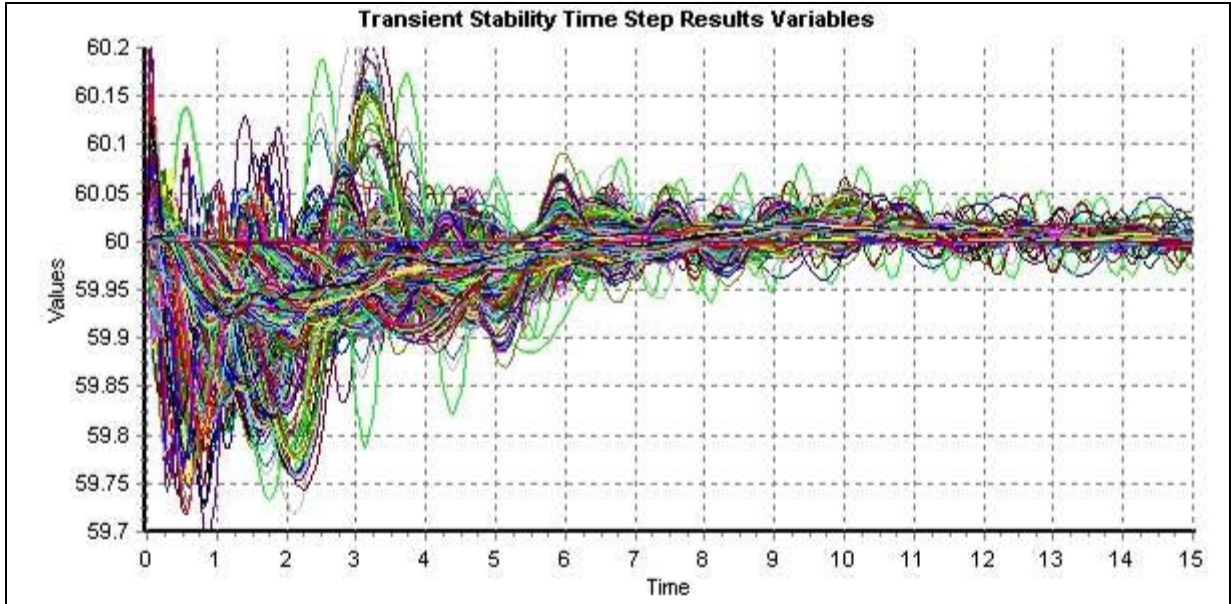


**Figure 3-15**  
 Frequency response for all generators with ten second ramping

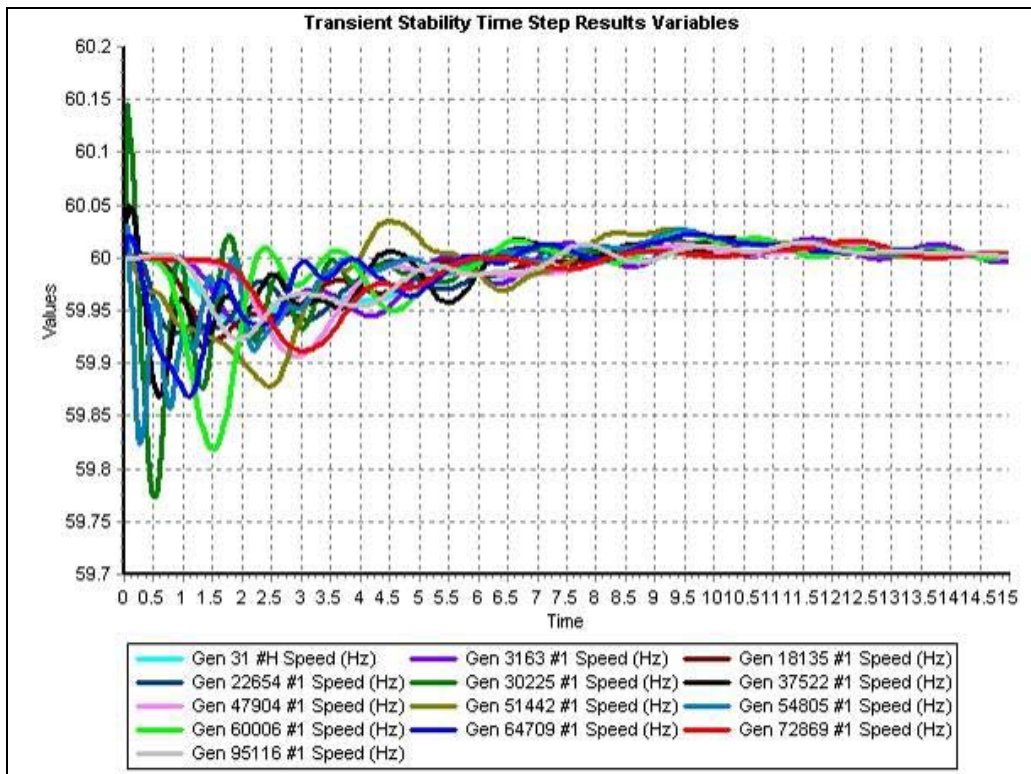


**Figure 3-16**  
 Frequency response for twelve large generators with ten second ramping

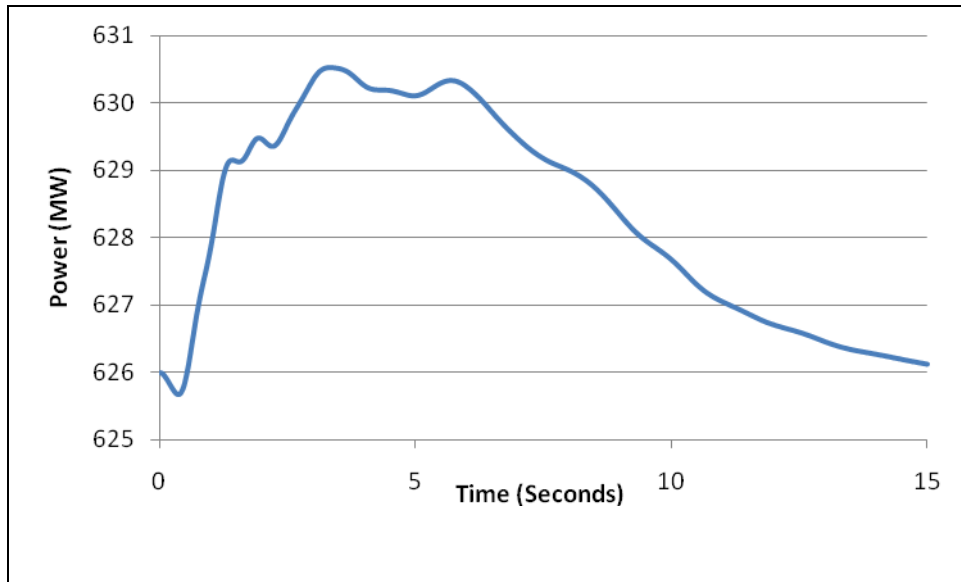


**Figure 3-17**  
**Governor response at generator 32461 with ten second ramping**

The next six figures show the frequency results for scenarios in which the power is ramped over five seconds (Figure 3-18 and Figure 3-19), three seconds (Figure 3-20 and Figure 3-21) and one second (Figure 3-22 and Figure 3-23). In comparing the figures it becomes clear that since the initial drop in generator frequency occurs within the first second or two, unless the power is ramped extremely rapidly (e.g. within one second) its ramping rate will have little impact on this initial decline. Rather, the decline depends upon the net rotating inertia of the interconnect. Also, faster ramping rates can actually exacerbate the transient over-frequency values at least to a small degree. Therefore, unsurprisingly given that these scenarios are less severe, they also indicate that the cable failure contingency is manageable (at least from a frequency perspective). The impact of the cable failure on system voltages is considered in the next section.

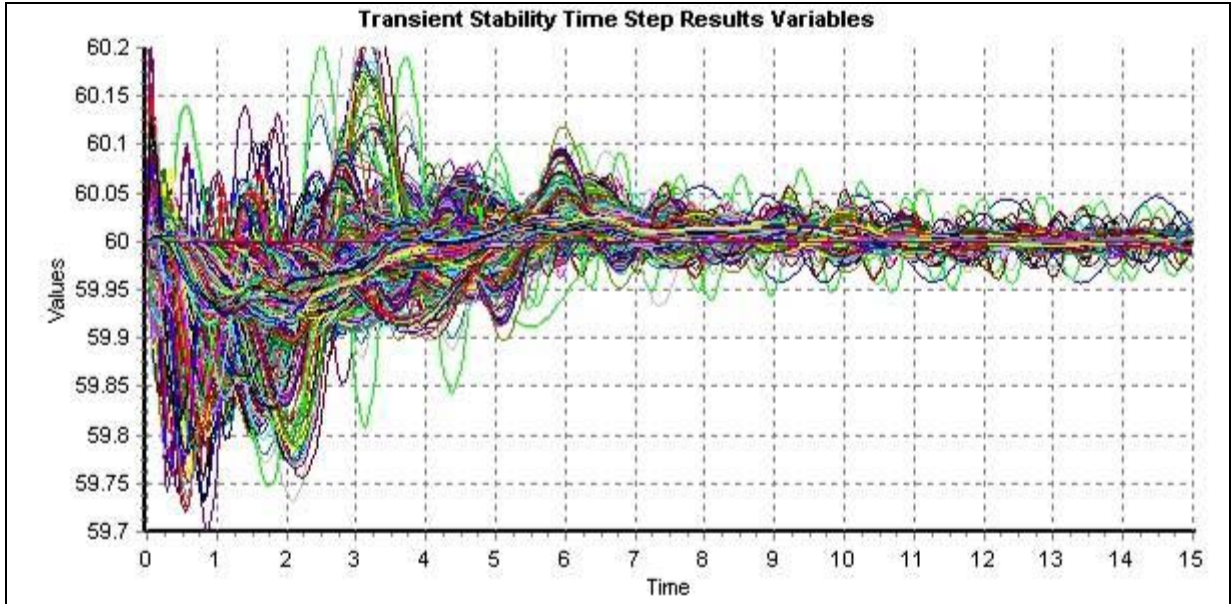


**Figure 3-18**  
**Frequency response for all generators with five second ramping**

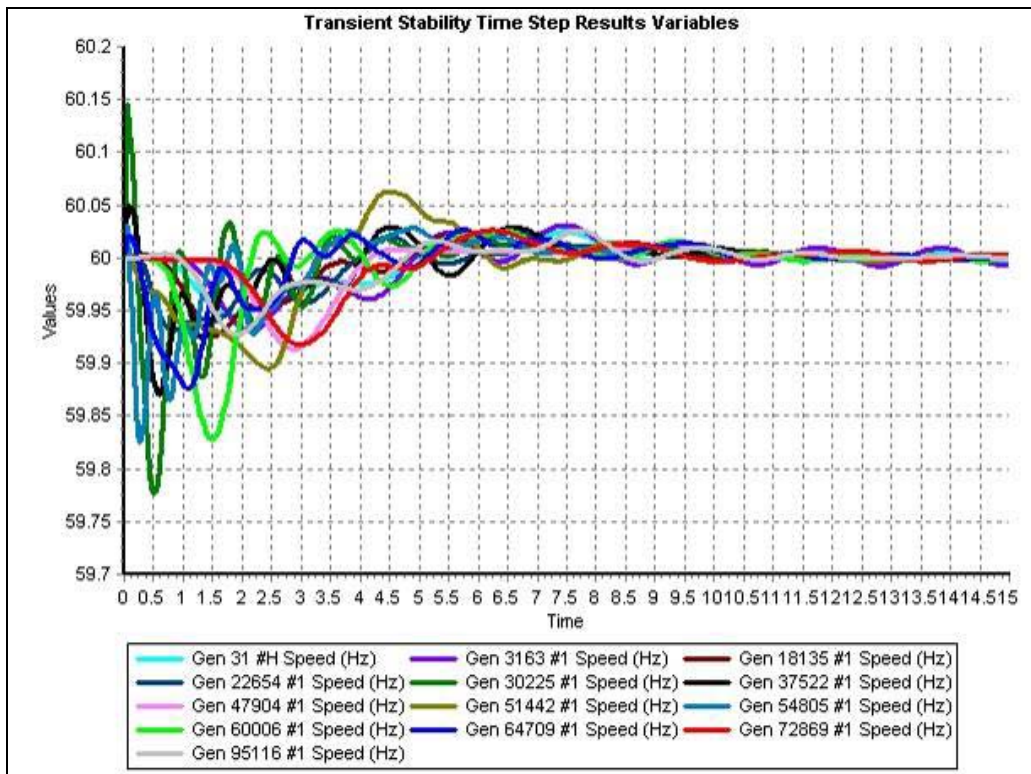


**Figure 3-19**  
**Frequency response for twelve large generators with five second ramping**

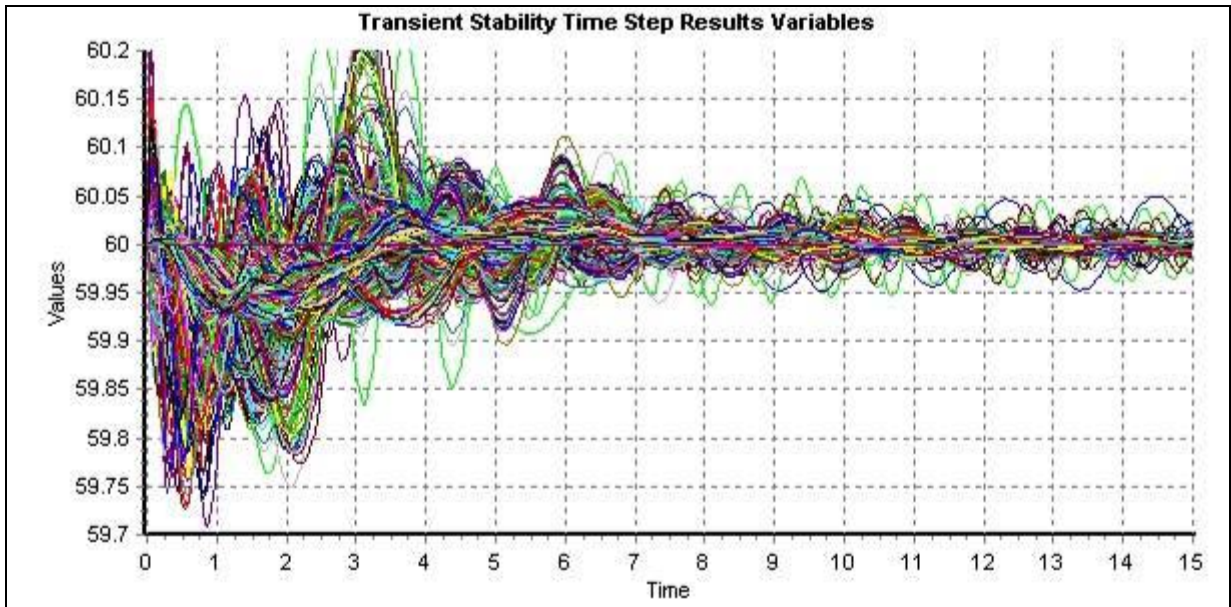


**Figure 3-20**  
**Frequency response for all generators with three second ramping**

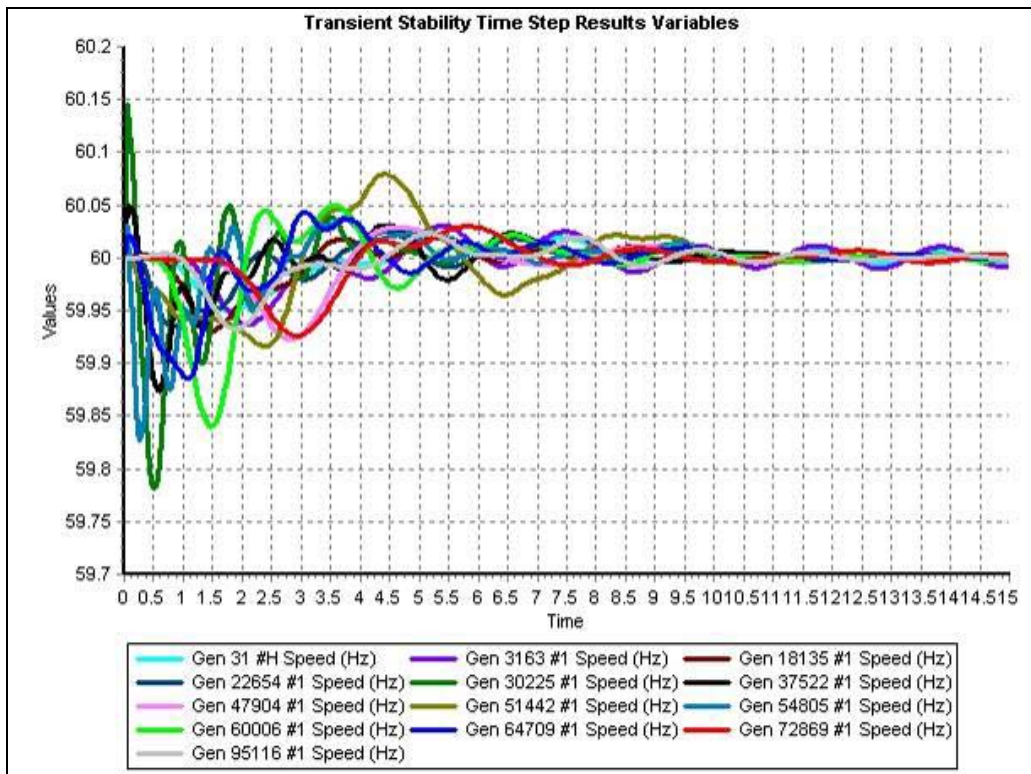


**Figure 3-21**  
**Frequency response for twelve large generators with three second ramping**

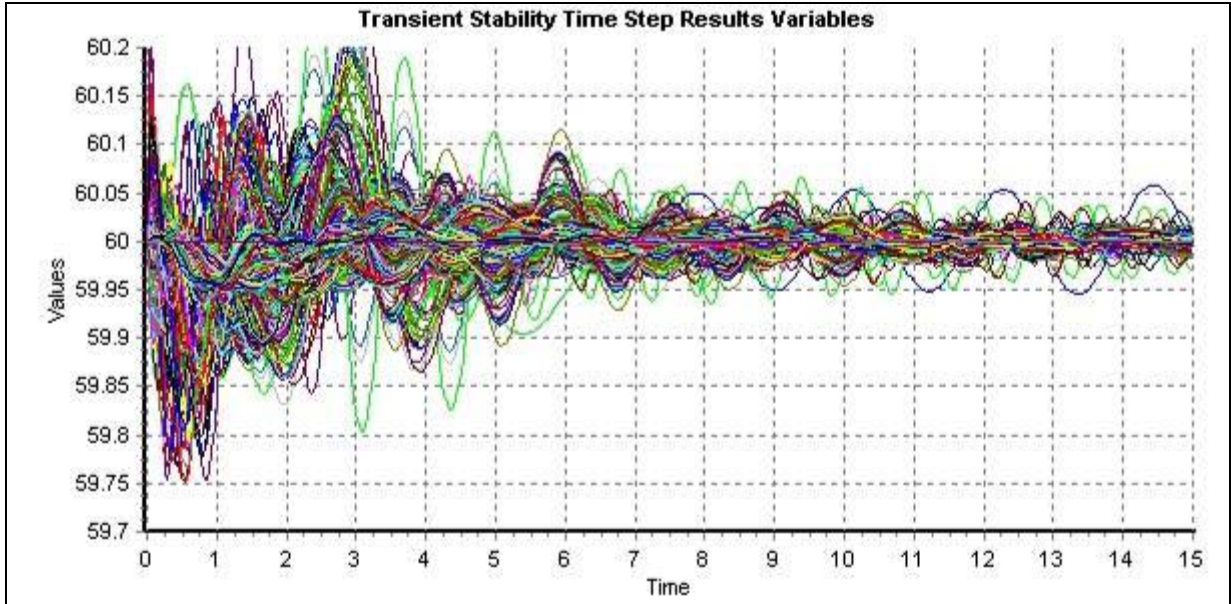


**Figure 3-22**  
 Frequency response for all generators with one second ramping

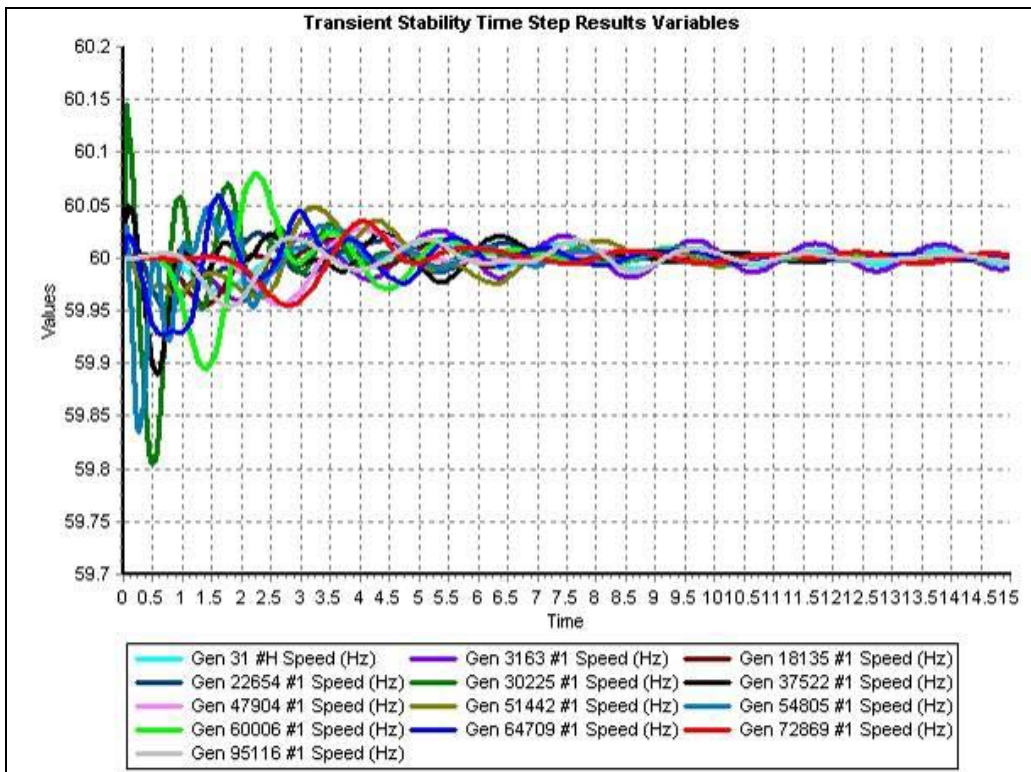


**Figure 3-23**  
 Frequency response for twelve large generators with one second ramping

## Transient Stability Results – Voltage Response

The second issue considered during the transient studies was the short-term voltage stability of the system. This section discusses the same results as presented in the previous section, but here the focus shifts from bus frequency to bus voltage. As was mentioned earlier, the transient stability voltage response is very dependent upon the assumed load model. If a static load model is assumed, such as constant current for the real power and constant impedance for the reactive power, then the voltage recovery following a fault is quite rapid. However, such a model is not realistic. The model used here consisted of a mix of 15% large induction motors, 45% small induction motors, 20% discharge lighting and the remainder as constant current for the real power and constant impedance for the reactive power.

To illustrate the impact of the load model on the voltage response, Figure 3-24 compares the voltage response for a fault at bus 5 of the WECC 3-machine, 9-bus system (described in [6]) between a static load model (constant current for the real power and constant impedance for the reactive power) and the model used here for two fault scenarios. With the static load model the voltage recovers quite quickly for both faults, whereas with the mixed load model the voltage recovery is slower for the 0.08 second fault case. For the 0.1 second fault case the small induction motor component of the load actually stalls, preventing the voltage from fully recovering (when stalled induction motors consume large amounts of reactive power).

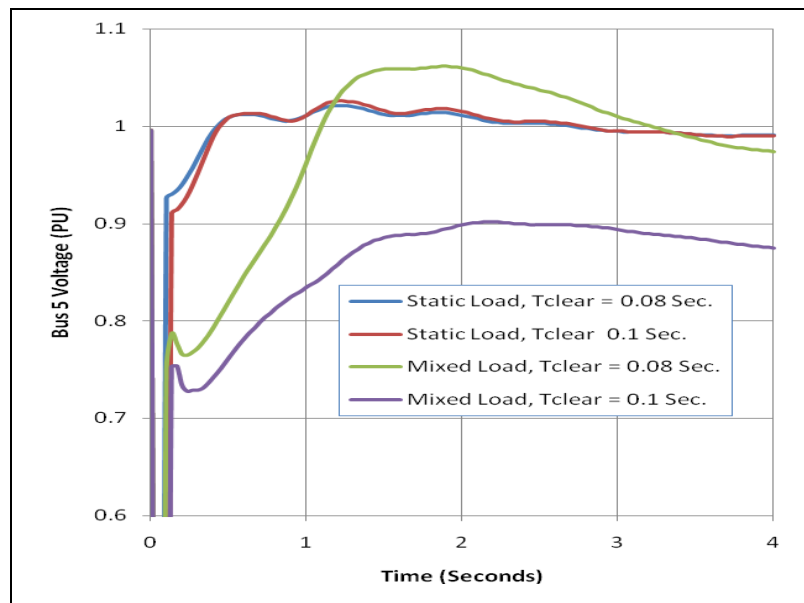


**Figure 3-24**  
Voltage response versus load model comparison

The system-wide impact of the cable fault is shown in the following four figures, each of which contours the per unit voltage at the high voltage buses (above 150 kV) for four different time points during the no ramping scenario (same as in Figure 3-6). Figure 3-25 shows the pre-fault voltage contour, representing a reasonable operating condition. Figure 3-26 then represents the situation at 0.1 seconds after the fault (0.05 seconds after the fault has been clear), a time when

many of the bus voltages are still quite low. Figure 3-27 shows the situation at 0.5 seconds, when many of the voltages have begun to recover. Finally, Figure 3-28 shows the situation at 1.0 seconds, indicating the voltage profile has almost recovered to its pre-fault condition.

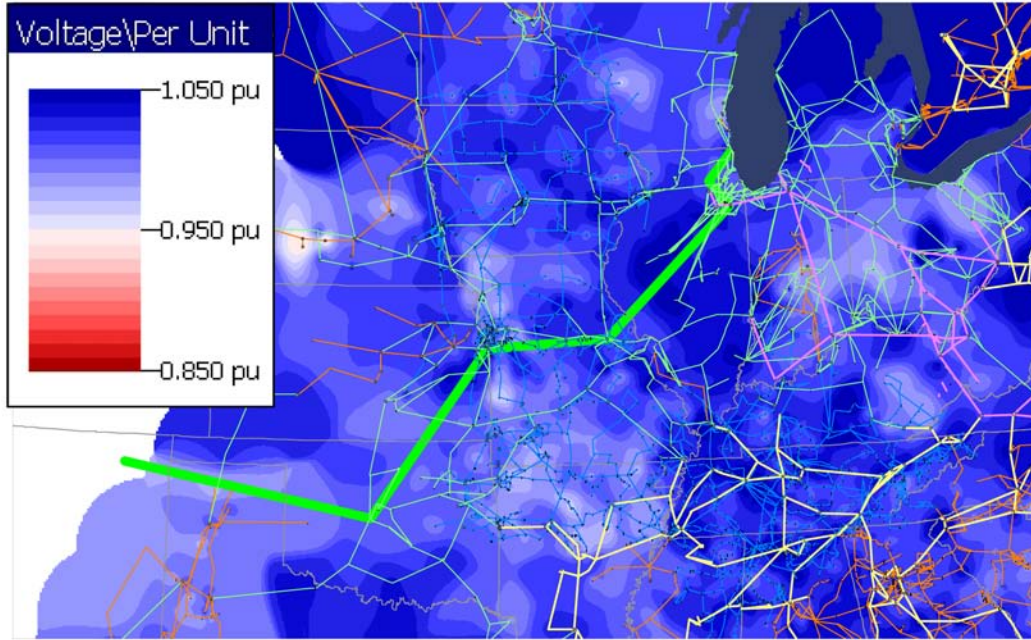


**Figure 3-25**  
Pre-fault voltage contour

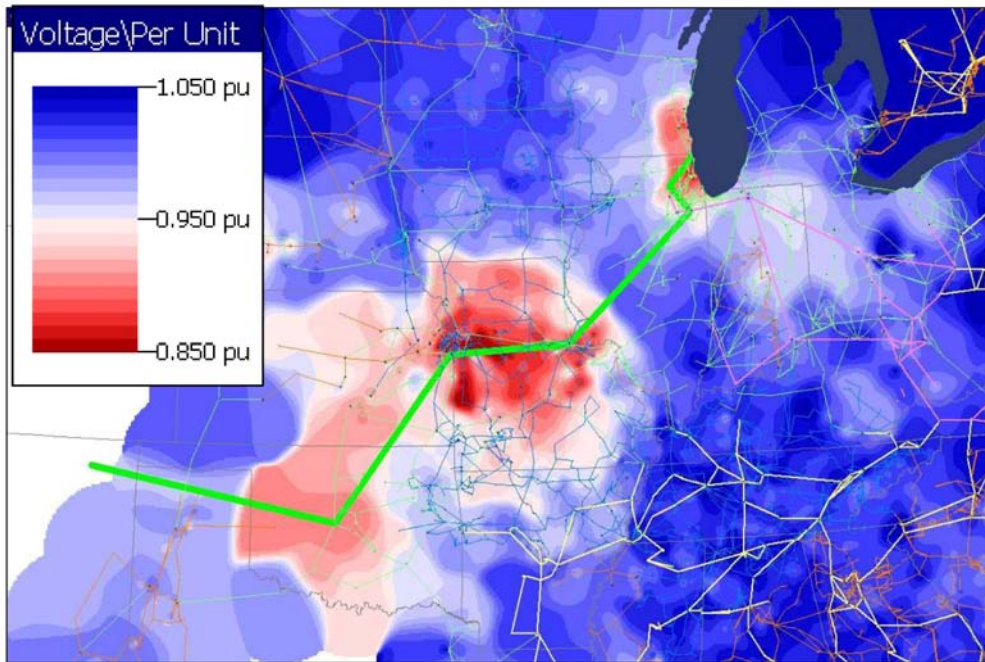


**Figure 3-26**  
Voltage contour for no ramp case at 0.1 seconds

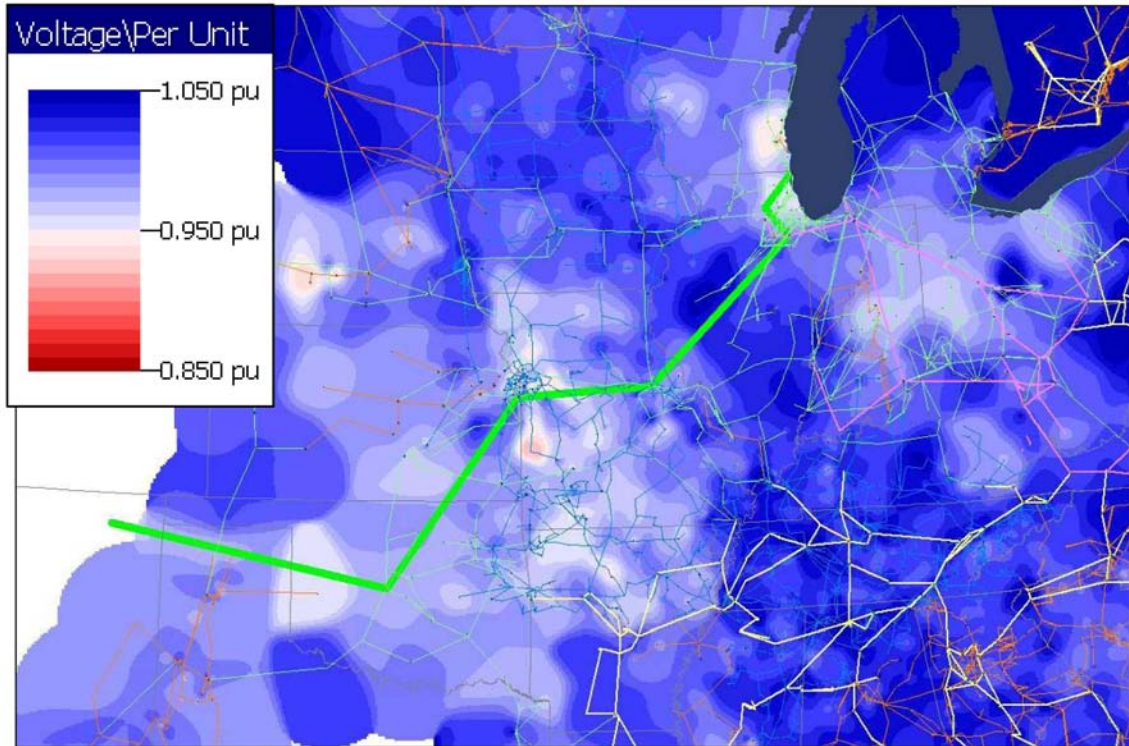


**Figure 3-27**  
Voltage contour for no ramp case at 0.5 seconds

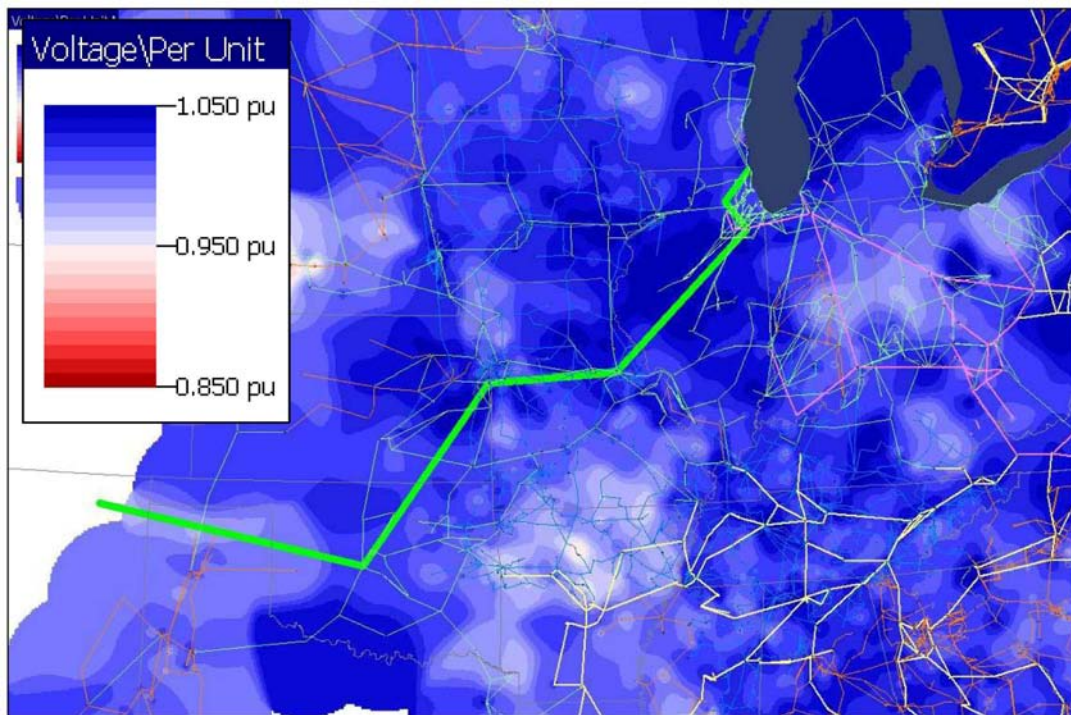


**Figure 3-28**  
Voltage contour for no ramp case at 1.0 second

From a generation perspective one of the key concerns addressed by transient stability studies is how quickly the voltage recovers at the generator terminal bus. This is known as “low voltage ride-through” and is of particular concern for nuclear and wind plants (for an overview of this issue see [7]). While no single standard exists, the proposed WECC standard, shown in Figure 3 of [7], requires that all generators stay connected as long as their voltage stays at zero for no more than 15 cycles (0.15 seconds), and then rises linearly to 0.9 per unit in 1.75 seconds. To address whether this criteria is met, Figure 3-29 presents a more traditional view of the same information as the contour displays, except showing the time variation in the per unit voltages at six buses and then at the worst performing load bus. The buses are as follows:

- Bus 30225 is a terminal bus for a nuclear power plant near St. Louis
- Bus 32435 is the terminal of a nuclear power plant in central Illinois
- Bus 37522 is the terminal of a nuclear power plant in the southern part of the Chicago metro area
- Bus 37524 is a nuclear power plant in north central Illinois
- Bus 56751 is a nuclear power plant in eastern Kansas
- Bus 53615 is the high side terminal for a power plant in northeast Texas, and
- Bus 30805 is a 69 kV load bus in eastern Missouri that exhibited the slowest voltage recovery in the case.

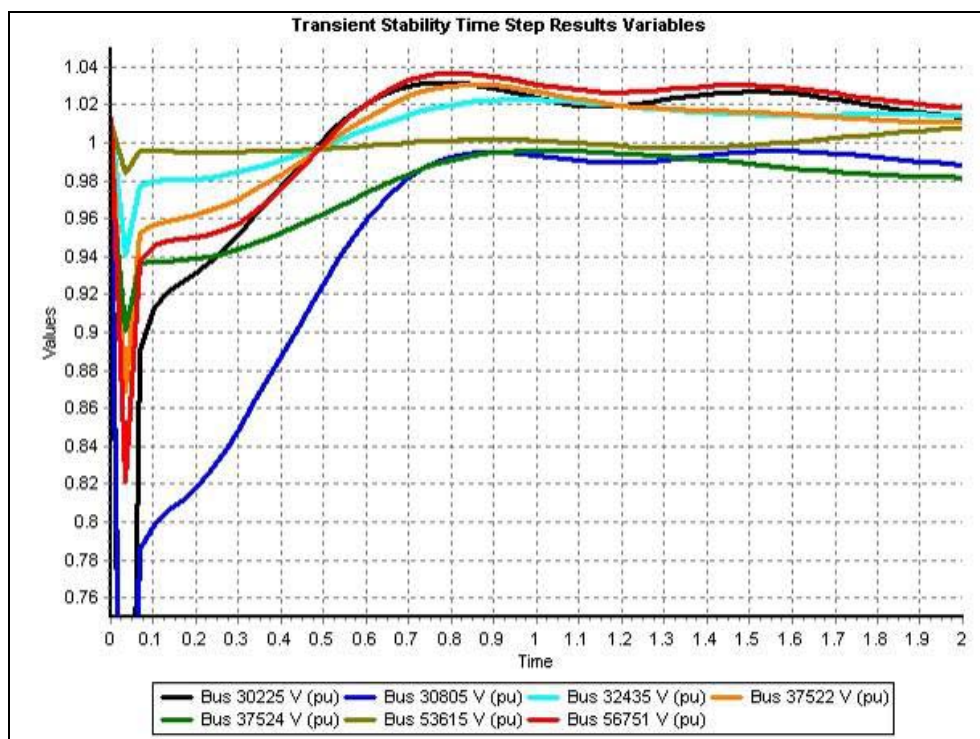


**Figure 3-29**  
Voltage response at selected buses for no ramp case for the first two seconds

Given that all the voltages have recovered to above 0.95 per unit within 0.4 seconds for the case of the generator buses, and within 0.6 seconds for the worst performing load bus, the studies indicate that the proposed WECC low voltage ride-through criteria is satisfied.

The same voltage analysis was also performed for the other scenarios. For example, Figure 3-30 repeats Figure 3-29 for the case in which the power on the unfaulted cable is ramped in three seconds. A comparison between the figures indicates that the voltage response is quite similar. This was also the case for other scenarios not shown. Based upon this analysis the conclusion is that from a short-term voltage stability point of view, all the plausible contingencies should be manageable.

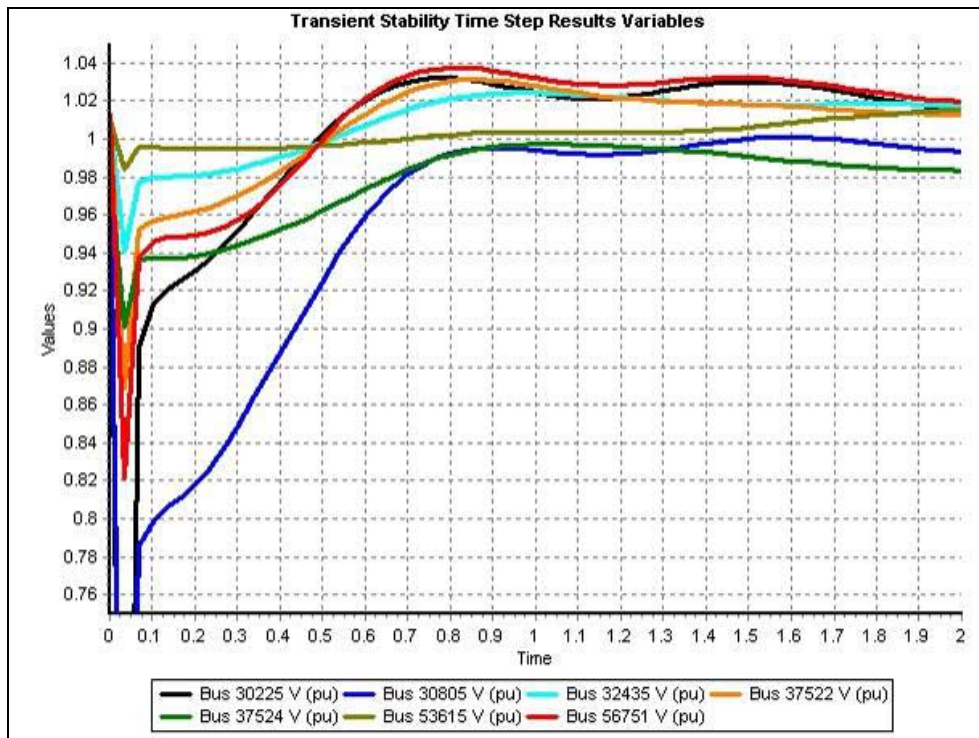


**Figure 3-30**  
Voltage response at selected buses for three second ramp case for the first two seconds

# 4

## WESTERN ELECTRICITY COORDINATING COUNCIL STUDIES

---

The second system studied for this project was the Western Electricity Coordinating Council (WECC) 2010 LA1-SA case, which models the WECC area for anticipated 2010 operating conditions. This case contains about 15,800 buses, 3100 generators, with a total system load of about 106 GW. To perform the transient stability studies the power flow case data was augmented with the associated 2006 series dynamic models.

A main challenge with integrating a superconducting dc cable system into the WECC system is that its size is only about 1/6 that of the Eastern Interconnect. This means that in the event of a cable fault, there will be proportionally less rotating inertia to make up for the lost generation. One would also assume that there would be a proportionally smaller governor response. However, based upon the actual results discussed in section 2.7 of [4], while the governor response is certainly less, it is not proportionally less. Whereas the Eastern Interconnect has a frequency response of around 2500 MW/0.1 Hz, the WECC response is on the order of 1000 MW/0.1 Hz, just 2.5 times smaller. Also, the WECC has placed a high priority on accurate governor modeling, with one result being that with the newer models the modeled governor response tends to duplicate the actual results fairly well [8].

Nevertheless, the smaller size of the WECC made it unlikely that a full 10GW cable could be successfully integrated. Therefore a slightly smaller 8.5 GW system was studied. This meant that the sustained loss of the power flowing on one cable would result in an anticipated frequency decline of 0.4 to 0.5 Hz, still above the 59.1 Hz WECC load shed threshold. The superconducting dc cable system scenario assumed 8.5 GW of asynchronous generation located somewhere in the southwest Great Plains. The design goal was then to supply this power to the load with taps near Denver, Albuquerque, Phoenix, San Diego and Los Angeles. Figure 4-1 shows the route for this system, superimposed on a map of the existing transmission grid.

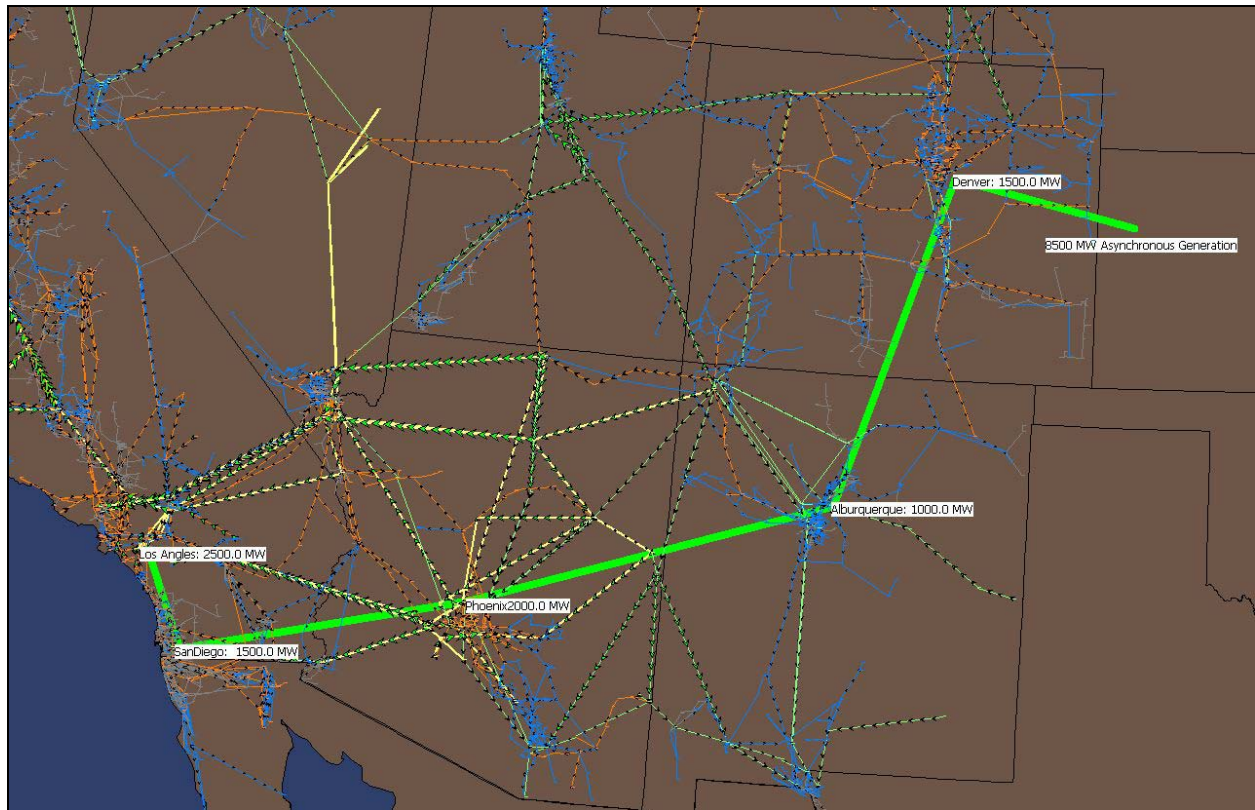


**Figure 4-1**  
**WECC route for a 8.5 GW, six station system**

## Power Flow Results and System Modifications

As was the case for the Eastern Interconnect case, the purpose for the power flow study was to determine locations in the existing grid that could accommodate the superconducting dc cable system power injections. Again, no attempt was made to do the detailed studies and system transmission additions that would be needed to make the system with the cable n-1 secure. Still, the study did identify locations in the existing grid that could accommodate at least one GW of power injection, with the amount varying by location. The selected locations were to have 1.5 GW injected in the Denver area (bus 70396 at 230 kV), 1 GW by Albuquerque (bus 10025 at 345 kV), 2 GW near Phoenix (bus 14005 at 500 kV), 1.5 GW near San Diego (bus 22464 at 230 kV) and 2.5 GW near Los Angeles (bus 24138 at 500 kV). All power injections were a unity power factor. Figure 4-2 shows the flows and voltages for the southern portion of the WECC with the cable system. Pie charts are used to highlight transmission lines loaded above 90% of their limit. The conclusion from the power flow study was the same as for the Eastern Interconnect. That is, integration of the superconducting dc cable system will certainly require modifications to the existing transmission grid similar to accommodating generators of equal size.

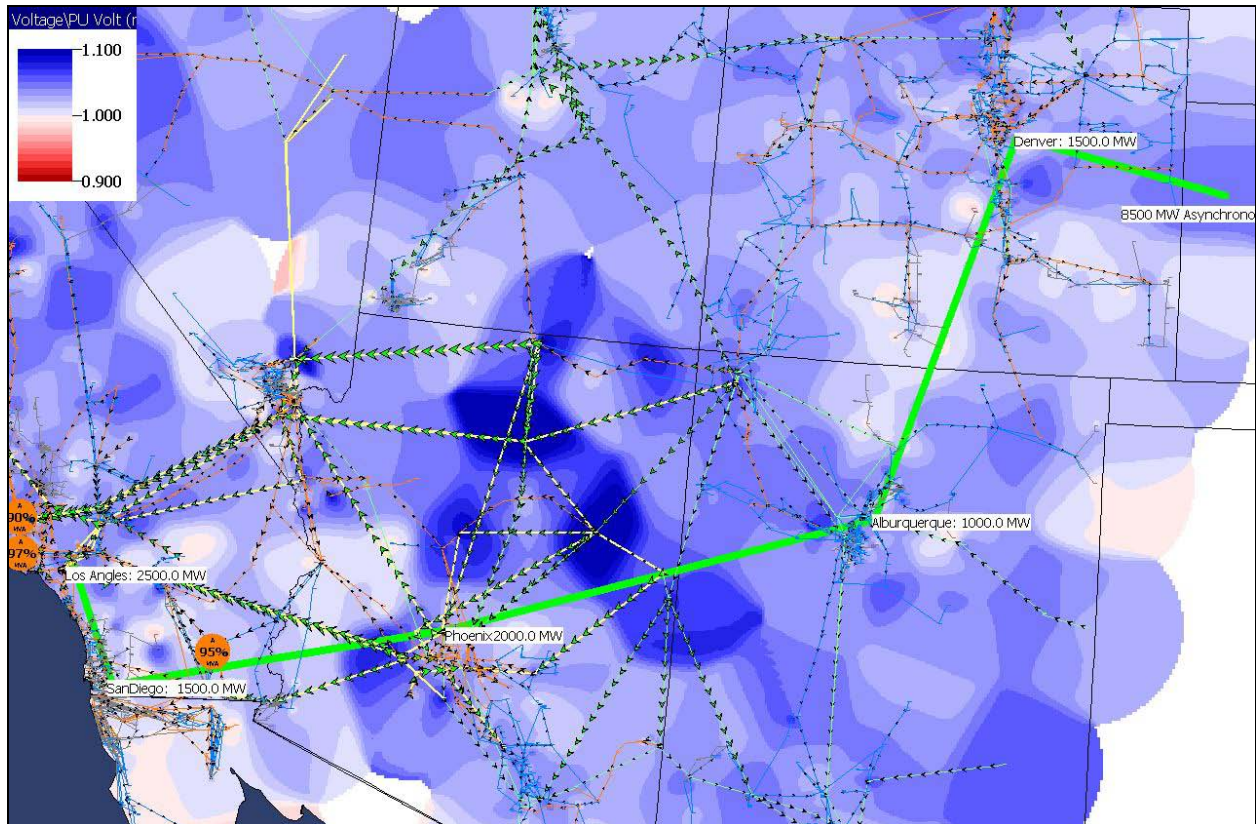


**Figure 4-2**  
WECC voltage contour and transmission flows with superconducting dc cable system

## Transient Stability Results – Frequency Response

The transient stability scenarios studied for the WECC system were the same as for the Eastern Interconnect. And the same mixed load model was used (i.e., 15% large motors, 45% small motors, 20% discharge lighting and the remainder as constant current for the real power and constant impedance for the reactive power).

Starting with the worst credible contingency in which one cable is lost and no power is transferred to the unfaulted cable, Figure 4-3 plots the individual frequencies at all of the generators, while Figure 4-4 highlights the frequencies at ten large generators. Since for this scenario there is 4.25 GW of lost generation, the final frequency does not return to 60 Hz. Rather it settles to a value of about 59.49 Hz, a value that is quite close to the frequency response reported in [8] and still 0.3 Hz above the 59.1 WECC load shed threshold.

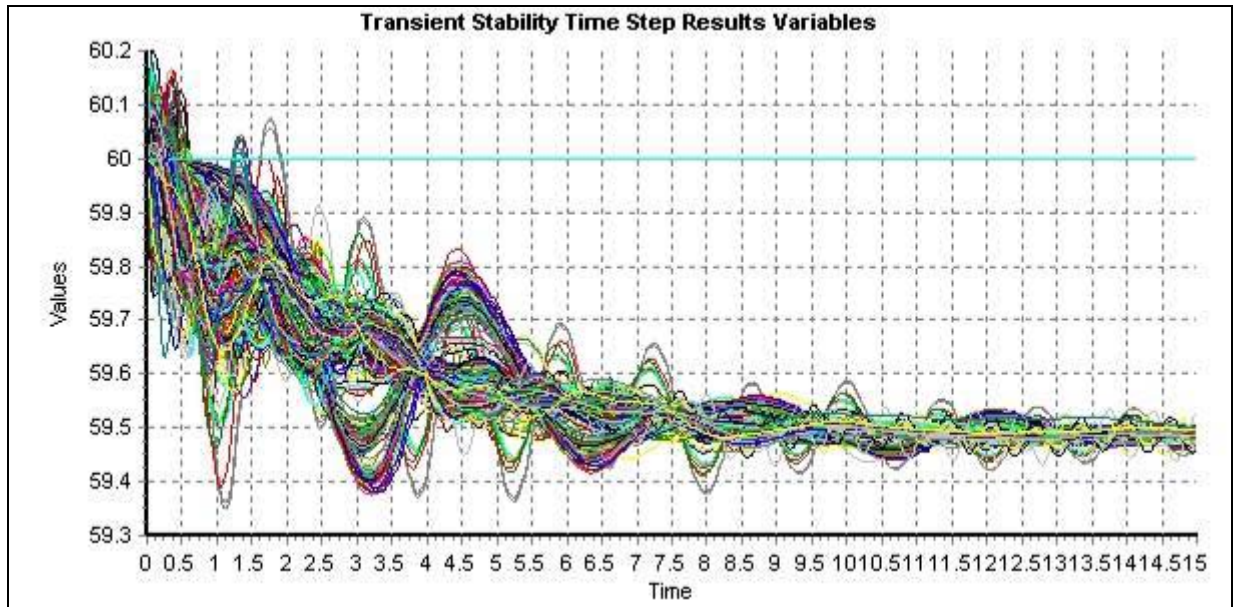


**Figure 4-3**  
Frequency response for all generators with no ramping

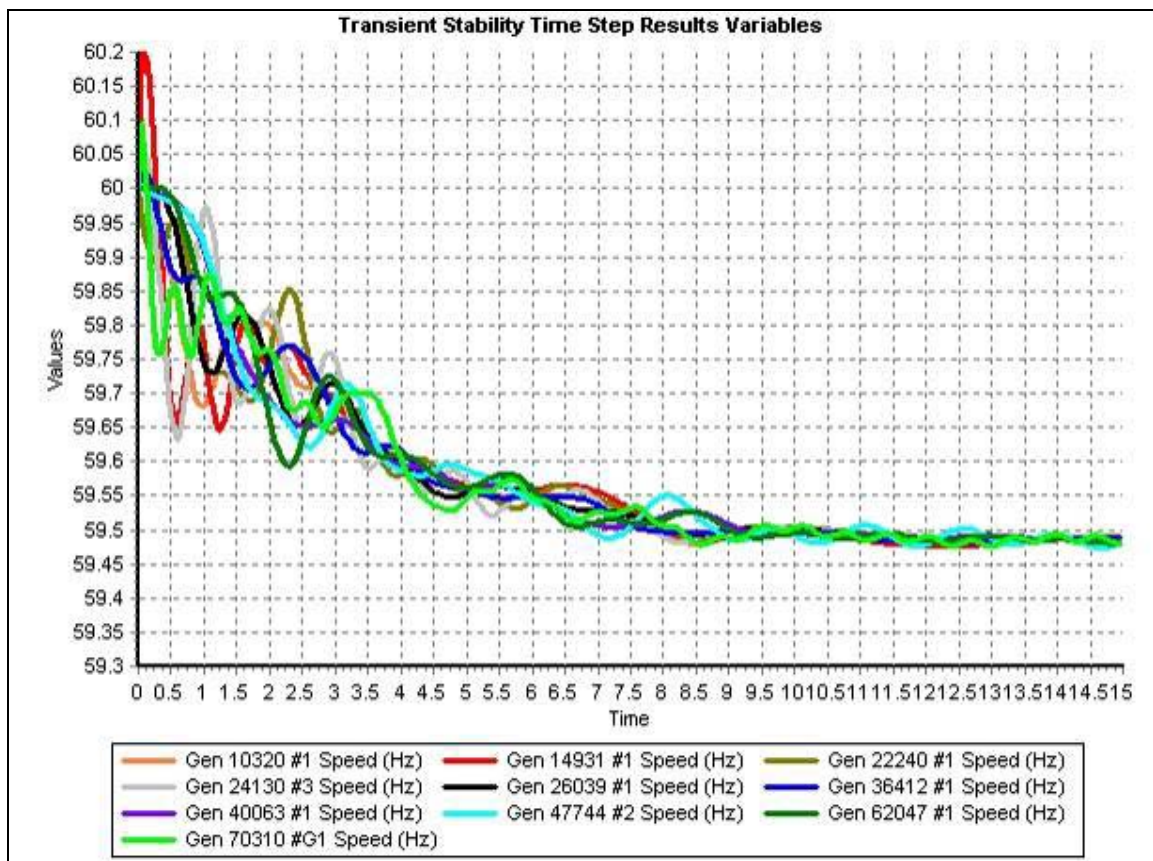


**Figure 4-4**  
Frequency response for ten large generators with no ramping

The next eight figures show how the frequency response changes as the power is ramped up on the unfaulted cable over ten seconds (Figure 4-5 and Figure 4-6), over five seconds (Figure 4-7 and Figure 4-8), over three seconds (Figure 4-9 and Figure 4-10) and over one second (Figure 4-11 and Figure 4-12). The conclusion from these scenarios is that from a system frequency point of view the failure of one cable without any power transfer should be a manageable contingency. However, since the frequency drop is relatively severe (down to about 59.5 Hz), ramping of the power onto the other cable is certainly preferable, and 8.5 GW would be a reasonable upper limit for the superconducting dc system size.

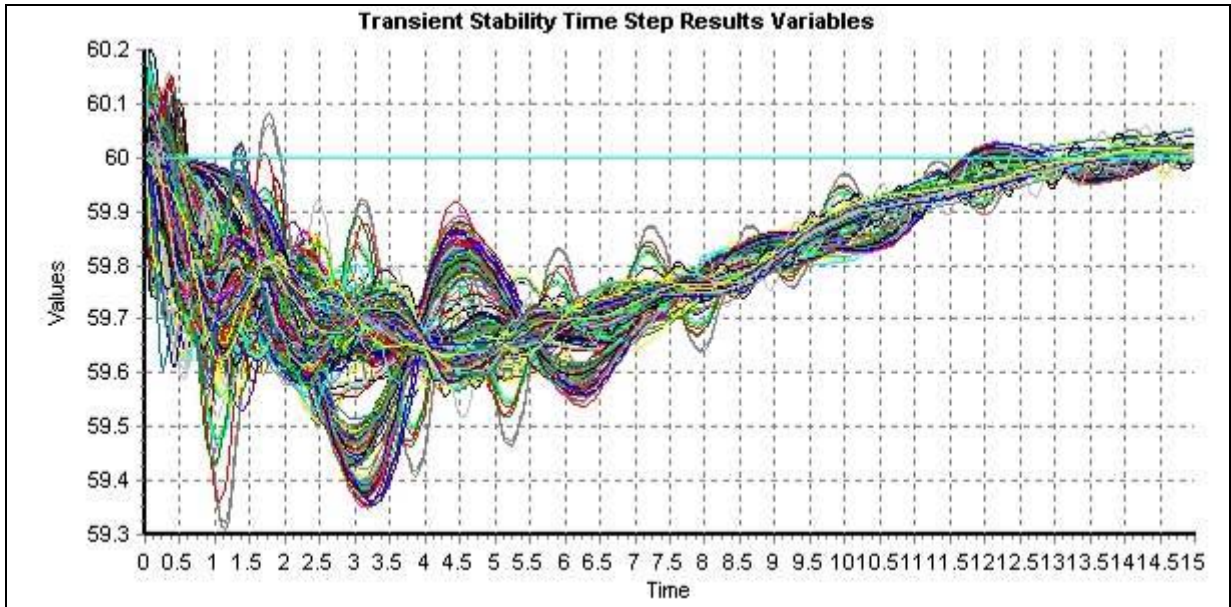


**Figure 4-5**  
Frequency response for all generators with ten second ramping

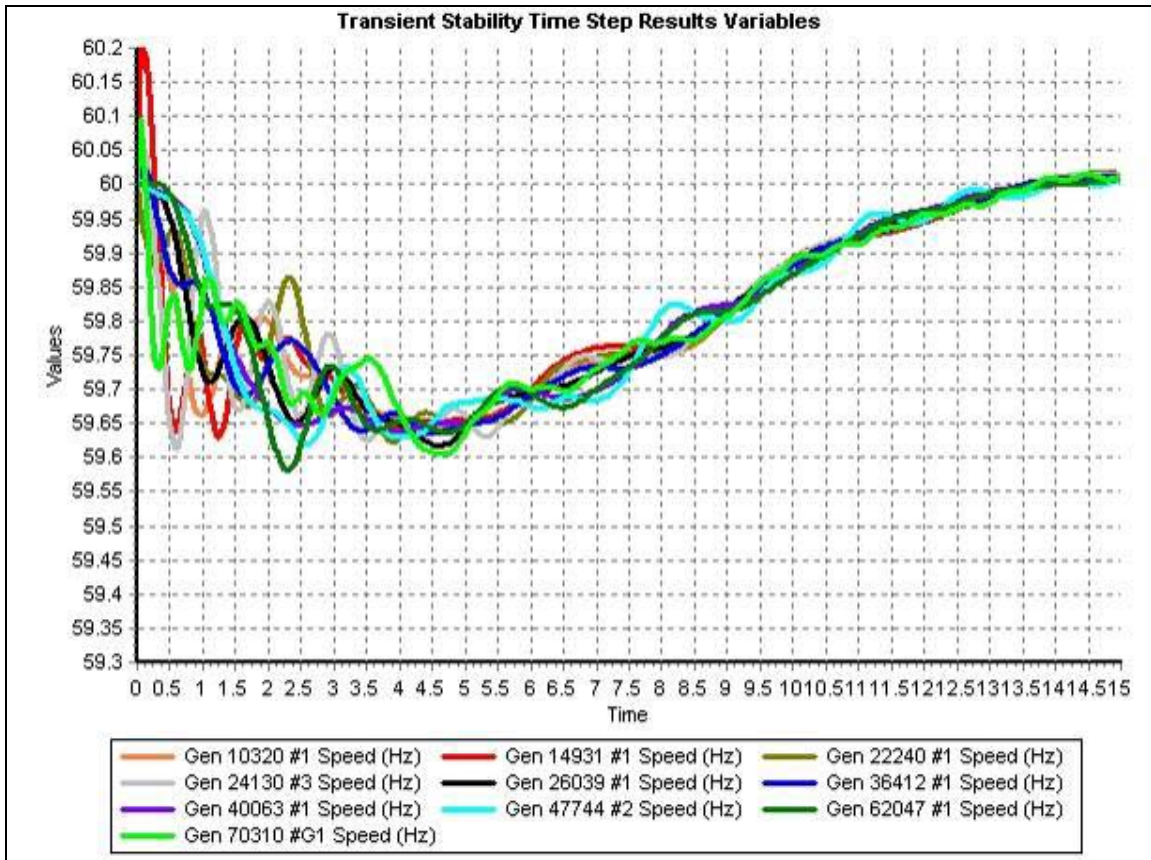


**Figure 4-6**  
Frequency response for ten large generators with ten second ramping

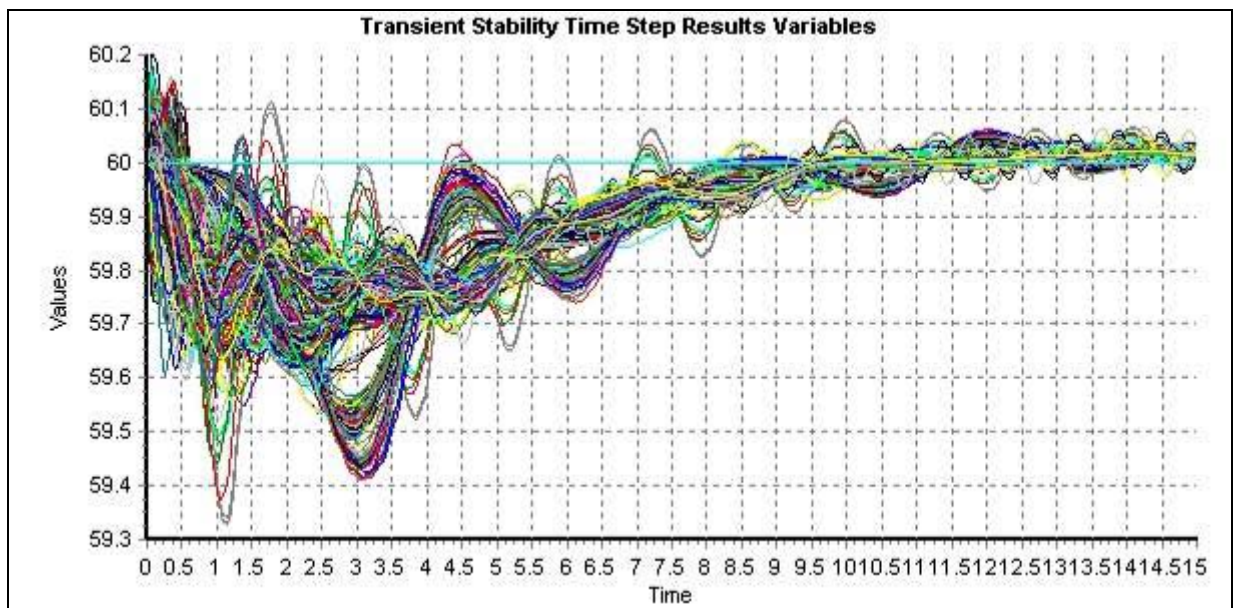


**Figure 4-7**  
Frequency response for all generators with five second ramping

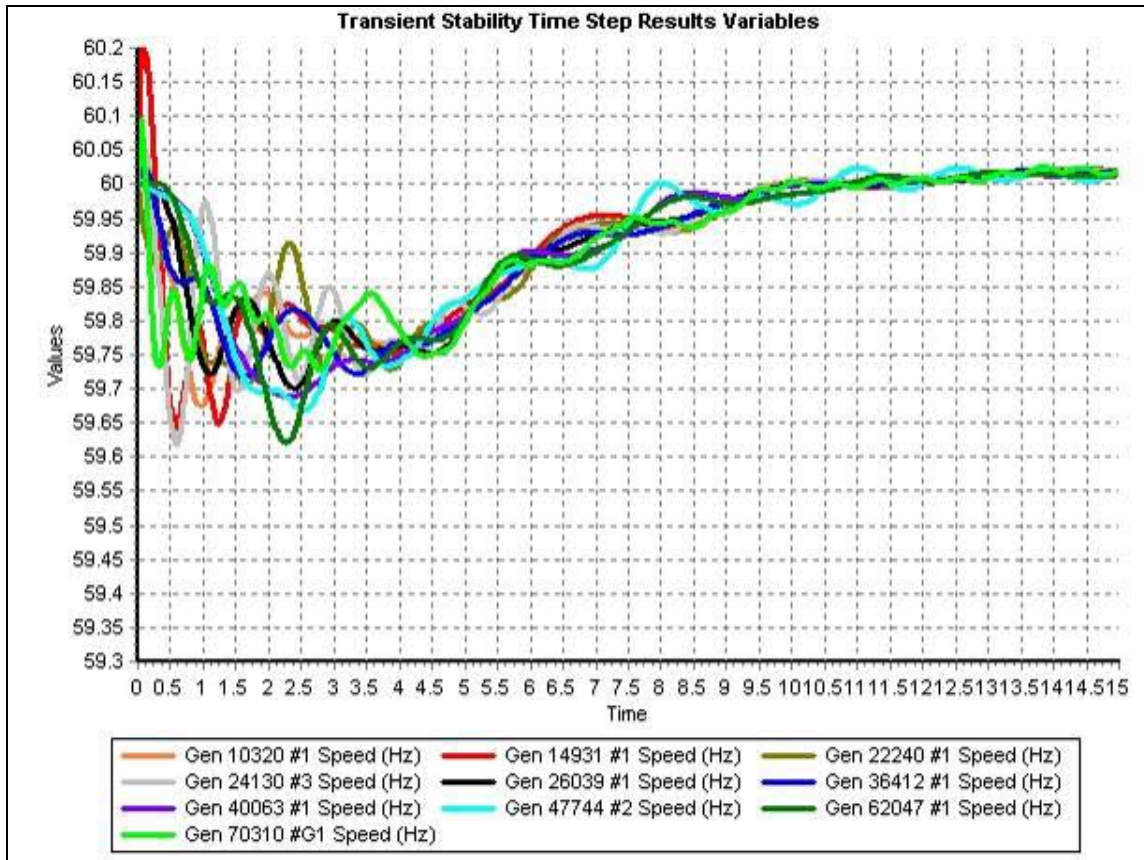


**Figure 4-8**  
Frequency response for ten large generators with five second ramping

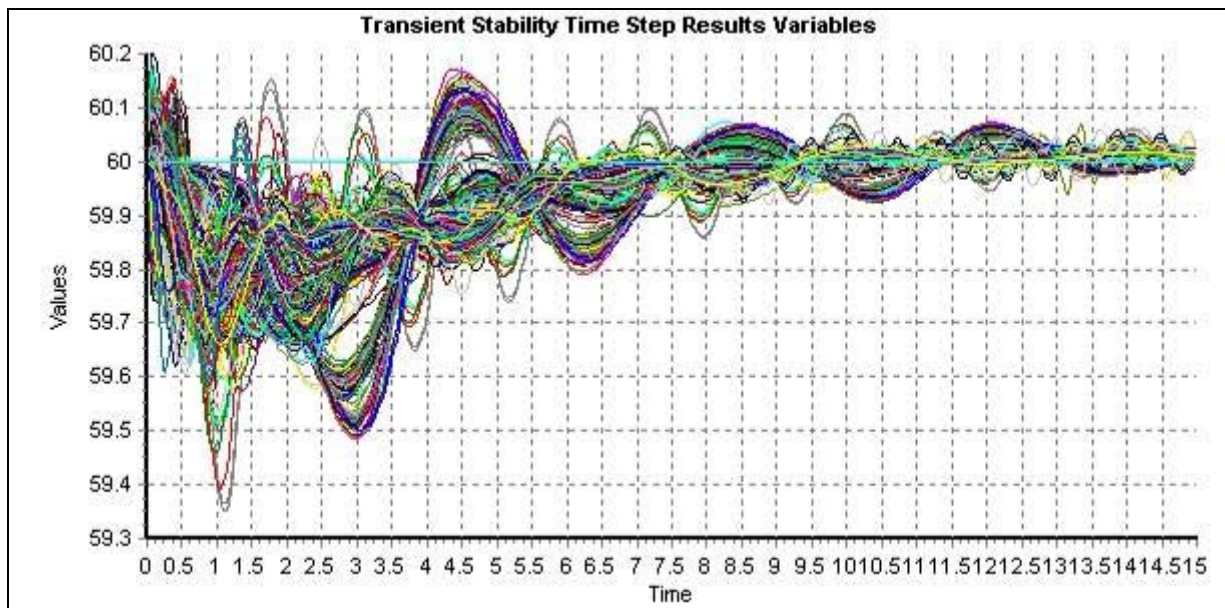


**Figure 4-9**  
Frequency response for all generators with three second ramping

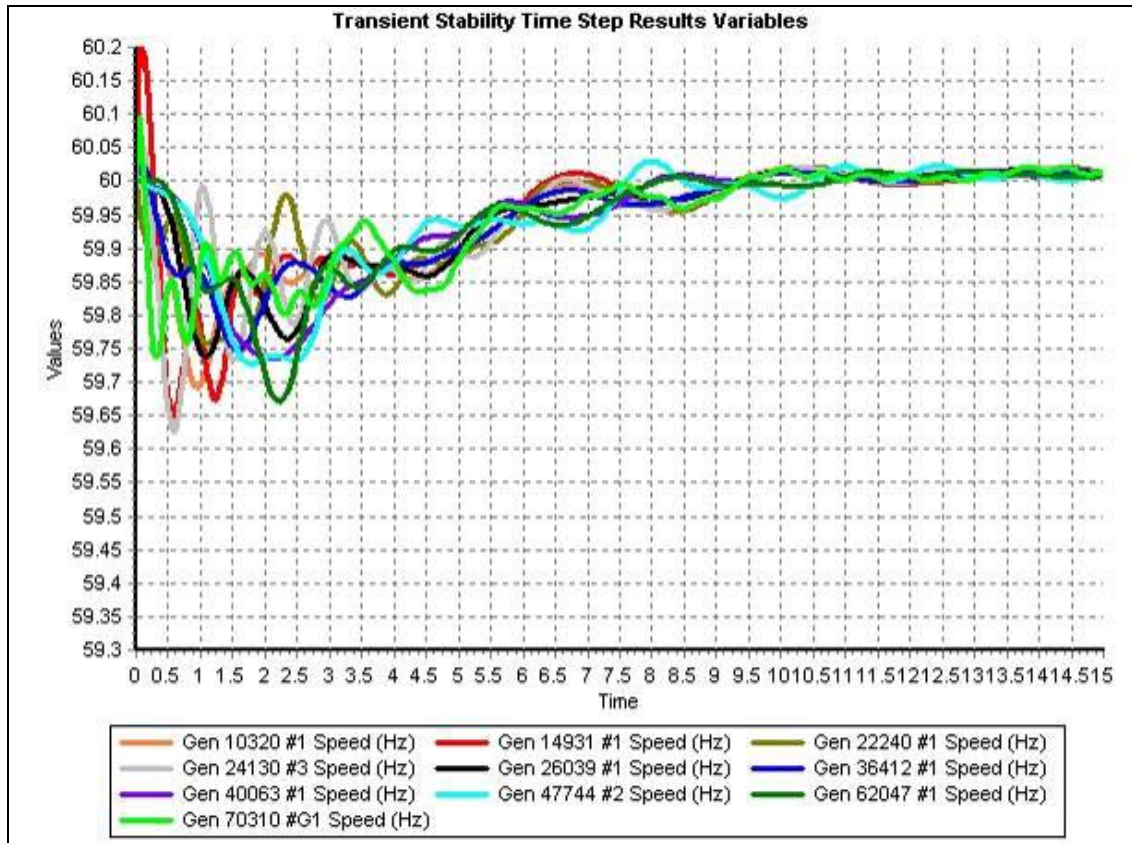


**Figure 4-10**  
Frequency response for ten large generators with three second ramping

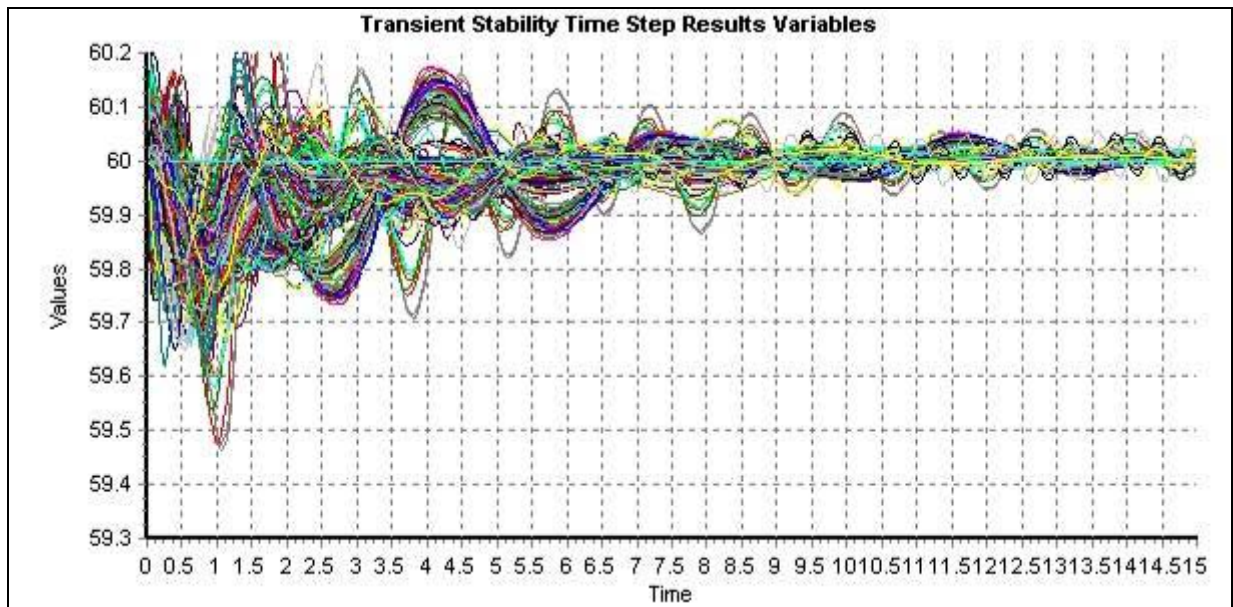


**Figure 4-11**  
Frequency response for all generators with one second ramping

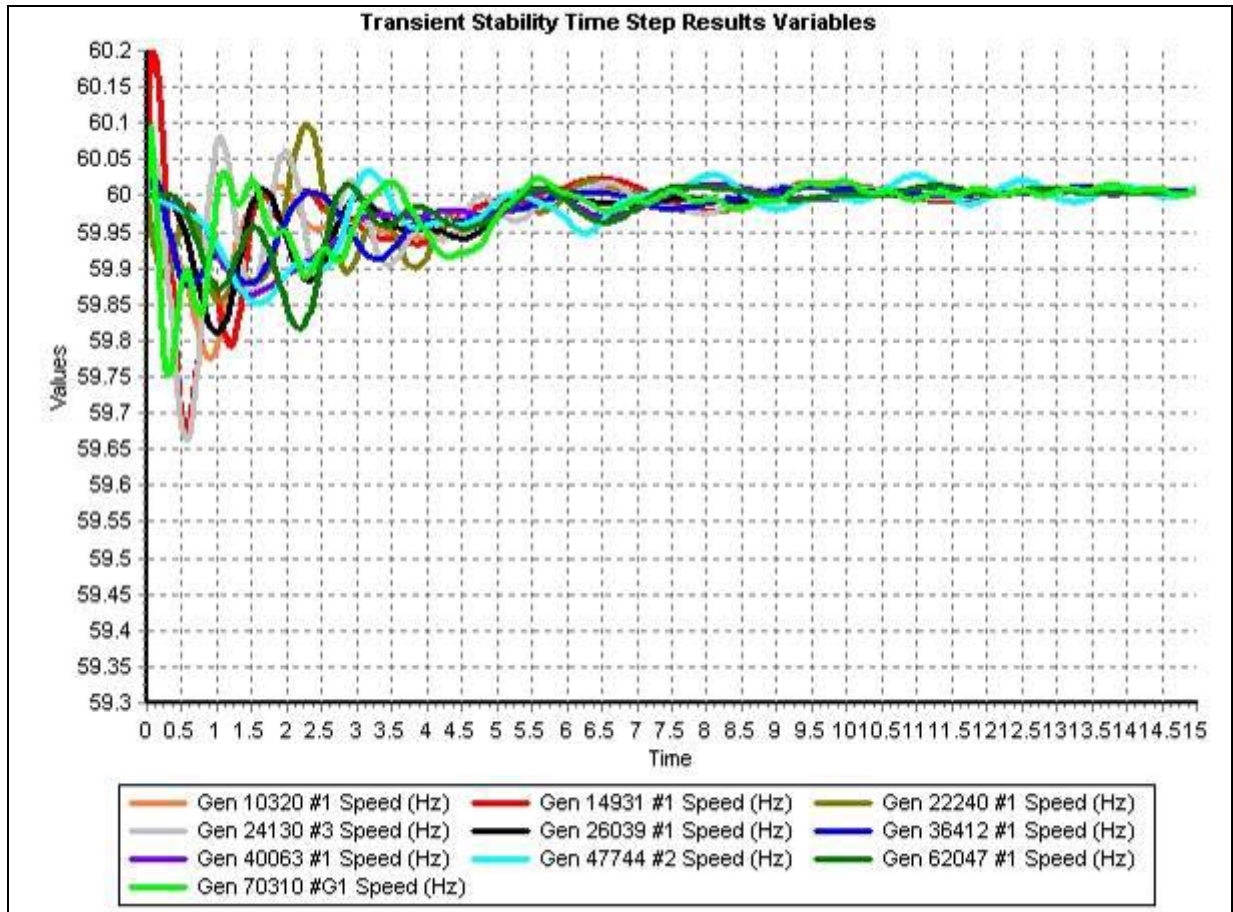


**Figure 4-12**  
Frequency response for ten large generators with one second ramping

### Transient Stability Results – Voltage Response

The short-term voltage issues seem to be more of a concern for the WECC system than was the case for the Eastern Interconnect. This is illustrated in the following five figures that show a contour of the southern WECC voltages for the no ramping scenario at the pre-fault time (Figure 4-13), 0.1 seconds after the fault (Figure 4-14 [0.05 seconds after the fault has cleared]), 0.5 seconds after the fault (Figure 4-15), 1.0 seconds after the fault (Figure 4-16) and 2.0 seconds after the fault. While practically all of the voltages eventually recover following the fault, their recovery is somewhat slower than for the Eastern Interconnect. Also, not all of the voltages recover, with the small induction motors stalling at a few buses.

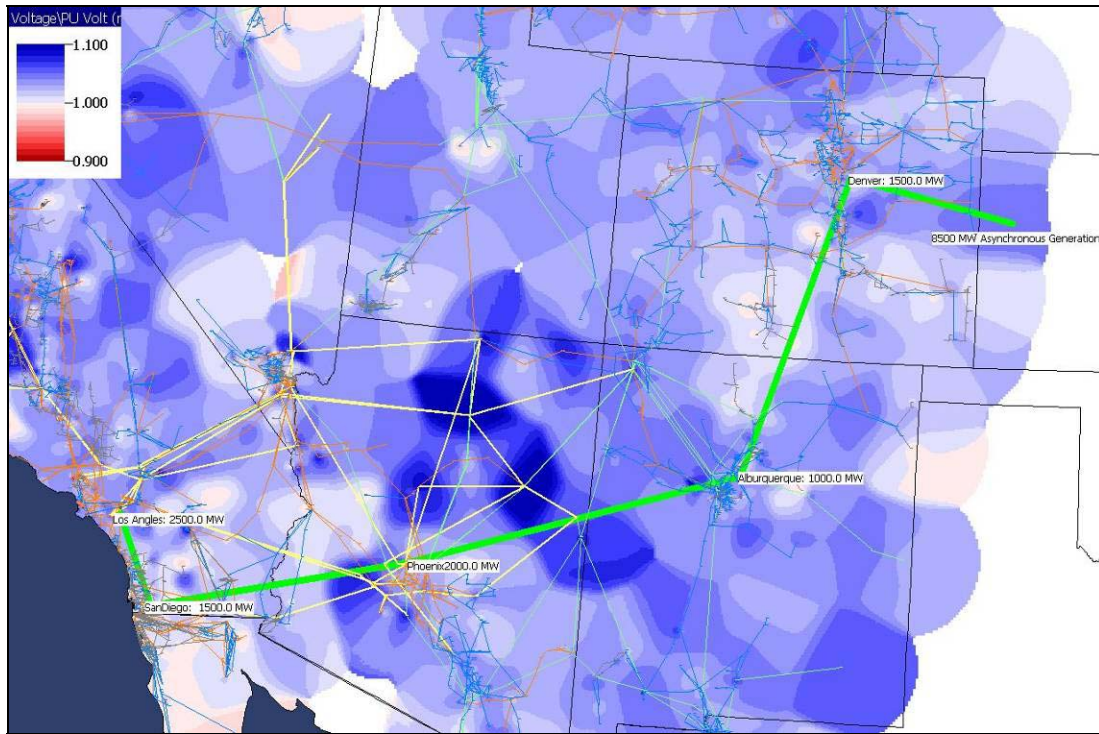


**Figure 4-13**  
**WECC case pre-fault substation PU voltage contour**

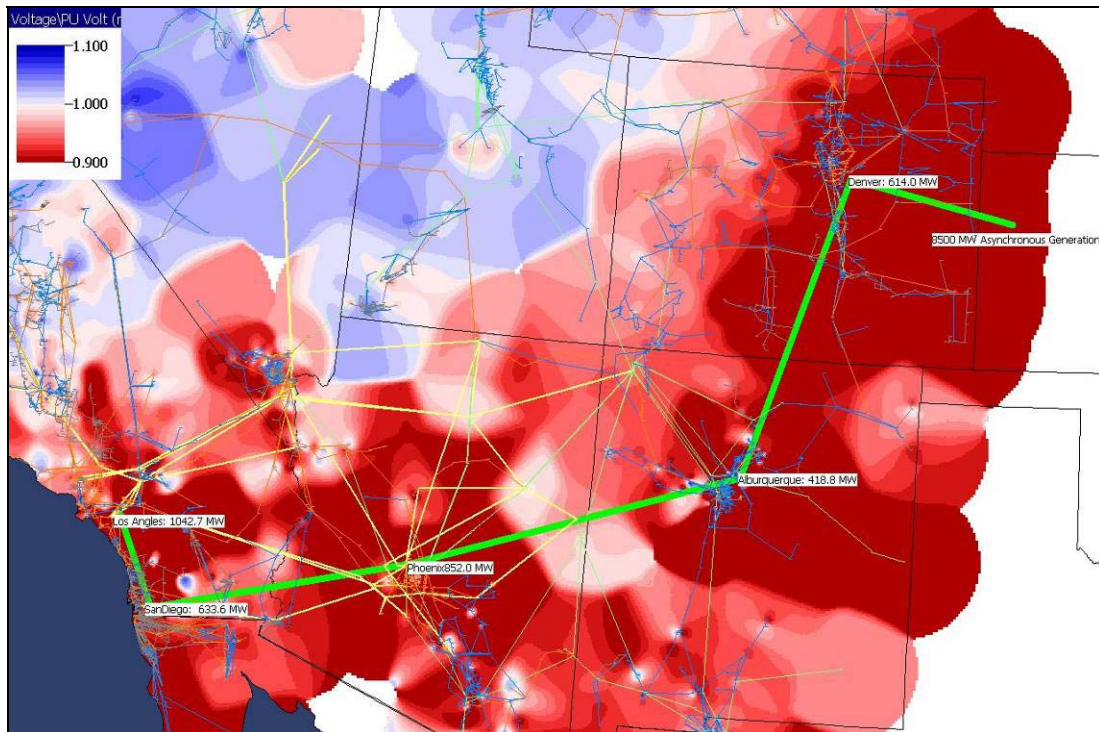


**Figure 4-14**  
**WECC no ramp case at 0.1 seconds**

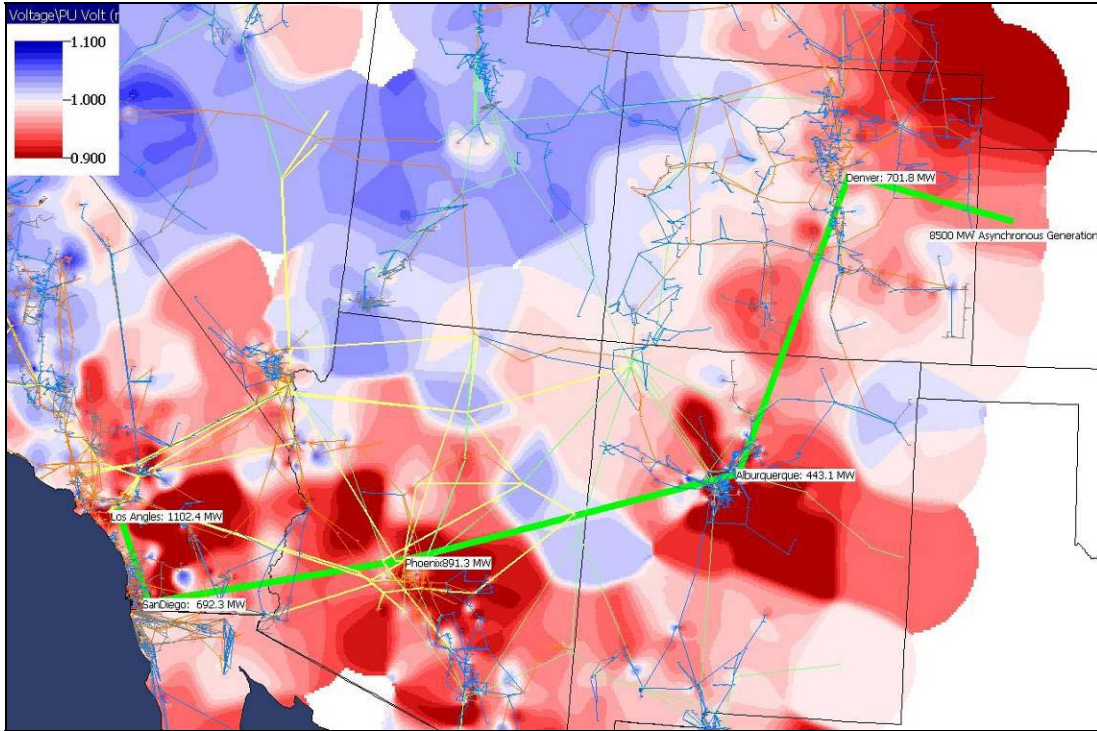


**Figure 4-15**  
**WECC no ramp case at 0.5 seconds**

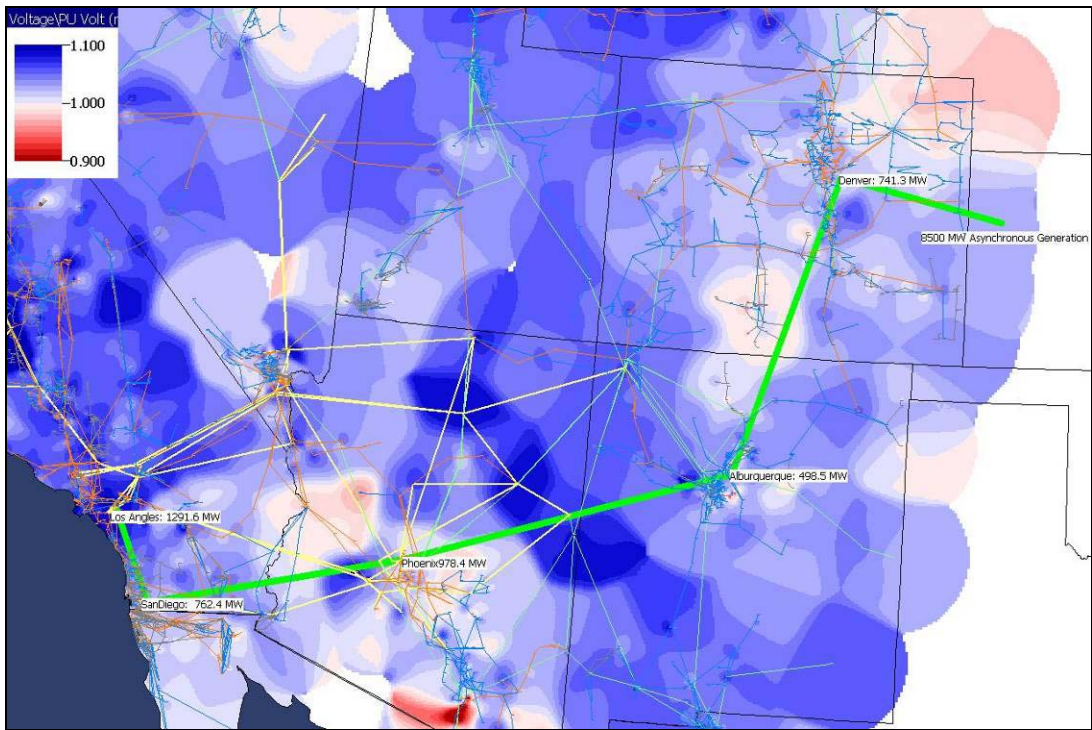


**Figure 4-16**  
**WECC no ramp case at 1.0 seconds**

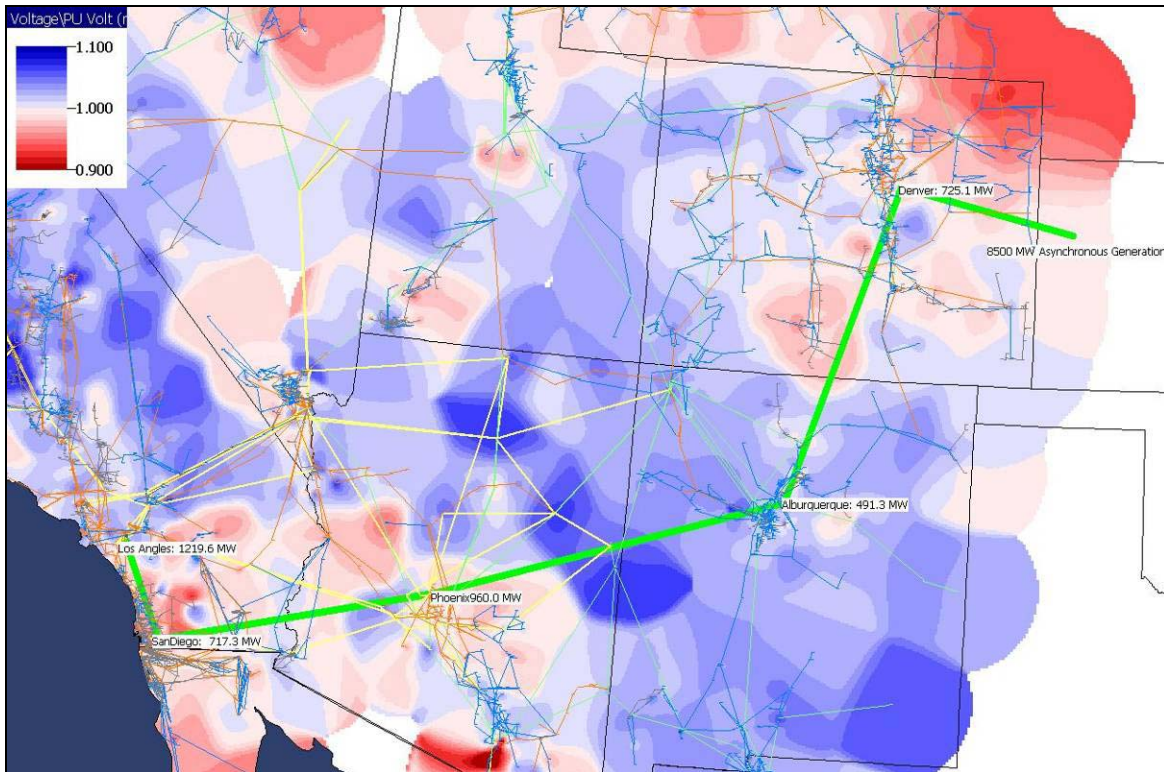


**Figure 4-17**  
**WECC no ramp case at 2.0 seconds**

The time variation in the voltage response at selected load buses and large generator buses for the no ramp case is shown in Figure 4-18. The effect of the small induction motors stalling is seen at bus 16710 in which the voltage does not recover for the duration of the simulation. However it should be noted that 16710 is a 13.2 kV bus with a relatively small load (less than 20 MW); whether its stalling is significant is not known. The bus with the second worst voltage behavior in the figure is a 66 kV bus in British Columbia. While its voltage has some oscillations it does recover. The remaining buses are for large generators, all of which eventually recover and actually would satisfy the proposed WECC standard from [7] that requires that all generators stay connected as long as their voltage stays at zero for no more than 15 cycles (0.15 seconds), and then rises linearly to 0.9 per unit in 1.75 seconds. Figure 4-19 duplicates the results from Figure 4-18 except for the case in which the power is ramped on the unfaulted cable over three seconds. While this ramping improves the overall voltage response it does not prevent the motor stall at bus 16710.

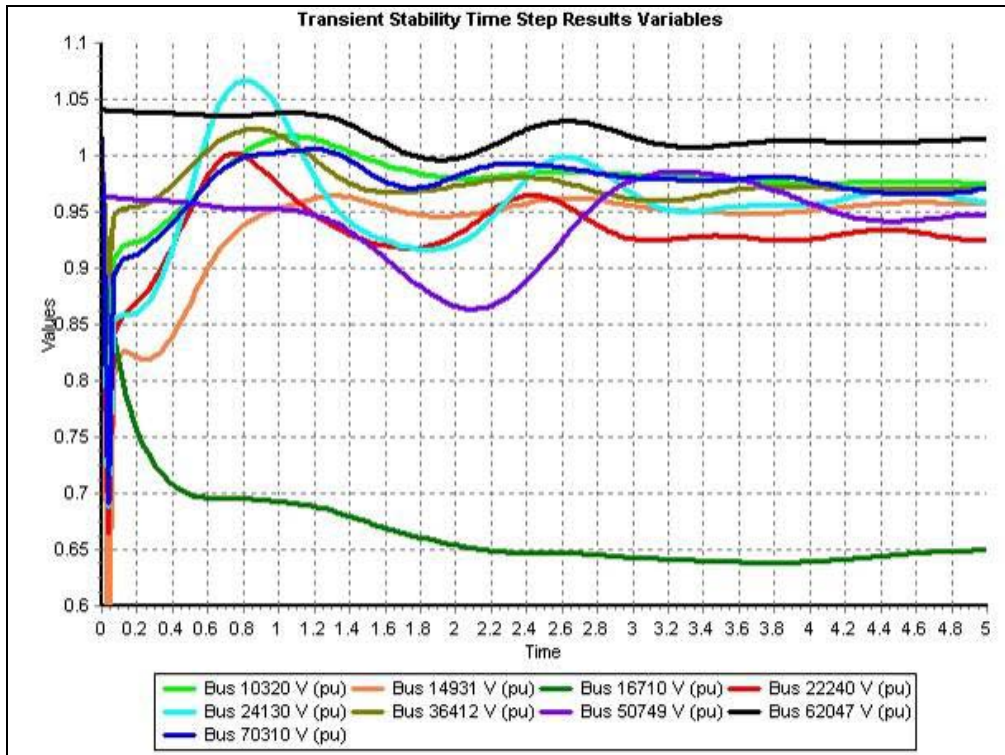


**Figure 4-18**  
Voltage response at selected buses for no ramp case for the first five seconds

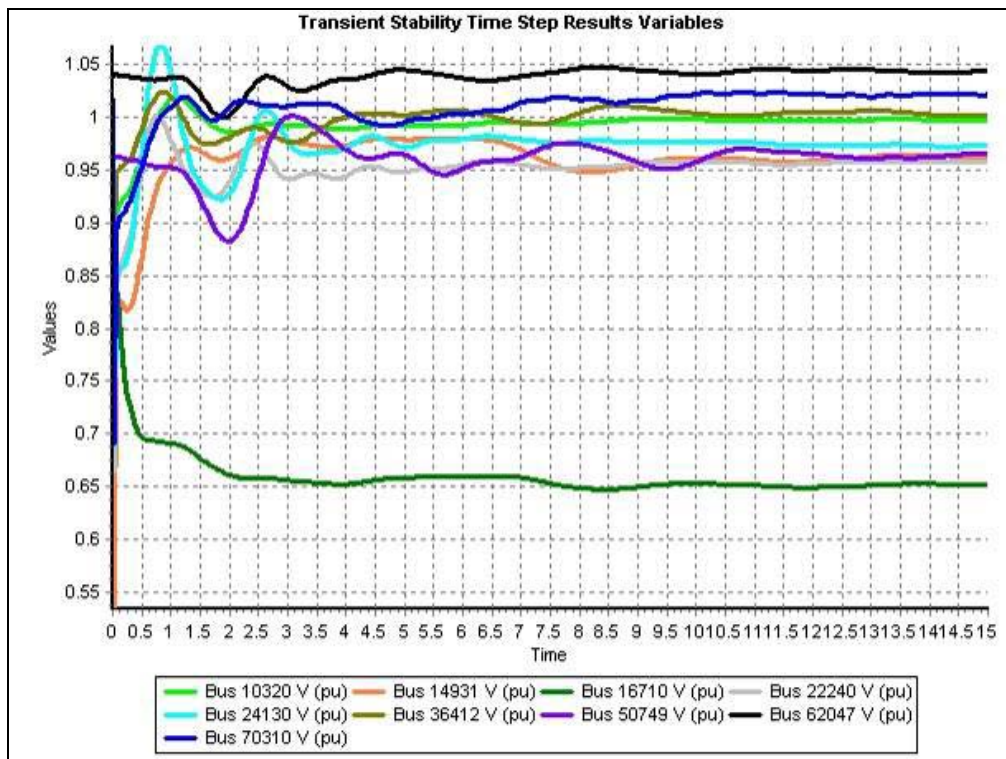


**Figure 4-19**  
**Voltage response at selected buses for no ramp case for the first fifteen seconds**

The conclusion for the WECC system is that from this preliminary study a 8.5 GW superconducting dc cable system could be integrated into the existing grid. The overall decline in frequency in the event of a single cable failure would be on the order of 0.5 Hz, a value still above the load shed frequency. The effect of a cable failure on the system voltage profile would be significant, at least for the first second or two, but almost all the system voltages recover sufficiently fast to meet the proposed WECC requirements, with voltage recovery improving if the power from the faulted cable can be ramped on to the unfaulted one quickly. Motors at several small buses did stall in all scenarios. Whether this stalling is significant, and if so what mitigation measures would be needed, has not been determined.

# 5

## CONSIDERATIONS ON THE OPERATION OF SUPERCONDUCTING DC CABLES FED BY MULTIPLE VOLTAGE SOURCE CONVERTERS

---

While high voltage dc (HVDC) transmission using current sourced converters has been in use for over 50 years, voltage sourced converter based HVDC transmission has only started coming into use in the last ten years. These systems are based on a modular design, thereby reducing the installation time. An EPRI Report [9] presented an excellent proposal and explanation of the issues associated with the converter stations for a possible superconducting dc cable system. In particular, converter topology and design, within the ratings and conditions of the cable system, is discussed. But the report also correctly points to several aspects which need to be more fully addressed, such as:

- Study of ac system performance with multiple voltage source converter infeeds to a major metropolitan area
- Optimization of the converter size
- Study of potential interactions between converters in close proximity to each other
- Voltage control of the dc cable and strategies dealing with loss of rectifiers and inverters
- Overall reliability assessment of the transmissions system, including identification of critical failure modes and their impact on the ac system.

### **Voltage Source Converter Superconducting DC Cable Topology**

Figure 5-1 shows the basic topology proposed. However, the assumption of decoupling or low transient interaction between converters of very large ratings such as the ones proposed for this project need to be thoroughly investigated as they are connected to the same ac node as illustrated in Figure 5-2. The general configuration of the multiple terminal voltage source converter for one cable is illustrated in Figure 5-3.

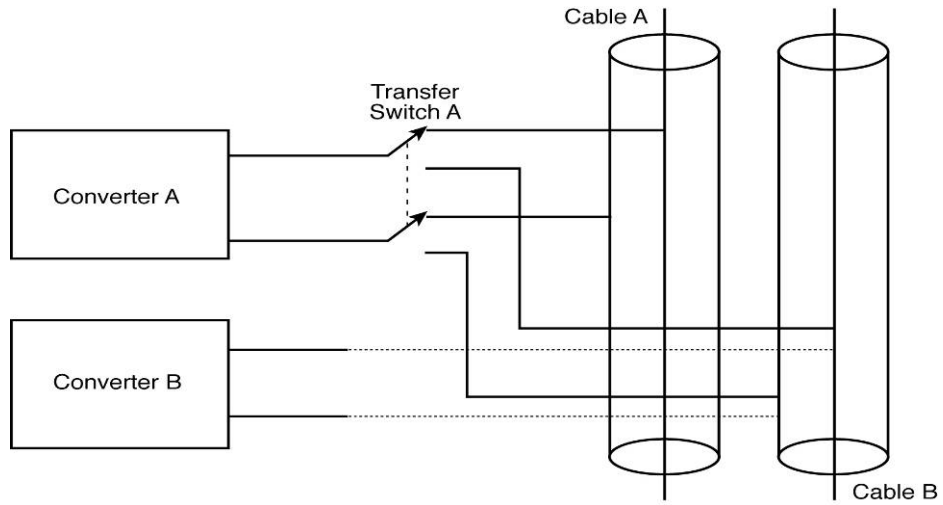


**Figure 5-1**  
Switching arrangement to transfer Converter A from a failed to a healthy cable; similar switches are required on Converter B

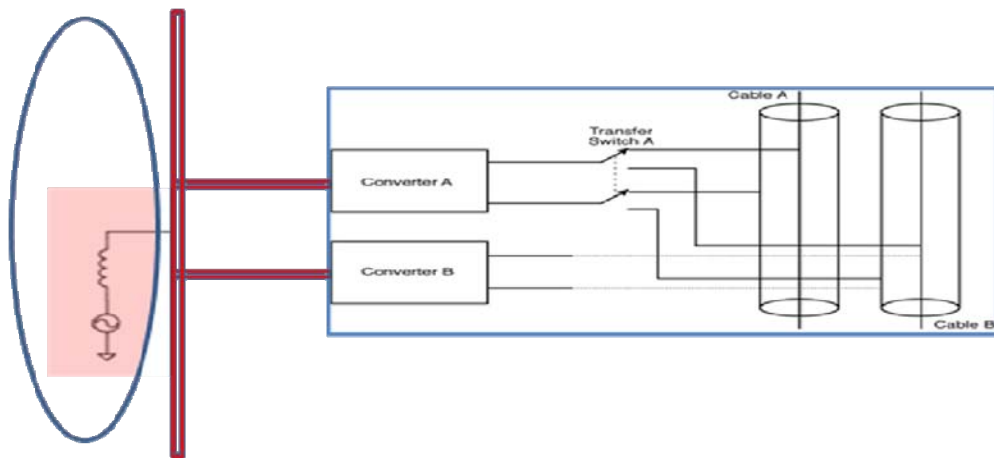


**Figure 5-2**  
Converters are connected at the same substation point and transients caused by switching of cables need to be investigated in detail

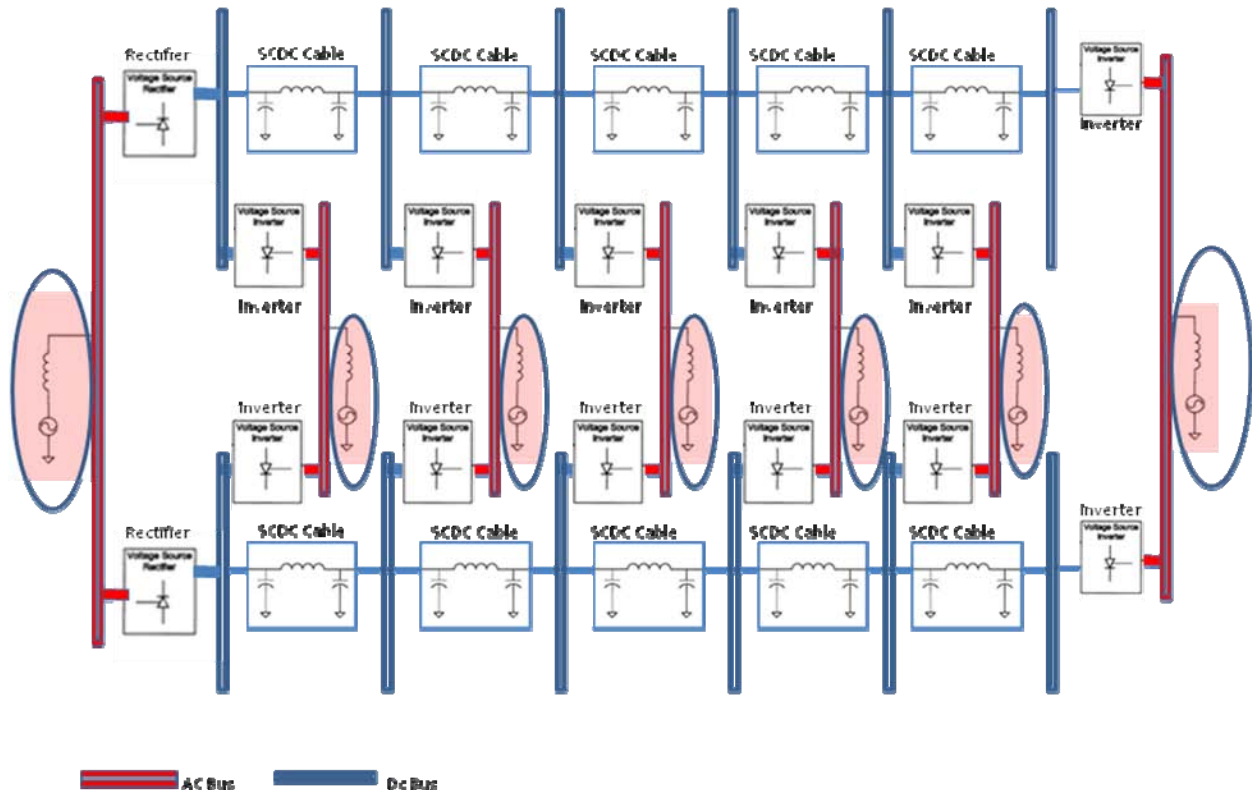


**Figure 5-3**  
**Superconducting DC general topology**

### Multi-Terminal Voltage Source Converter Design Issues

A distributed voltage control system strategy based on voltage droop for the converters acting as rectifiers (to automatically adjust the power flows based on small changes in the dc voltage) as proposed in [9] would work for a superconducting system with a mesh connected or parallel system, since all of the terminals will have the same steady-state dc voltage. However, more detailed modeling of a truly multi-terminal system with the power and current levels proposed for the superconducting dc system must be developed. Converter controls will be an issue for multi-terminal systems when converters hit their limits. Existing HVDC systems have one converter acting as the master voltage controller (for the parallel system) or the master current controller (for the series system), but they struggle with handling converter limits and get into complicated modes of operation and mode switching. A summary of issues for multi-terminal voltage source converter systems with superconducting dc cables is found in [10].

Transients that appear during faults on the dc cable must be investigated. Damping with active and passive filters on the dc side and by converter controls as pulse-width modulated (PWM) voltage source converters can be efficiently used in such situations. Active filters and transient damping issues are further discussed in [9] and [11]. An example of the use of active filters in PSCAD® modeling studies of a superconducting dc cable is presented in [11].

Multi-terminal HVDC systems have not been commonly used to date, due to the cost of the additional converter stations, complexity of the control system, and the need for dc circuit breakers, etc. However, recently the manufacturers for HVDC using voltage source converters have marketed their systems as working well for mesh connected multi-terminal systems.

A key challenge is the possible need for a dc circuit breaker and the voltage source converter control issues. BPA tested HVDC breakers on the Pacific Intertie in the late 80's and it can be done, but probably not with present technologies for the current levels discussed for the presently conceived superconducting dc cable system. See [11] for additional discussion of the need for dc circuit breakers.

## **Ramp Rate Limits for Long Cables**

A proper voltage profile is maintained at the converter with voltage control. The voltage at a converter with current control sags and swells due to the inductance of the superconducting dc cable. The propagation delay and mismatch between the cable's characteristic impedance and the converter's impedance, results in a decaying oscillation. The ramp rate of the current affects the magnitudes of the voltage sags, swells, and ringing. See Table 5-1 below.

**Table 5-1**  
**Sags for the 2000-mile superconducting DC cable**

<b>Case</b>	<b>Peak <math>I_{dc}</math> Ramp Rate</b>	<b>Greatest <math>V_{dc}</math> Sag</b>	<b>Average <math>V_{dc}</math> Sag</b>
Run #1	1 kA/s	-0.38% (79.7 kV)	-0.19% (79.85 kV)
Run #2	2 kA/s	-0.88% (79.3 kV)	-0.44% (79.65 kV)
Run #3	5 kA/s	-2.75% (77.8 kV)	-1.38% (78.90 kV)
Run #4	10 kA/s	-5.50% (75.6 kV)	-2.75% (77.80 kV)
Run #5	20 kA/s	-11.0% (71.2 kV)	-5.50% (75.60 kV)

## **Impact of Cable Length**

Figure 5-4 through Figure 5-6 show the dc voltage ripple for different cable lengths. The simulation parameters considered were: 80 kV, 10 kA, two-terminal superconducting dc cable, current control terminal: 2 kA / sec ramp rate.

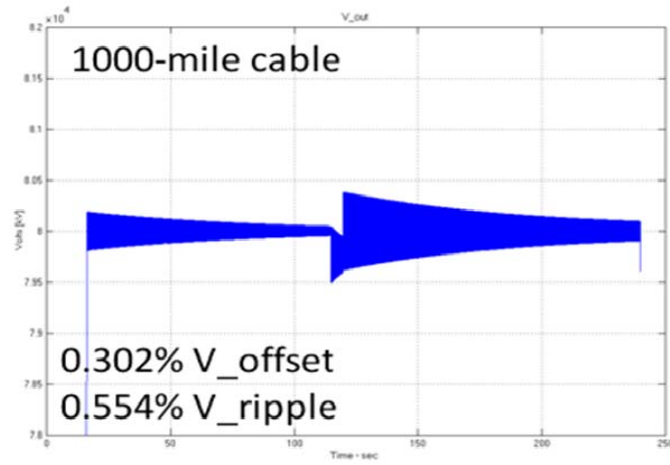


**Figure 5-4**  
1000-mile cable voltage ripple

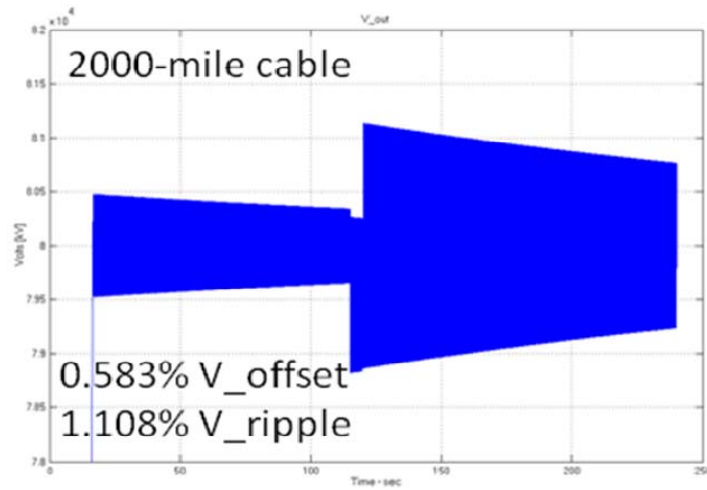


**Figure 5-5**  
2000-mile cable voltage ripple

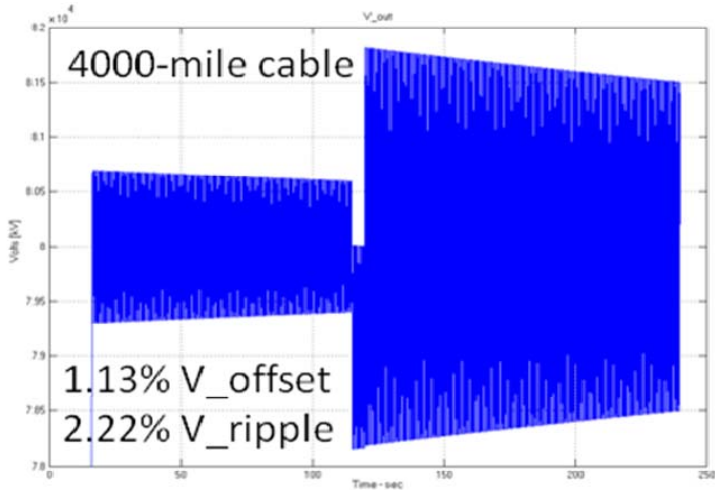


**Figure 5-6**  
4000-mile cable voltage ripple

# 6

## ELECTROMAGNETIC TRANSIENT STUDIES FOR A SUPERCONDUCTING DC CABLE SYSTEM

For this project a multi-tap superconducting dc cable system was assumed capable of carrying up to 10 GW over a distant of up to about 1000 miles. In order to achieve good reliability the system was assumed to be completely redundant, including two parallel cables each capable of carrying the entire loading.

Simplified models of two and three voltage source converters (one operating as a rectifier and the others as inverters) connected by a dc cable and fed by two separate ac systems were modeled to study the interaction and dynamics of the system as discussed in the previous section. The resistivity of the dc cable was varied to investigate the impact of a superconducting cable on system-to-system events and faults. Figure 6-1 shows the basic topology of the two voltage source converter system as implemented in PSCAD® Version 4.2.0 Educational. In order to provide a baseline, a typical HVDC plus conventional cable system was simulated. This was followed by simulations in which the conventional cable is replaced by the superconducting cable.

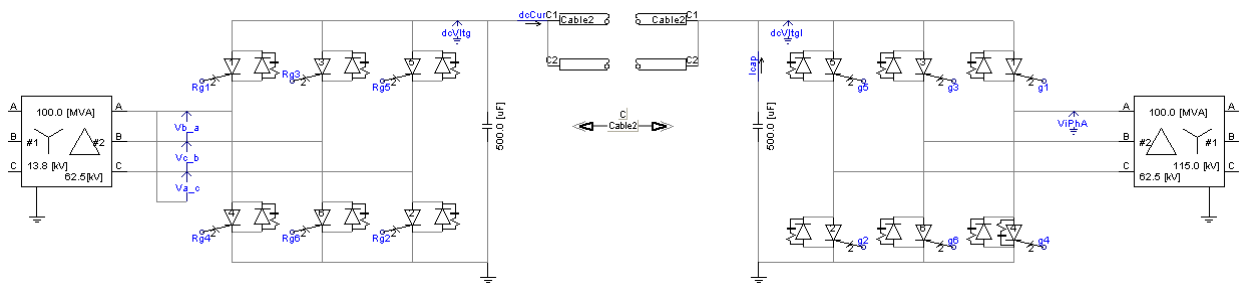


**Figure 6-1**  
PSCAD® voltage source converter topology

### Typical HVDC System Results – Single Line-to-Ground Fault with Two Voltage Source Converters

The following figures show the electromagnetic transient study results for a typical HVDC transmission system with several different cable lengths. A single line-to-ground fault at the ac receiving end of the system was applied at 2.1 seconds in each case. These cases are included to demonstrate the stability of the proposed voltage source converter model, and provide a basis for comparison to the superconducting dc system results presented in subsequent sections. Figure 6-2, Figure 6-3, Figure 6-4, Figure 6-5, and Figure 6-6 show the PSCAD® simulation results for the 1000km HVDC transmission system case described above.

The results show that the system performs more than adequately as far as voltage control and dc current control are concerned. After the fault, ac and dc voltage at the receiving end recover quickly, while dc current transients appear to subside as well. The dc voltage set point is 118kV, a value that is accurately maintained by the system as shown in Figure 6-5.

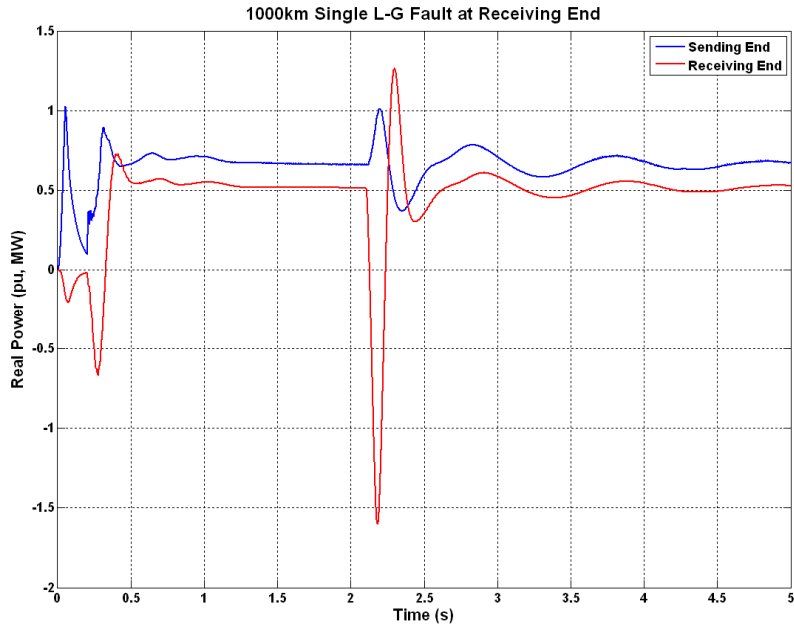


**Figure 6-2**  
1000km HVDC real power

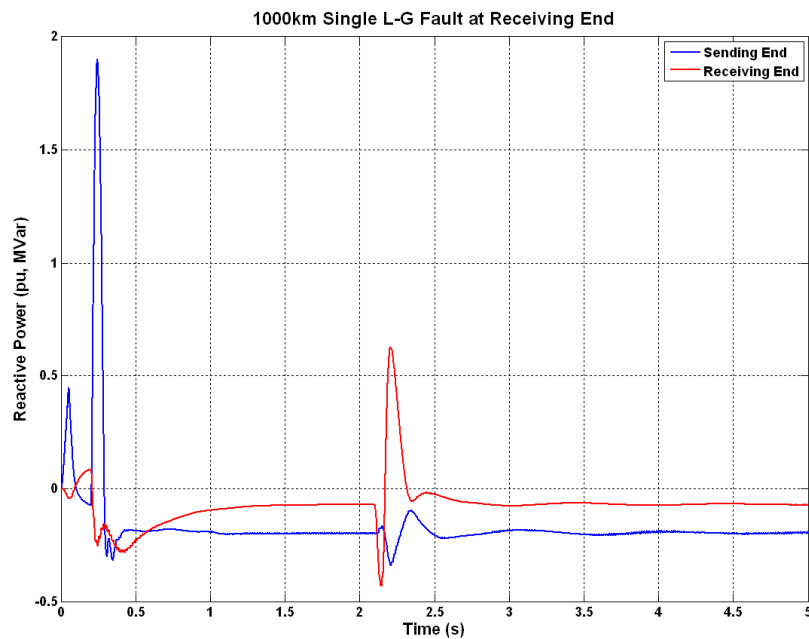


**Figure 6-3**  
1000km HVDC reactive power

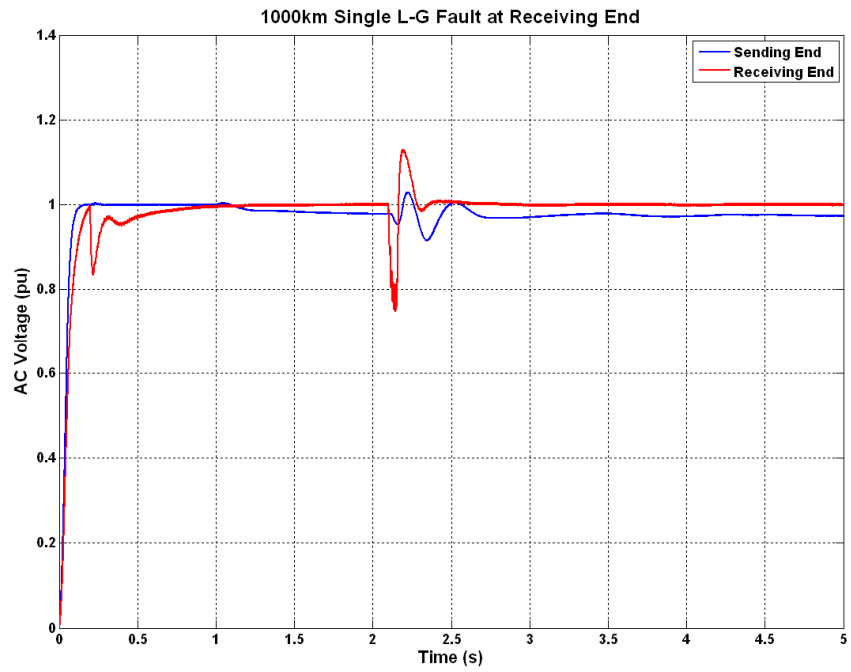


Figure 6-4  
1000km HVDC AC voltage

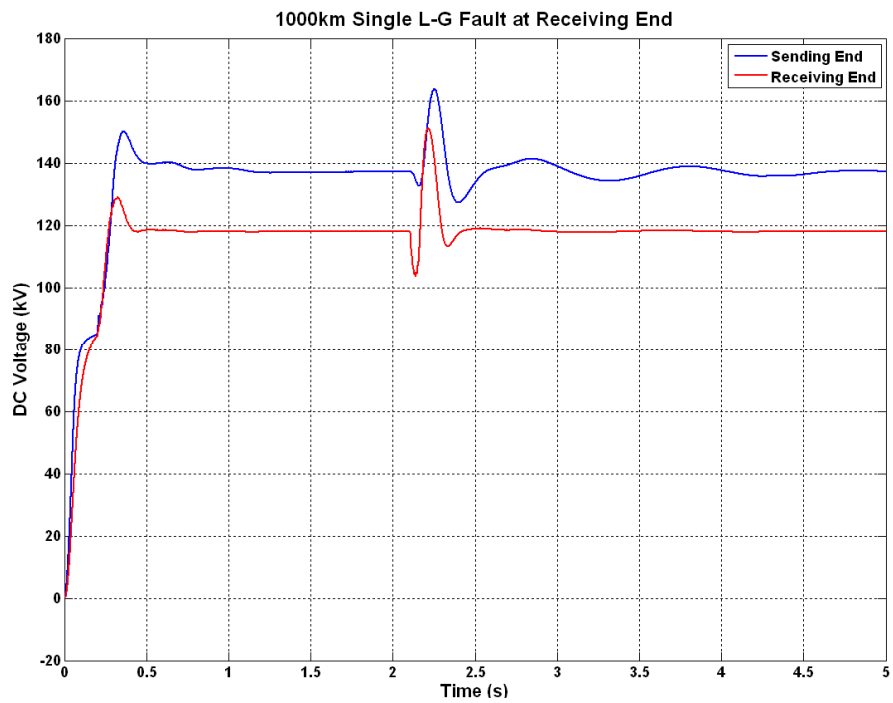
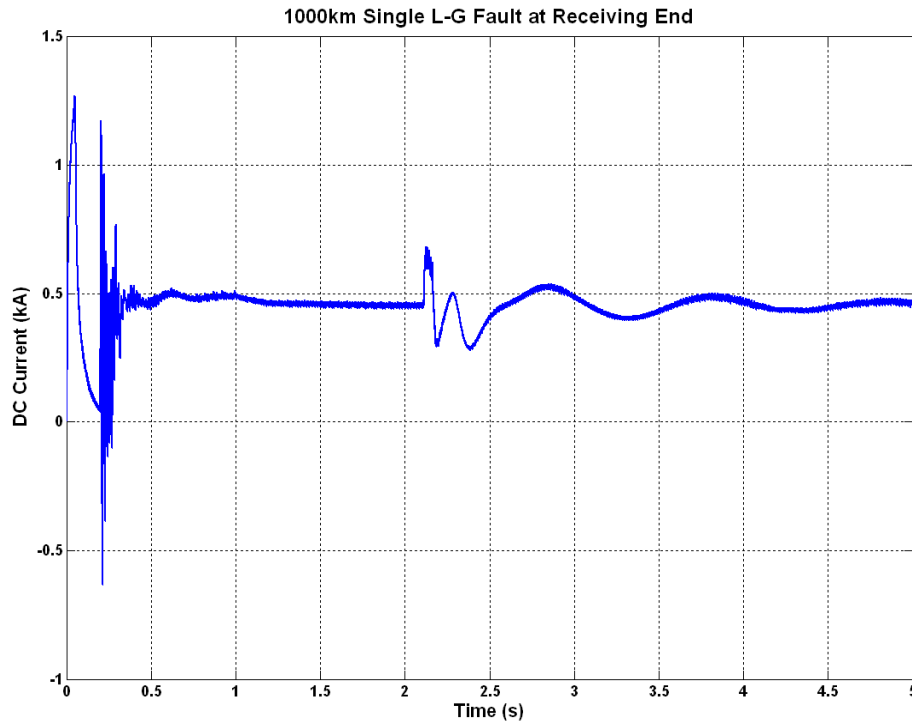


Figure 6-5  
1000km HVDC DC voltage



**Figure 6-6**  
**1000km HVDC DC current**

Figure 6-7, Figure 6-8, Figure 6-9, Figure 6-10, and Figure 6-11 show the results for a similar case with the HVDC cable length increased to 2000km. These plots reveal similar control successes following the receiving end fault. Receiving end ac and dc voltage recover quickly, while dc voltage at the receiving end is maintained at 118kV. Steady state dc voltage at the sending end in the 2000km case increases by approximately 15kV (compare Figure 6-5 and Figure 6-10). DC current also decreases just slightly in comparison to the 1000km case (compare Figure 6-6 and Figure 6-11).

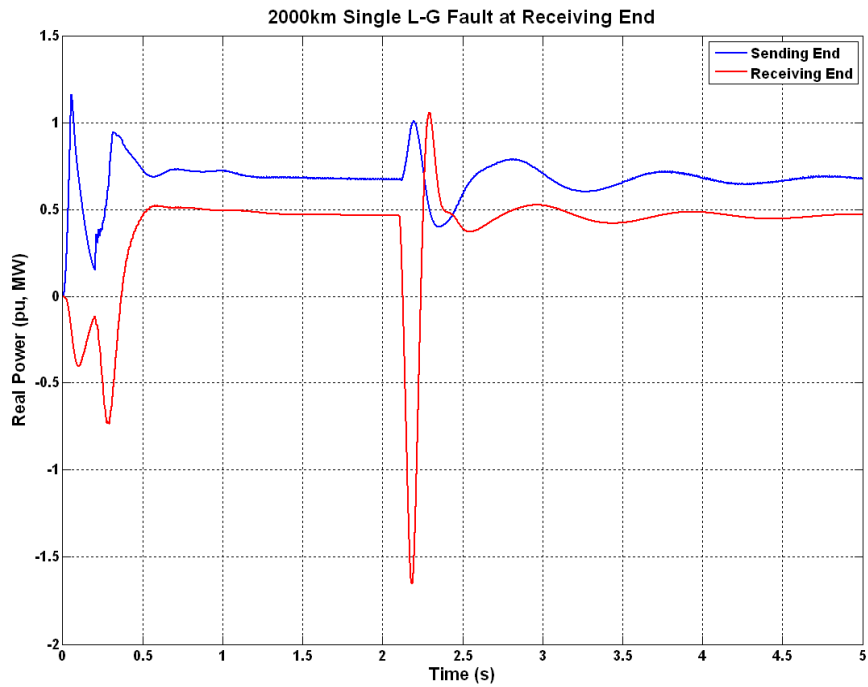


Figure 6-7  
2000km HVDC real power

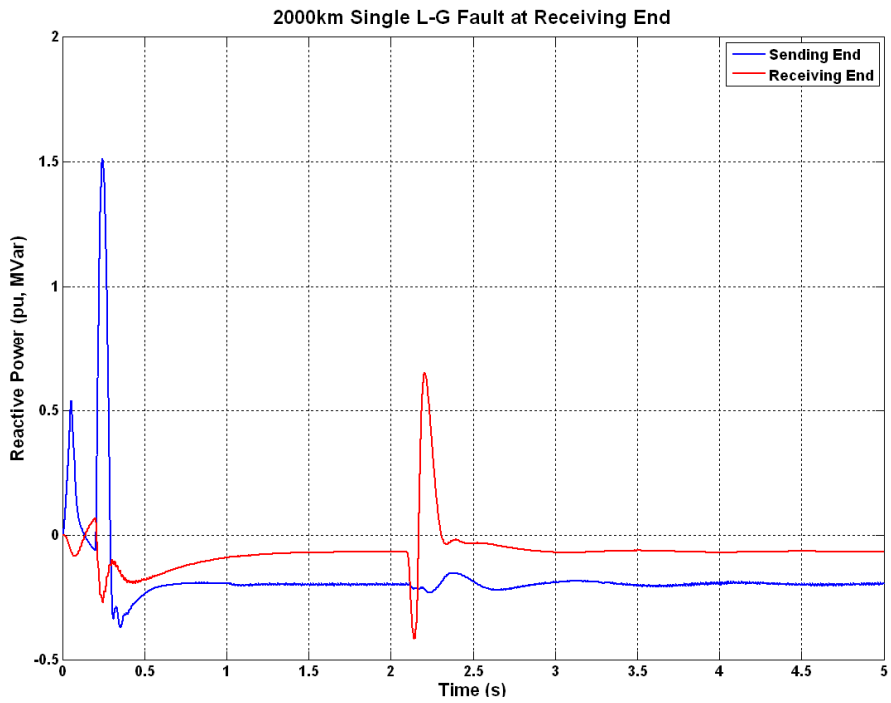


Figure 6-8  
2000km HVDC reactive power

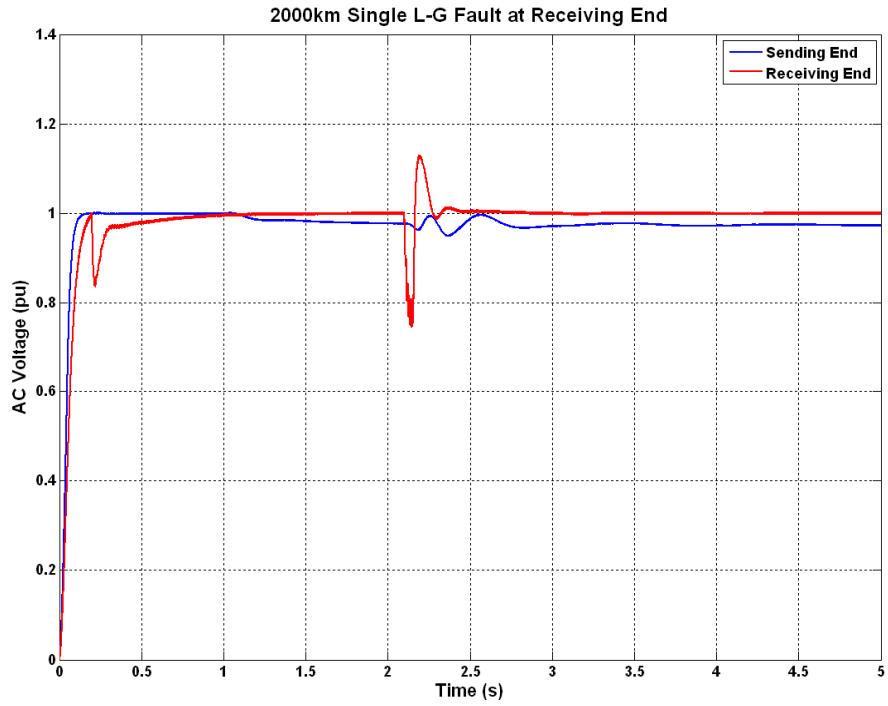


Figure 6-9  
2000km HVDC AC voltage

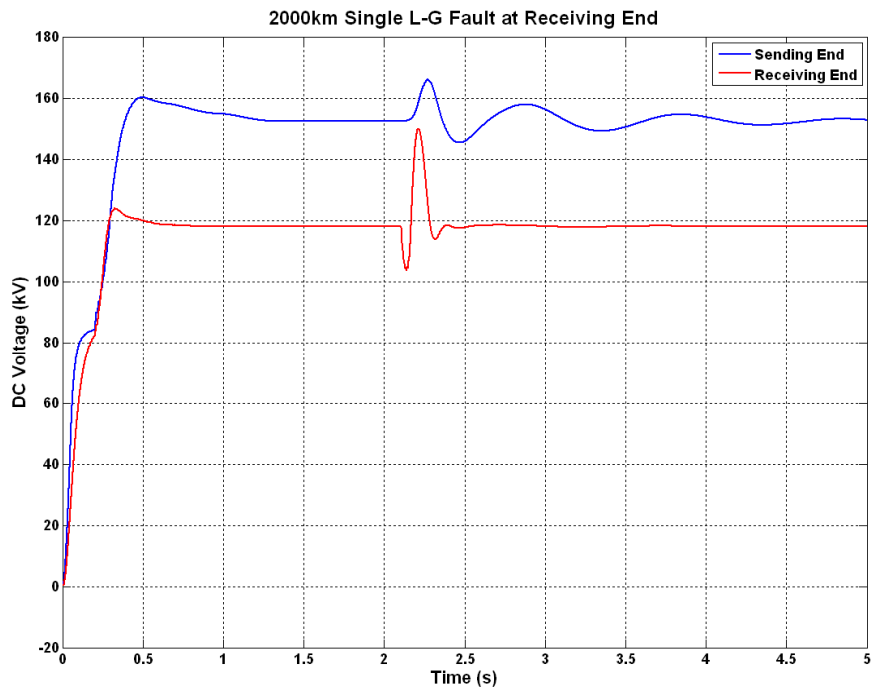
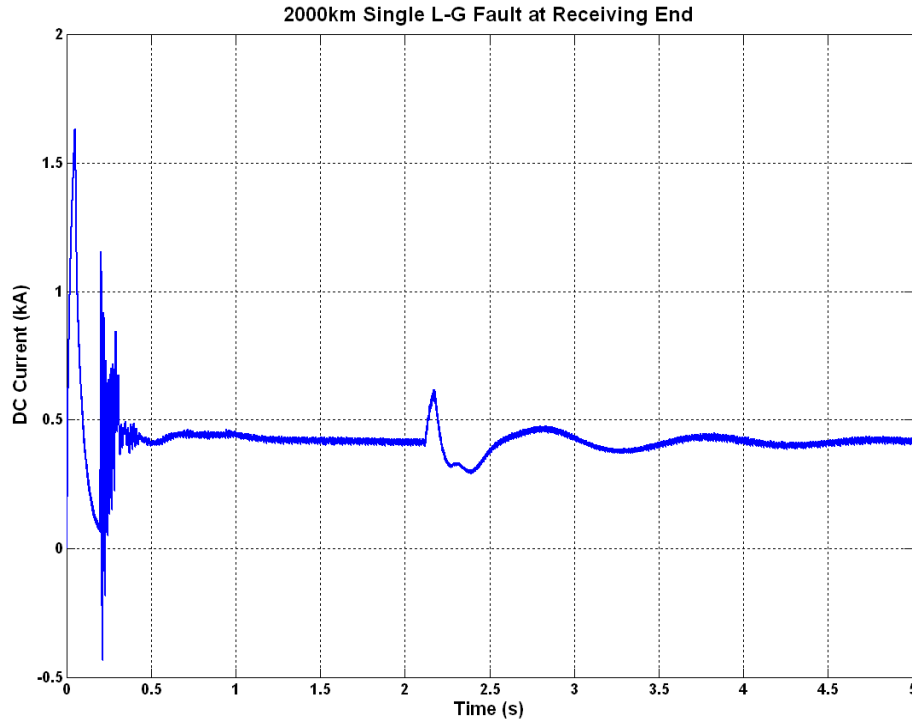


Figure 6-10  
2000km HVDC DC voltage



**Figure 6-11**  
**2000km HVDC DC current**

Figure 6-12, Figure 6-13, Figure 6-14, Figure 6-15, and Figure 6-16 outline the results for a typical HVDC system with cable length increased to 4000km. Once again, following the receiving end fault, ac and dc voltage at both ends remain well regulated. Comparing the three cases, several trends begin to appear. While dc voltage at the receiving end for all three cases is maintained at the set point of 118kV, steady state dc voltage at the sending end increases as cable length is increased (compare Figure 6-5, Figure 6-10, and Figure 6-15). DC current also decreases as cable length increases (compare Figure 6-6, Figure 6-11, and Figure 6-16). These results are consistent with a modern HVDC transmission system and are useful for comparison, but are not necessarily trends that will appear in the superconducting dc system results documented in the following sections.

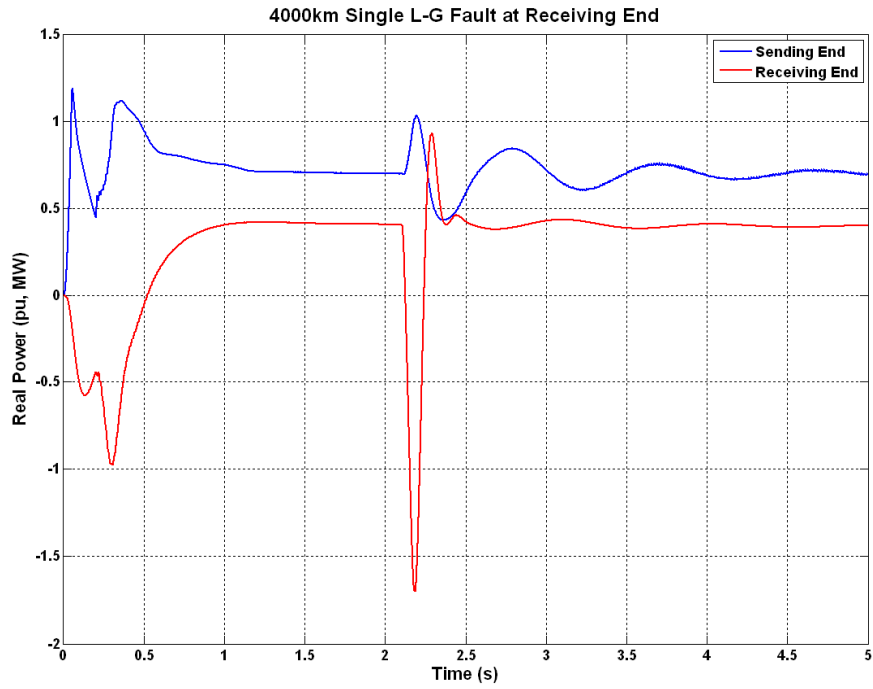


Figure 6-12  
4000km HVDC real power

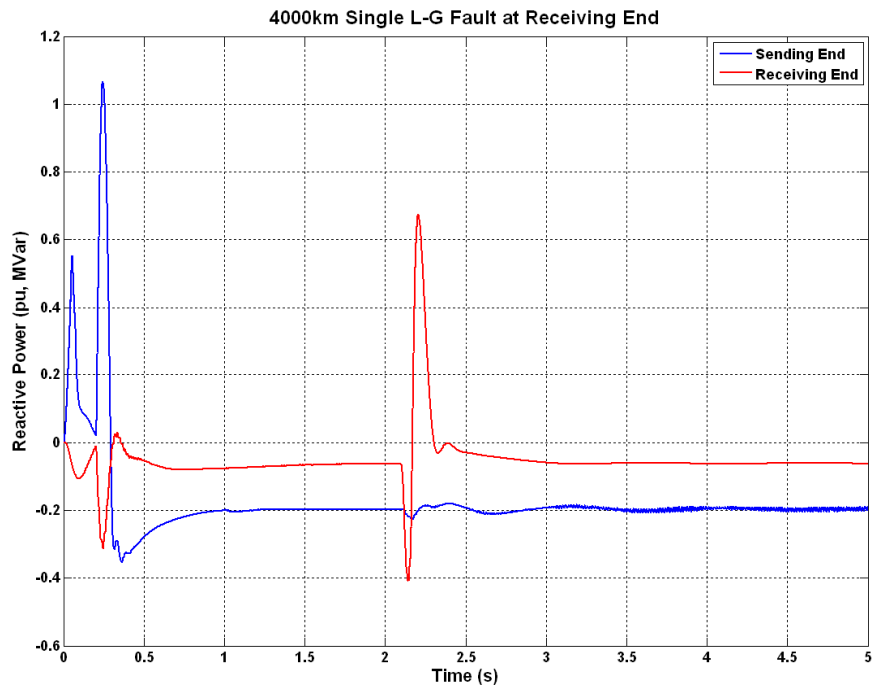


Figure 6-13  
4000km HVDC reactive power

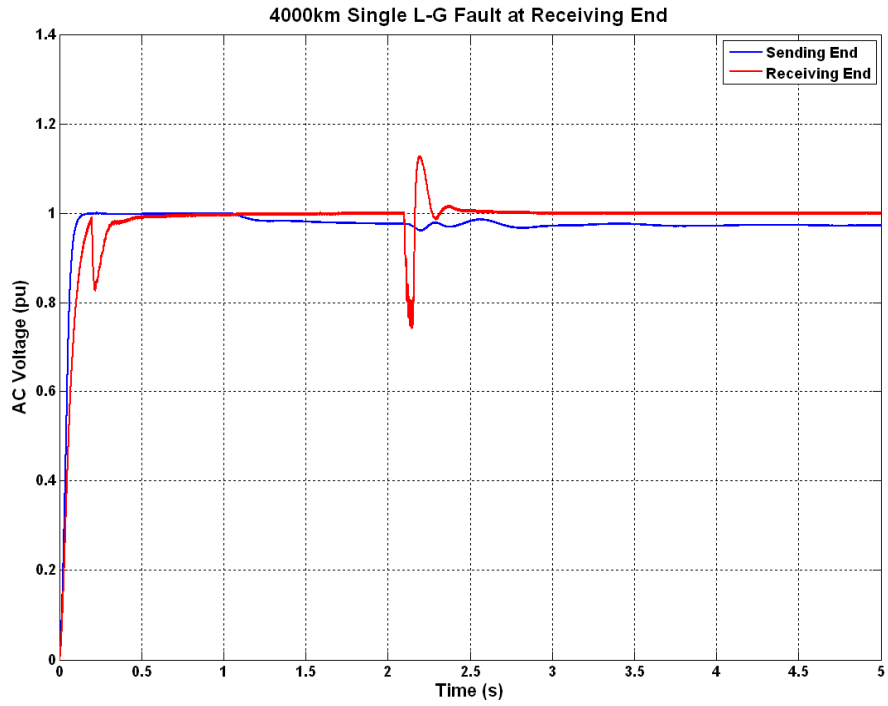


Figure 6-14  
4000km HVDC AC voltage

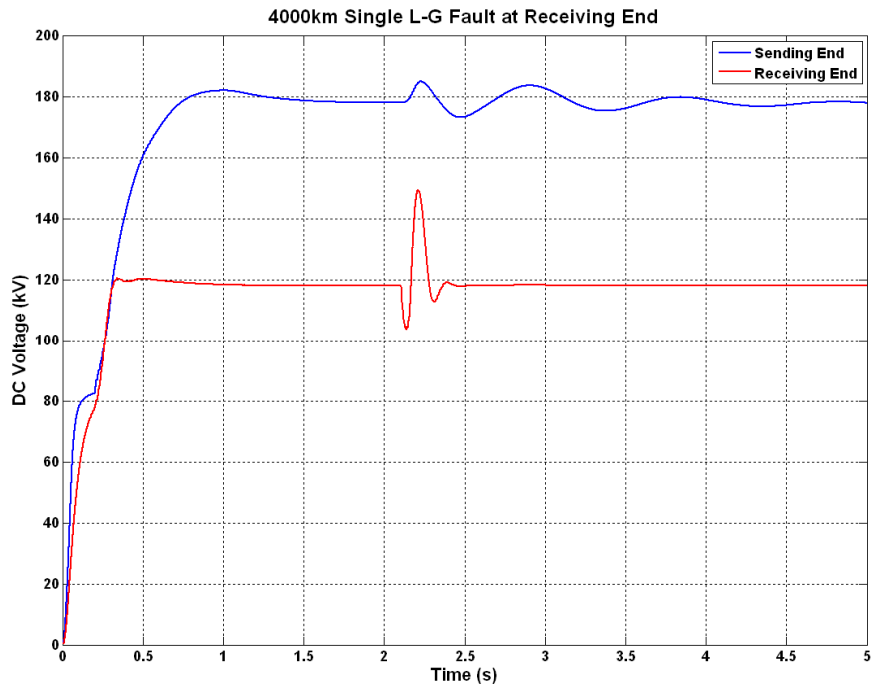
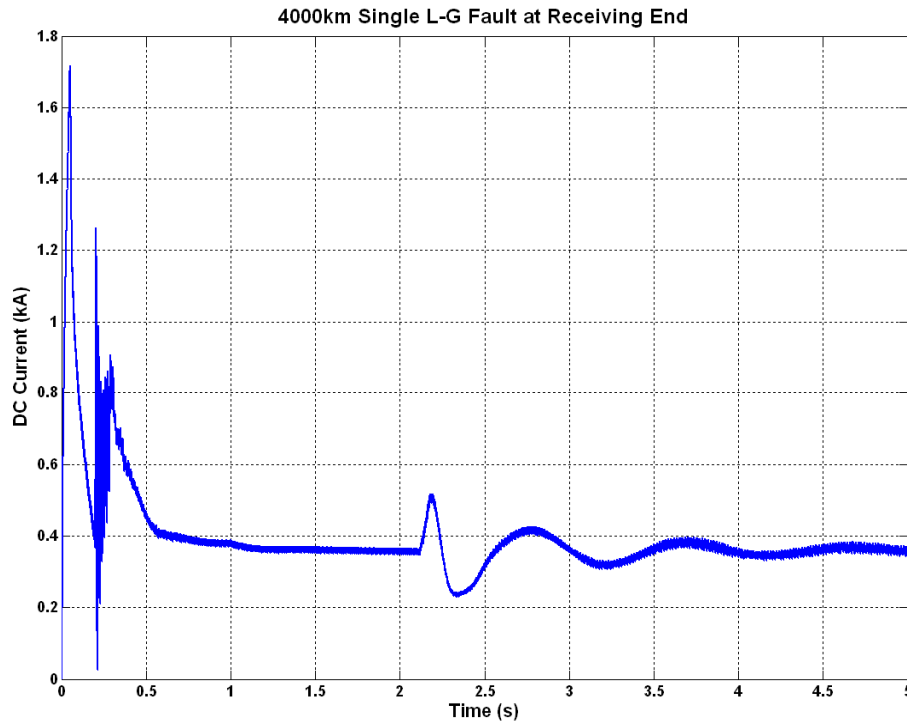


Figure 6-15  
4000km HVDC DC voltage



**Figure 6-16**  
4000km HVDC DC current

## Superconducting DC System Results – DC Fault with Two Voltage Source Converters

The following sections show the electromagnetic transient study results for a superconducting dc transmission system with three distinct cable lengths. In this section, a fault on the superconducting dc cable was applied at 2.1 seconds in each case. These cases begin to demonstrate the instability of the proposed voltage source converter model under dc fault conditions, revealing the large transients that can arise on a long superconducting cable. Figure 6-17, Figure 6-18, Figure 6-19, Figure 6-20, and Figure 6-21 show the PSCAD® simulation results for the 1000km superconducting dc transmission system with only two voltage source converters.

The severe transients predicted in section five are on display in the subsequent plots. After the fault, ac and dc voltage at both ends of the system plummet. When the system attempts to recover, large swings occur in each of the measured variables. While real power, reactive power, and dc voltage seem to be settling, dc current oscillations appear to be increasing, reaching over 2kA as shown in Figure 6-21.

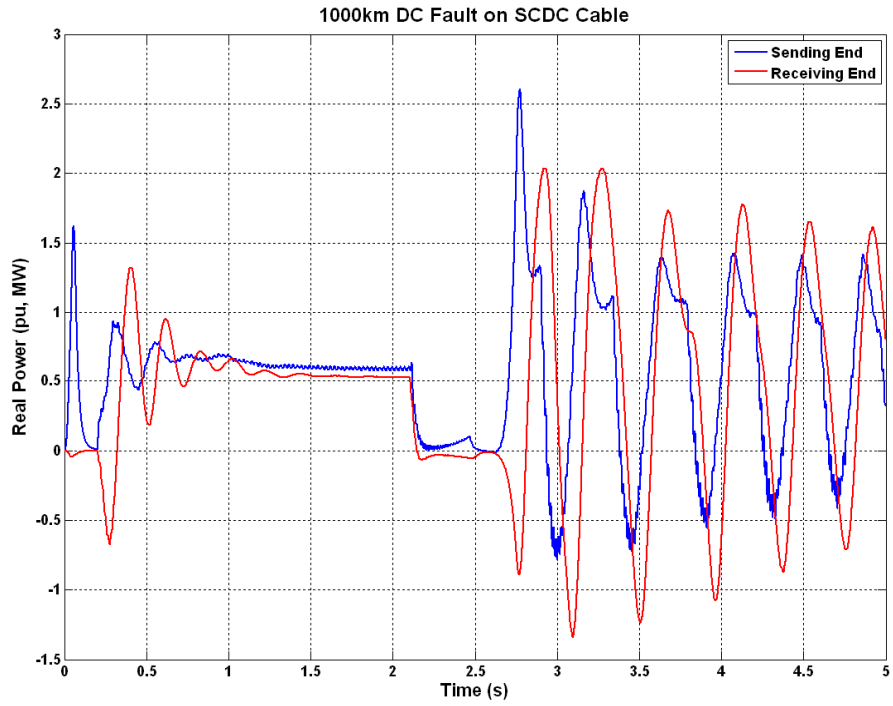


Figure 6-17  
1000km cable DC fault two voltage source converters, real power

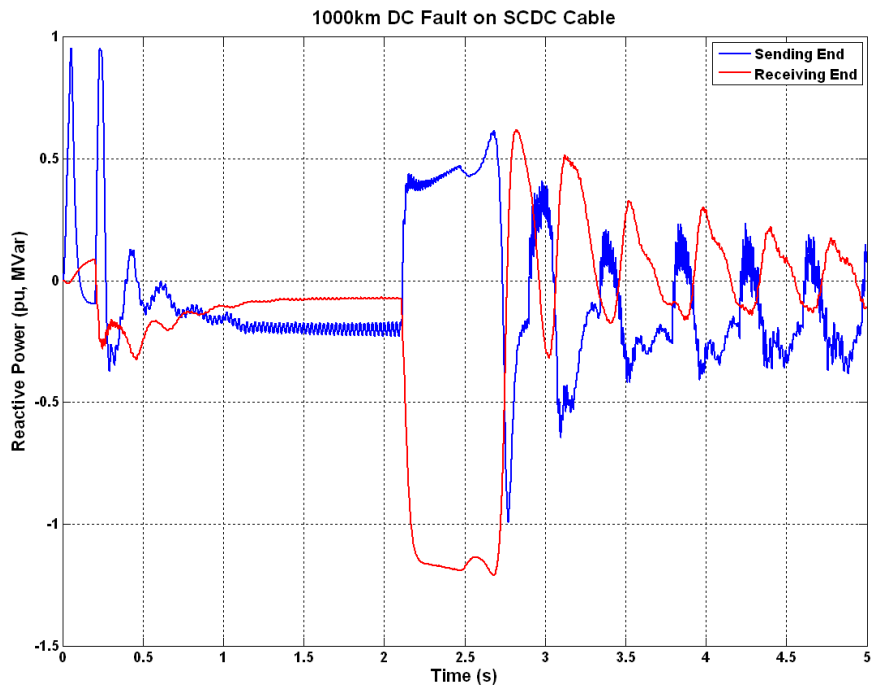
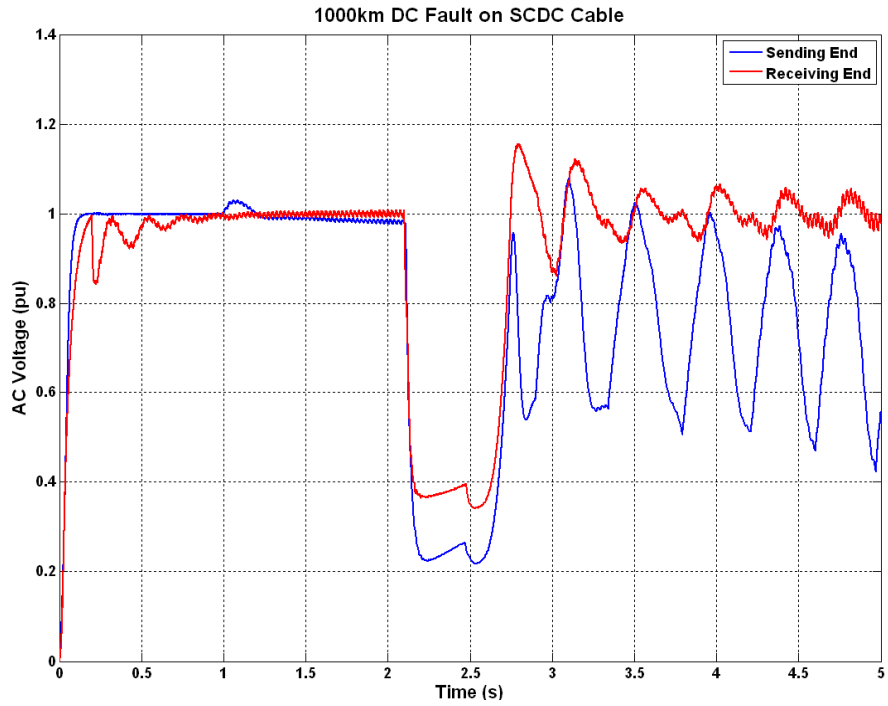
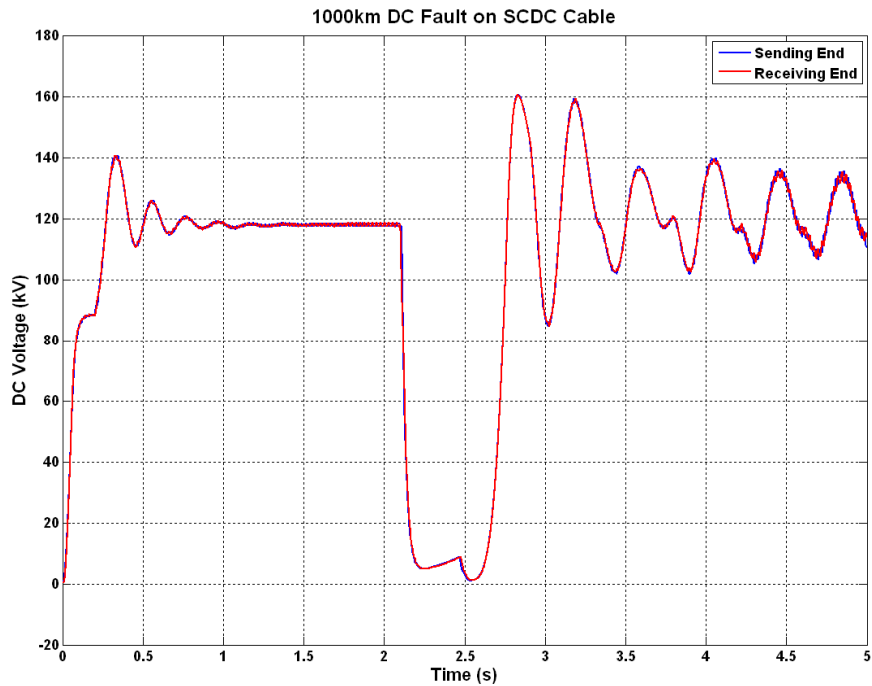


Figure 6-18  
1000km cable DC fault two voltage source converters, reactive power



**Figure 6-19**  
1000km cable DC fault two voltage source converters, AC voltage



**Figure 6-20**  
1000km cable DC fault two voltage source converters, DC voltage

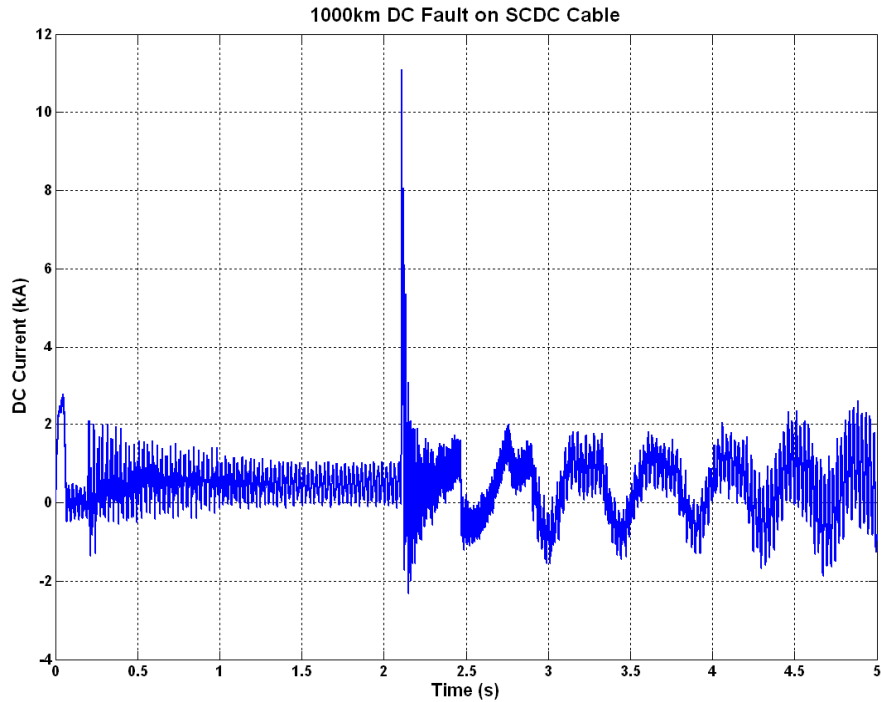


**Figure 6-21**  
1000km cable DC fault two voltage source converters, DC current

With cable length increased to 2000km, nearly identical system dynamics result. Figure 6-22, Figure 6-23, Figure 6-24, and Figure 6-25 again illustrate the large transients that result from a lack of cable damping.

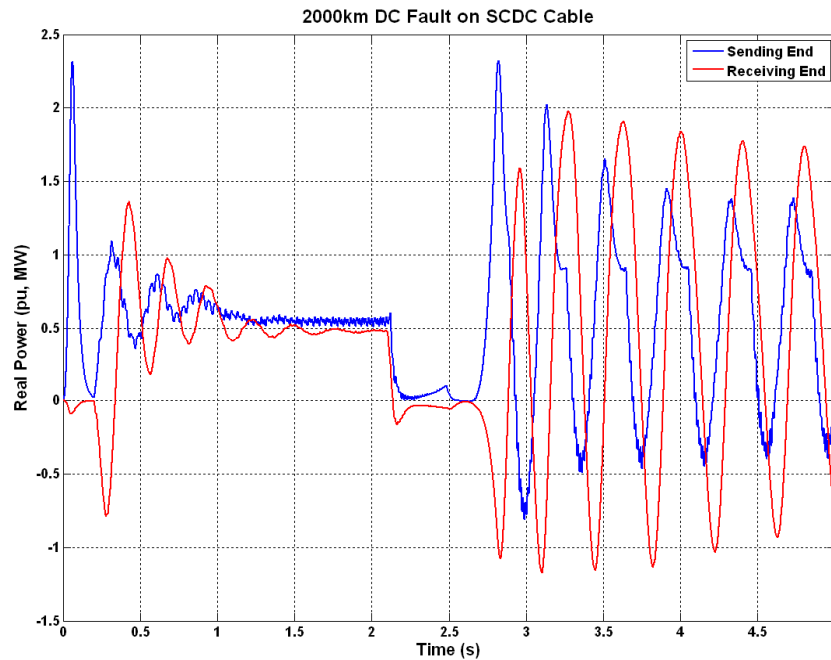


**Figure 6-22**  
2000km cable DC fault two voltage source converters, real power

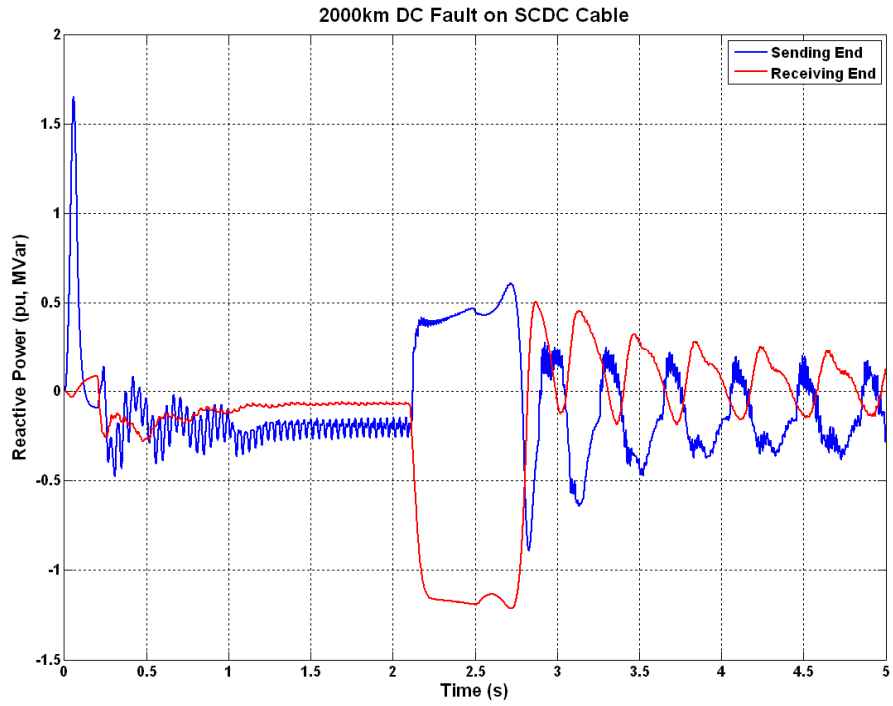


**Figure 6-23**  
2000km cable DC fault two voltage source converters, reactive power

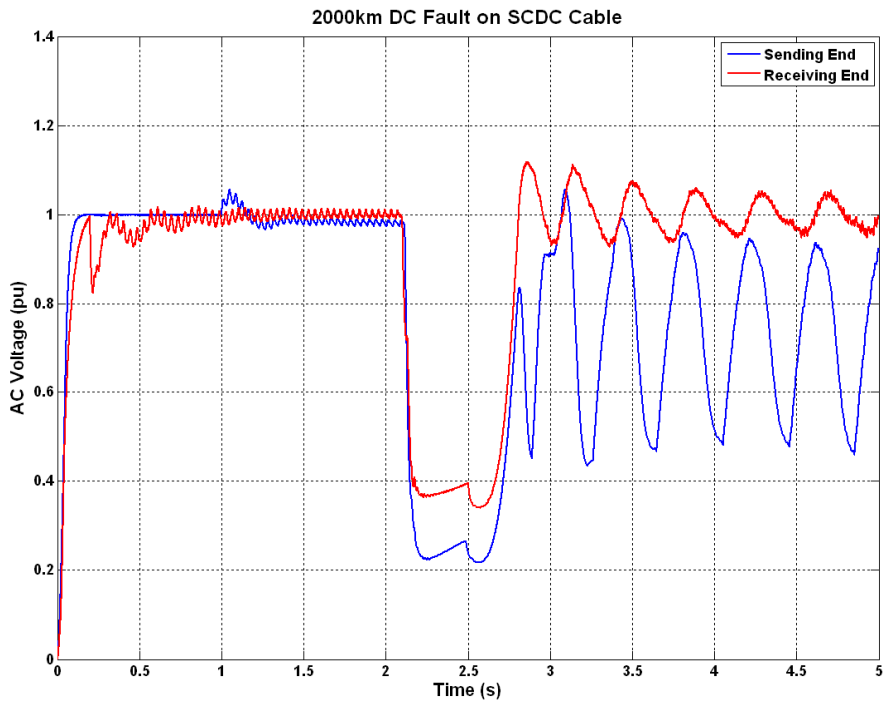


**Figure 6-24**  
2000km cable DC fault two voltage source converters, AC voltage

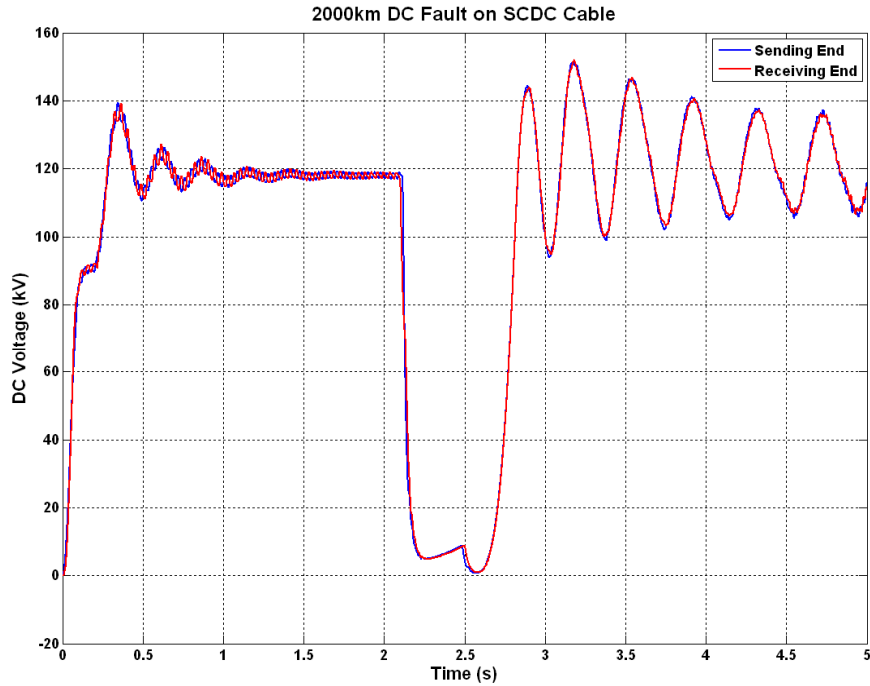


**Figure 6-25**  
2000km cable DC fault two voltage source converters, DC voltage

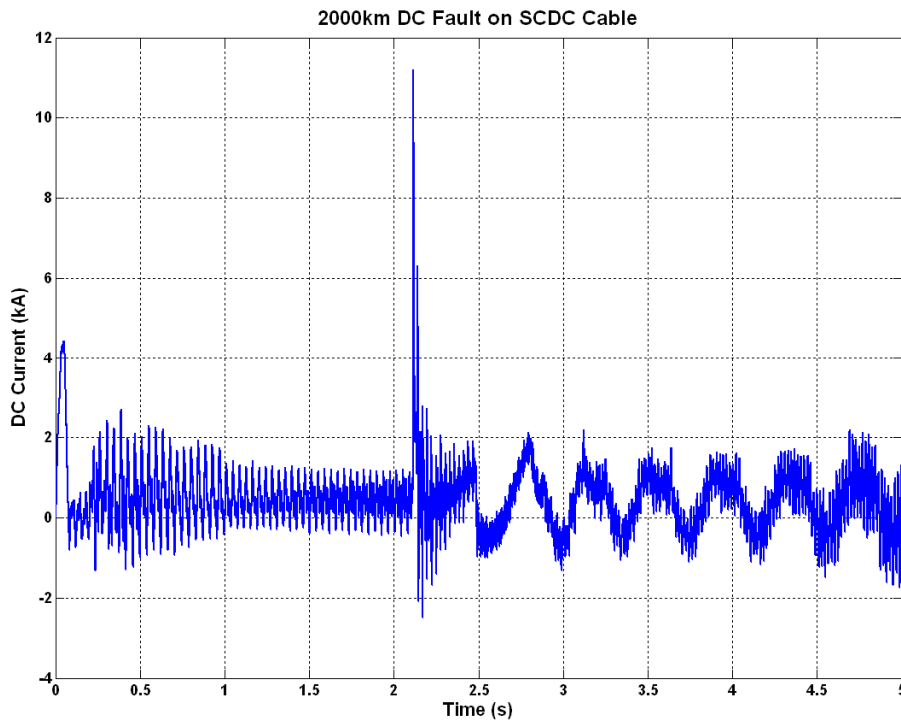


**Figure 6-26**  
2000km cable DC fault two voltage source converters, DC current

The 4000km cable results shown below in Figure 6-27, Figure 6-28, Figure 6-29, Figure 6-30, and Figure 6-31 reveal even more severe transients. This case not only takes over three times longer to attempt recovery (compare Figure 6-24 and Figure 6-29), but current on the superconducting cable reaches over 4kA (compare Figure 6-26 and Figure 6-31). Again, the low damping of the superconducting cable and the need for specialized filtering is evident.

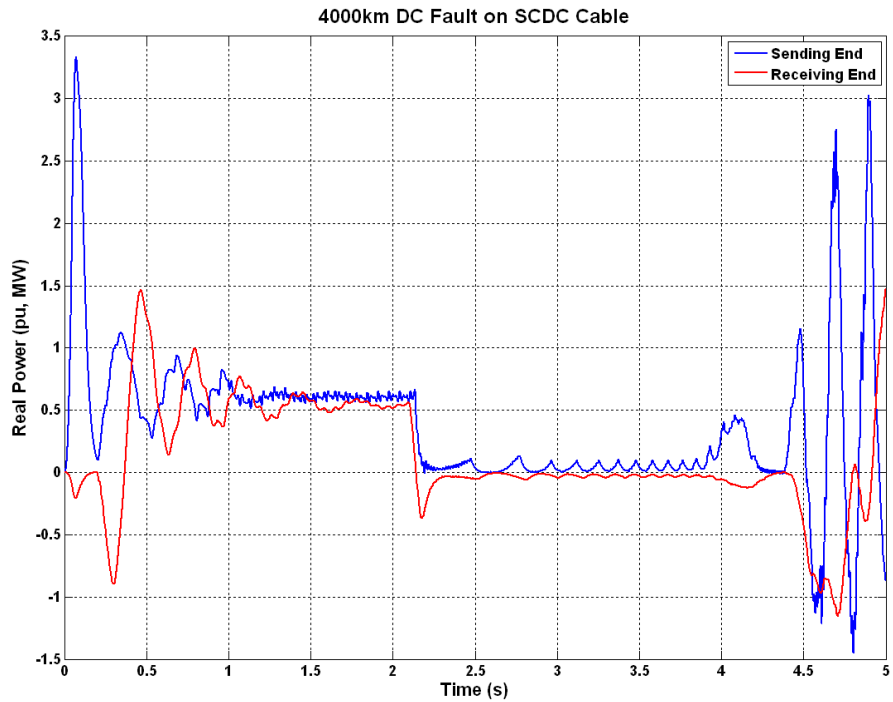


**Figure 6-27**  
4000km cable DC fault two voltage source converters, real power

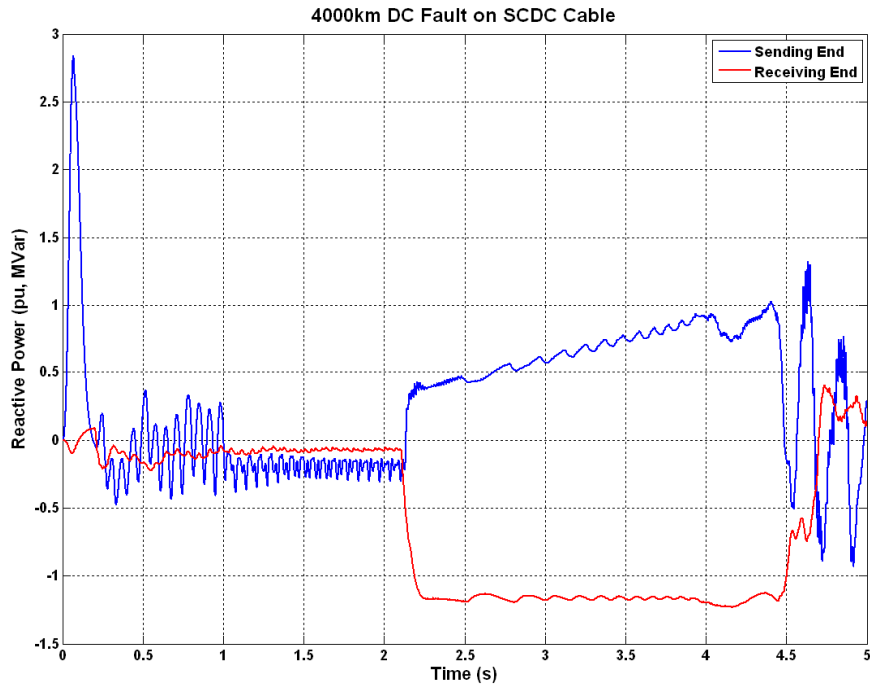


**Figure 6-28**  
4000km cable DC fault two voltage source converters, reactive power

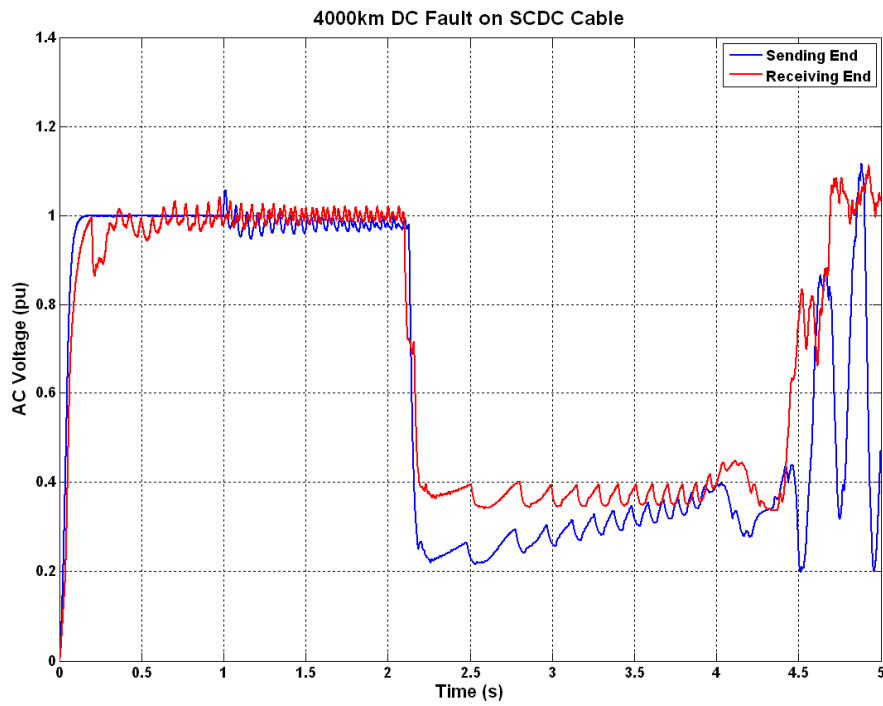


**Figure 6-29**  
4000km cable DC fault two voltage source converters, AC voltage

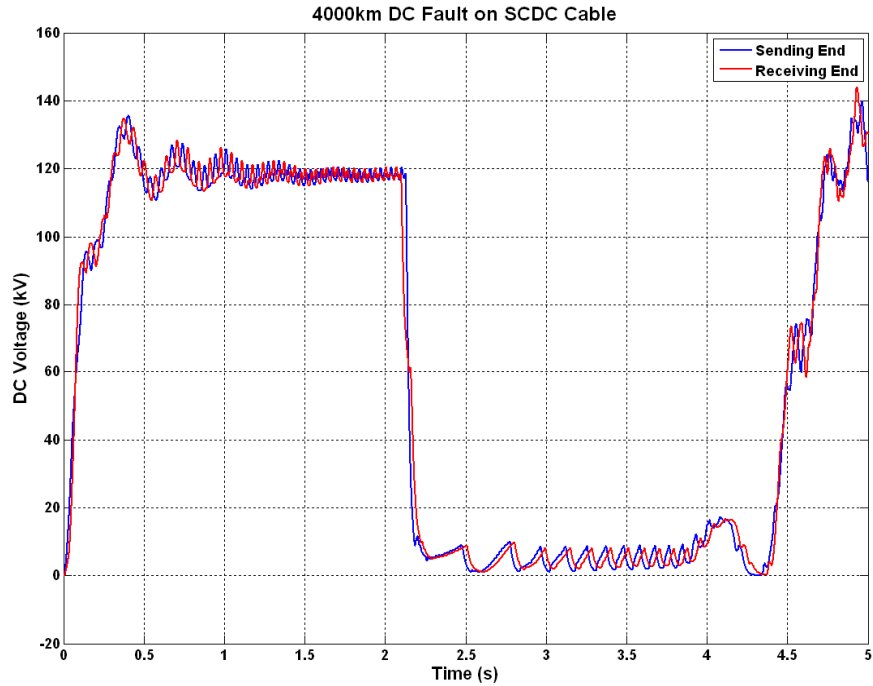


**Figure 6-30**  
4000km cable DC fault two voltage source converters, DC voltage

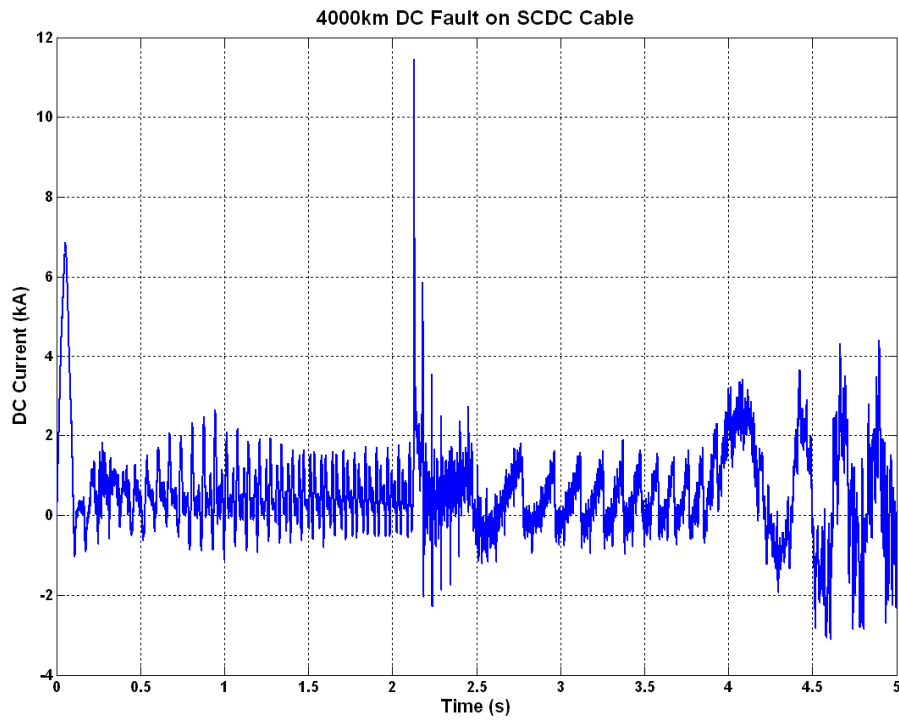


**Figure 6-31**  
4000km cable DC fault two voltage source converters, DC current

## Superconducting DC System Results – AC Fault with Two Voltage Source Converters

The following figures show the electromagnetic transient study results for a two voltage source converter superconducting dc transmission system with three distinct cable lengths and a single fault condition. A three-phase ac fault at the receiving end of the system was applied at 2.1 seconds in each case. These plots indicate greater system-wide stability than that of the superconducting dc system under dc fault conditions. Figure 6-32, Figure 6-33, Figure 6-34, Figure 6-35, and Figure 6-36 show the PSCAD® simulation results for the 1000km superconducting dc transmission system with only two voltage source converters, in an ac fault scenario.

Severe dc current transients reaching close to 4kA are still evident, but at a much higher frequency than in the dc fault scenario (compare Figure 6-21 and Figure 6-36). AC and dc voltage are also less oscillatory than in the dc fault cases (compare Figure 6-19 and Figure 6-20 with Figure 6-34 and Figure 6-35).

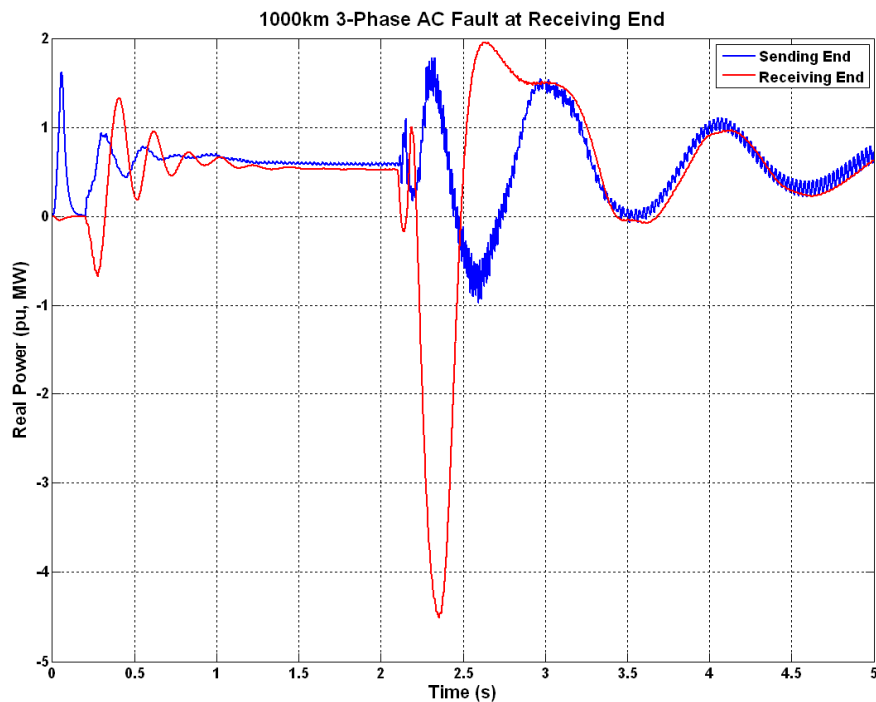


**Figure 6-32**  
1000km cable AC fault two voltage source converters, real power

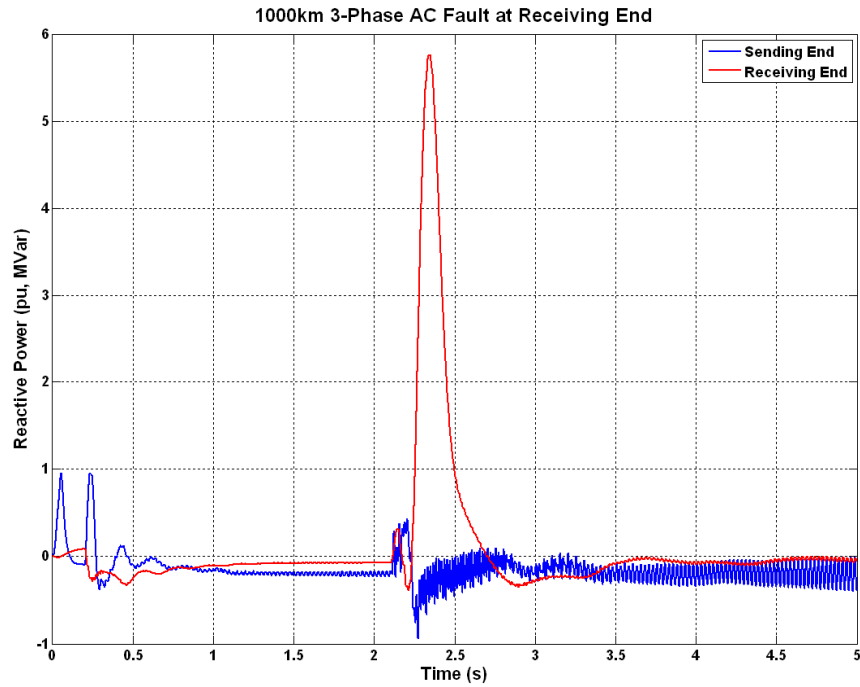


Figure 6-33  
1000km cable AC fault two voltage source converters, reactive power

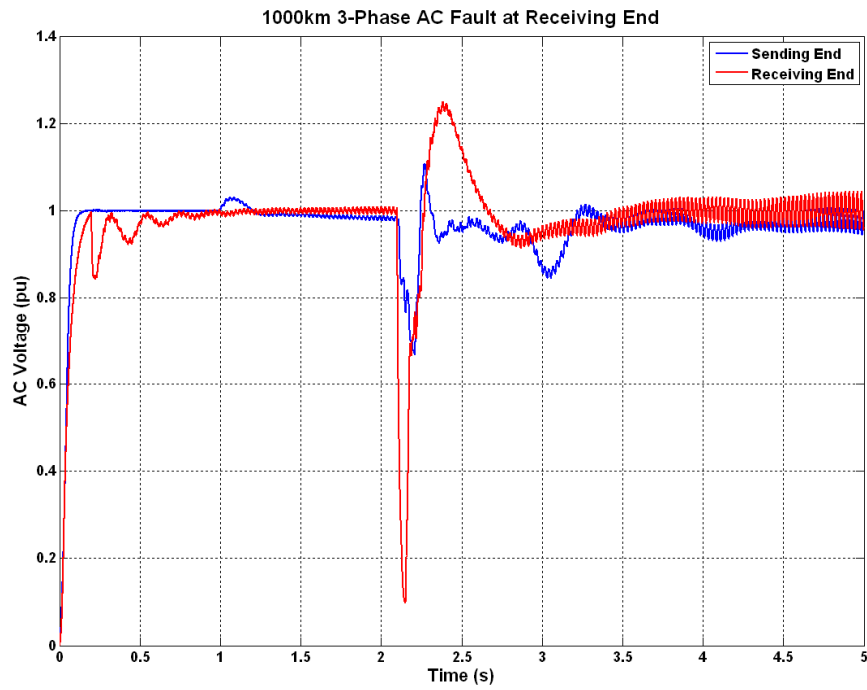
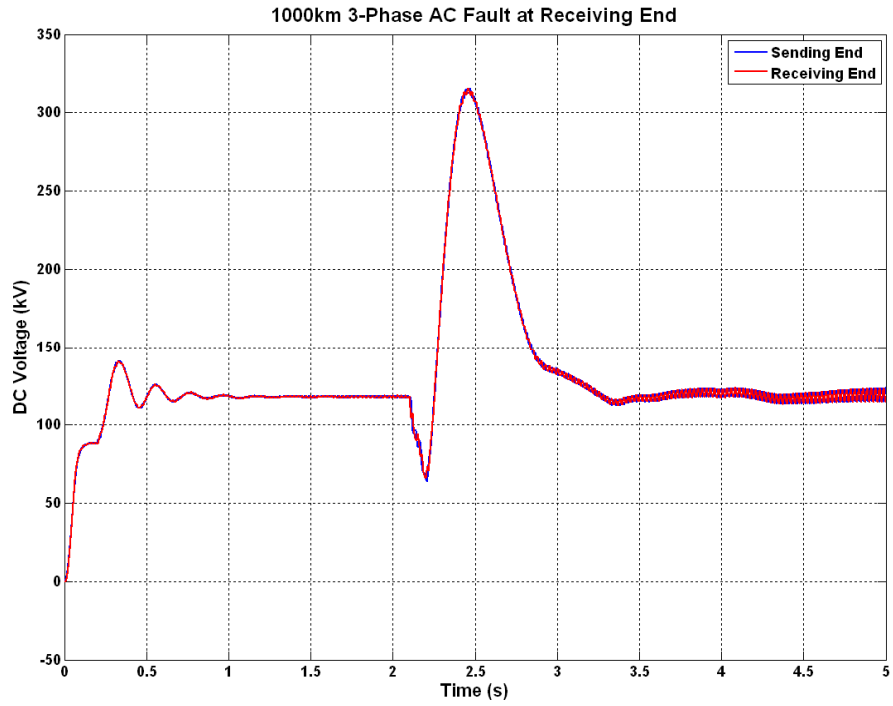
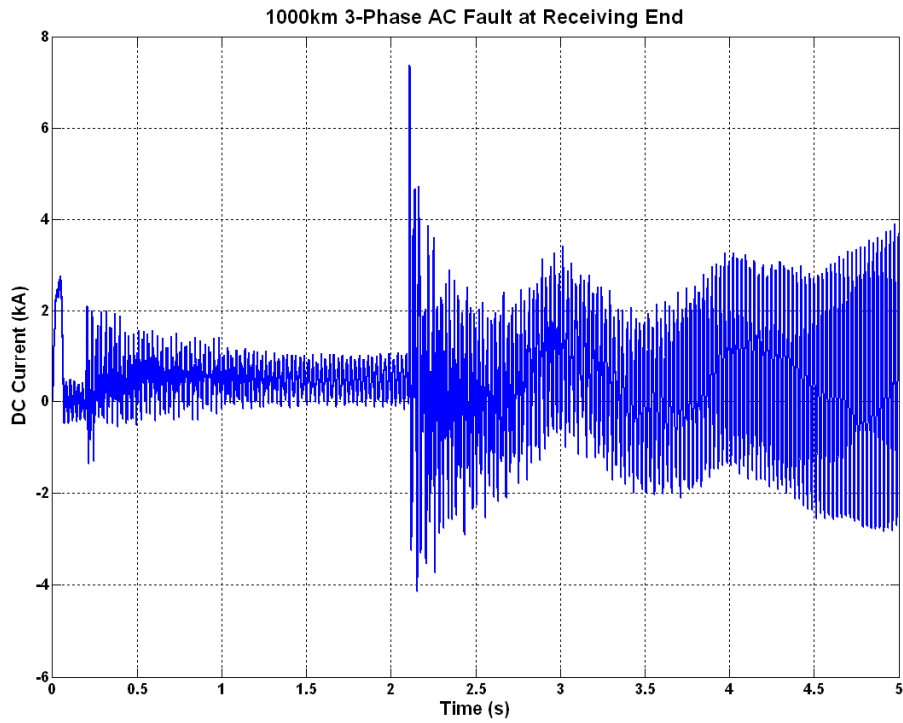


Figure 6-34  
1000km cable AC fault two voltage source converters, AC voltage



**Figure 6-35**  
1000km cable AC fault two voltage source converters, DC voltage



**Figure 6-36**  
1000km cable AC fault two voltage source converters, DC current

With cable length increased to 2000km, nearly identical system performance results. Figure 6-37, Figure 6-38, Figure 6-39, Figure 6-40, and Figure 6-41 reveal the close similarity. Peak dc current transients appear to drop just slightly in comparison with the 1000km case (compare Figure 6-36 and Figure 6-41).

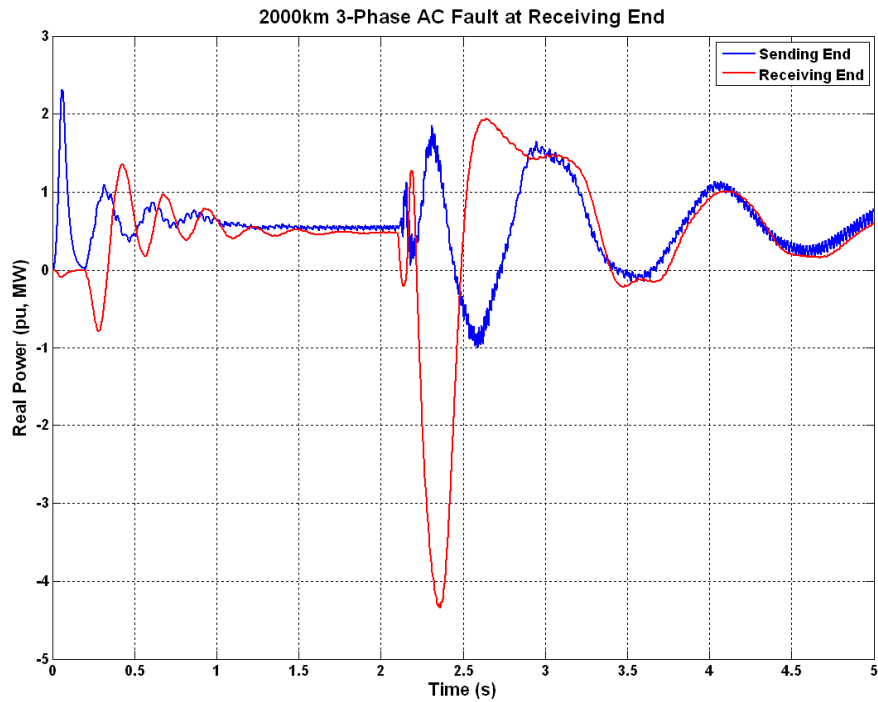


**Figure 6-37**  
2000km cable AC fault two voltage source converters, real power

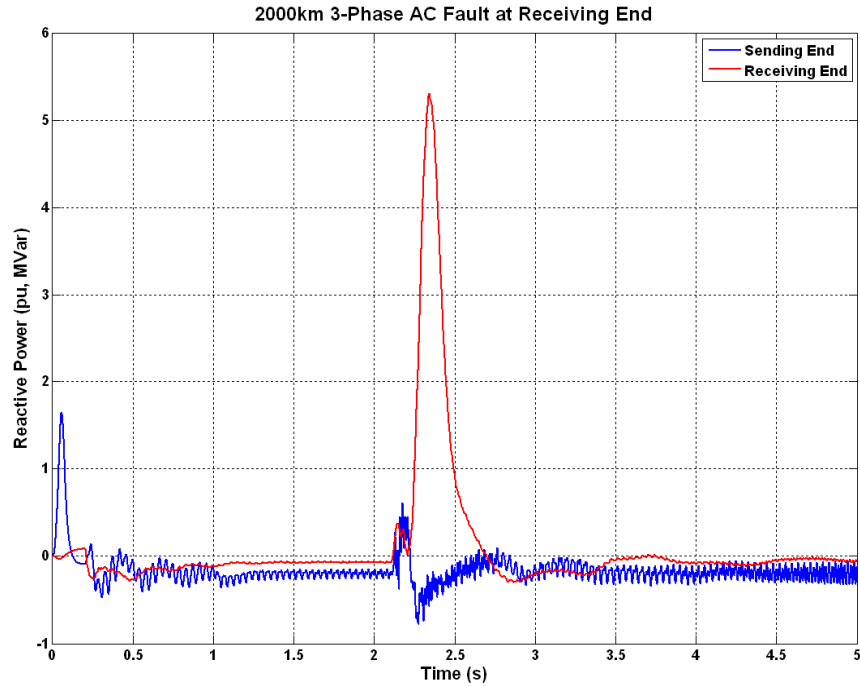


**Figure 6-38**  
2000km cable AC fault two voltage source converters, reactive power

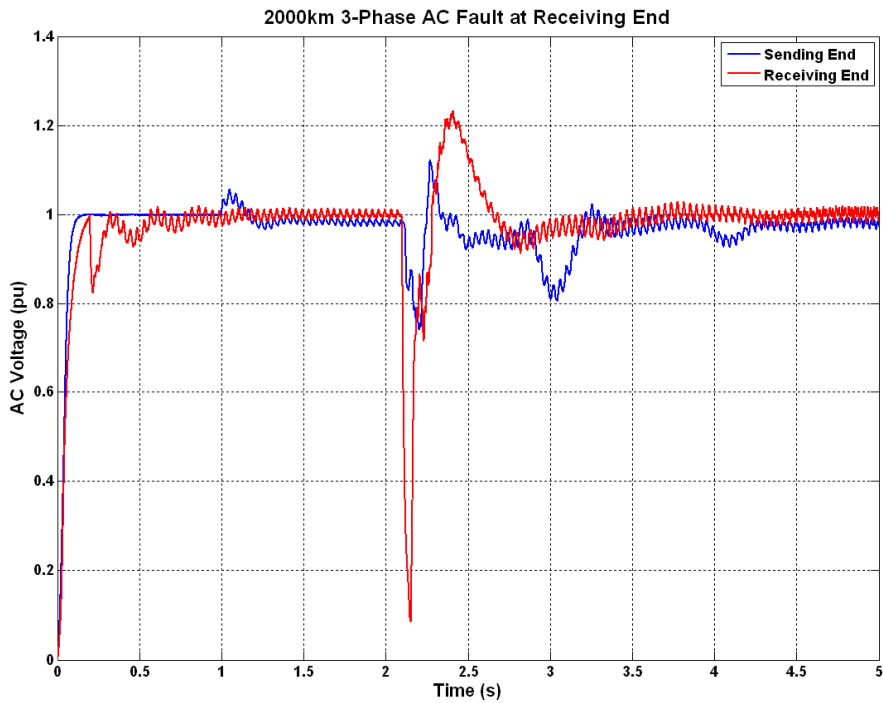


**Figure 6-39**  
2000km cable AC fault two voltage source converters, AC voltage

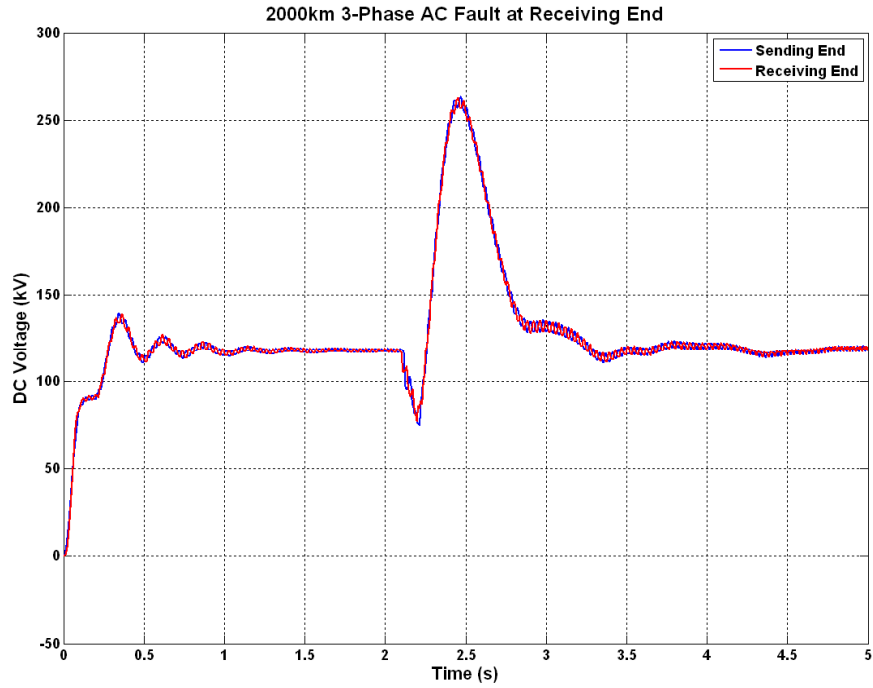


**Figure 6-40**  
2000km cable AC fault two voltage source converters, DC voltage

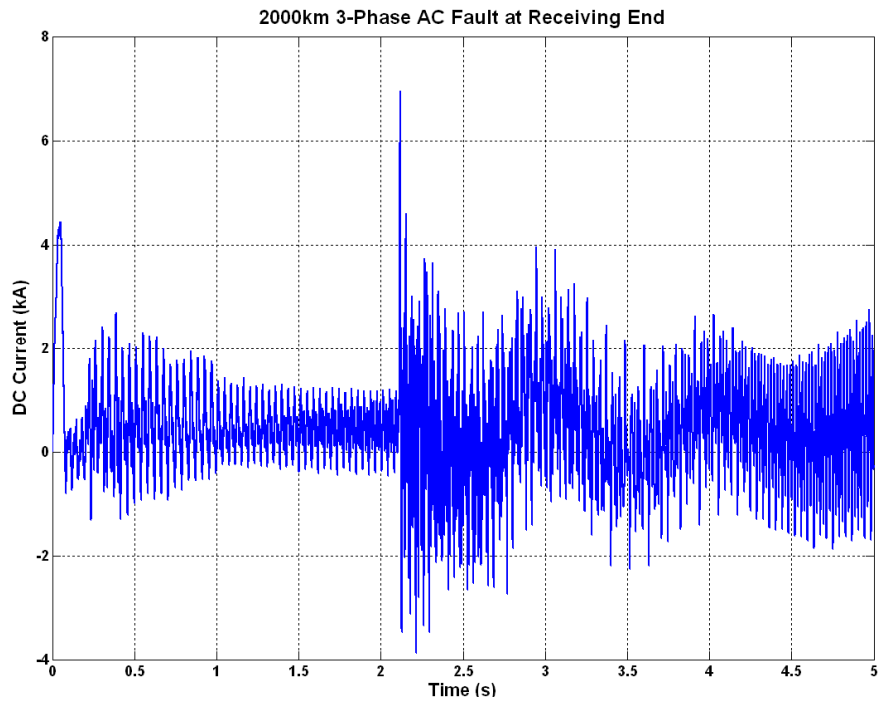


**Figure 6-41**  
2000km cable AC fault two voltage source converters, DC current

Increasing the cable length to 4000km reveals how long superconducting cables can generate rather severe oscillations in the ac systems and dc link. Figure 6-42, Figure 6-43, Figure 6-44, Figure 6-45, and Figure 6-46 are the relevant system plots for this simulation. Each of the figures shows a high frequency ripple content, especially the ac and dc voltages (see Figure 6-44 and Figure 6-45).

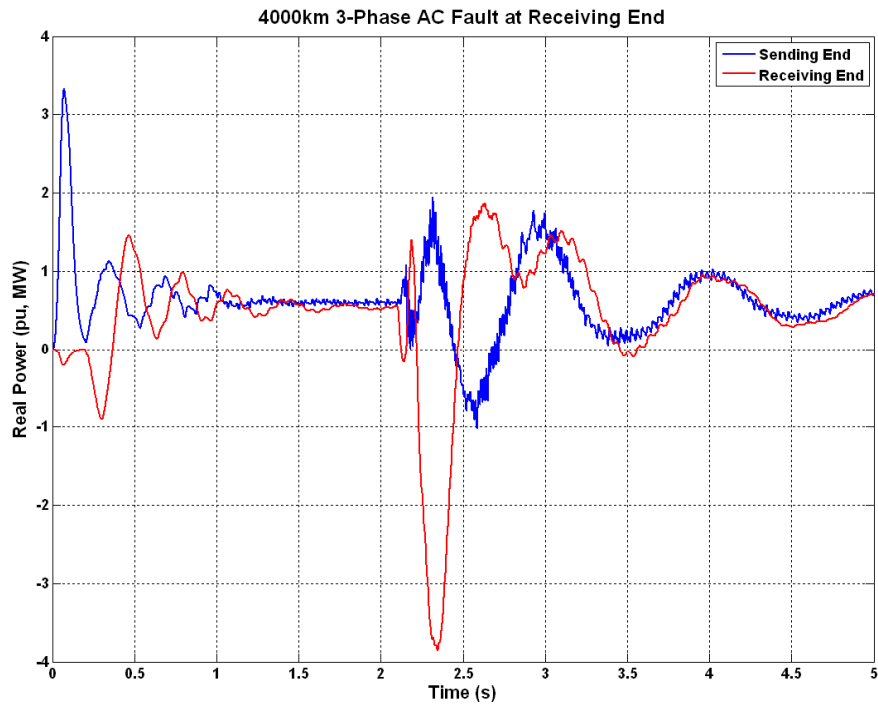


**Figure 6-42**  
4000km cable AC fault two voltage source converters, real power

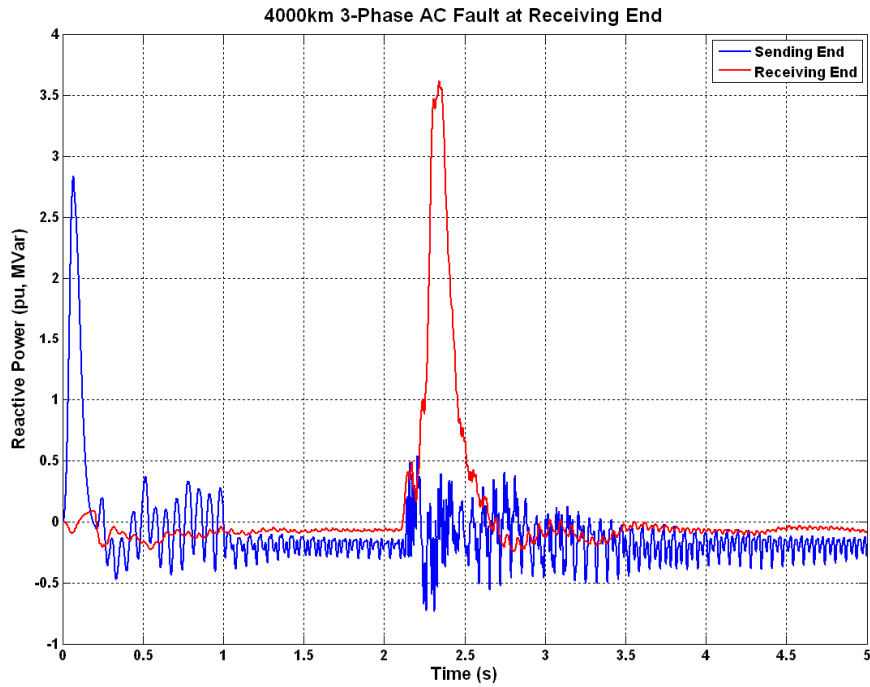


**Figure 6-43**  
4000km cable AC fault two voltage source converters, reactive power

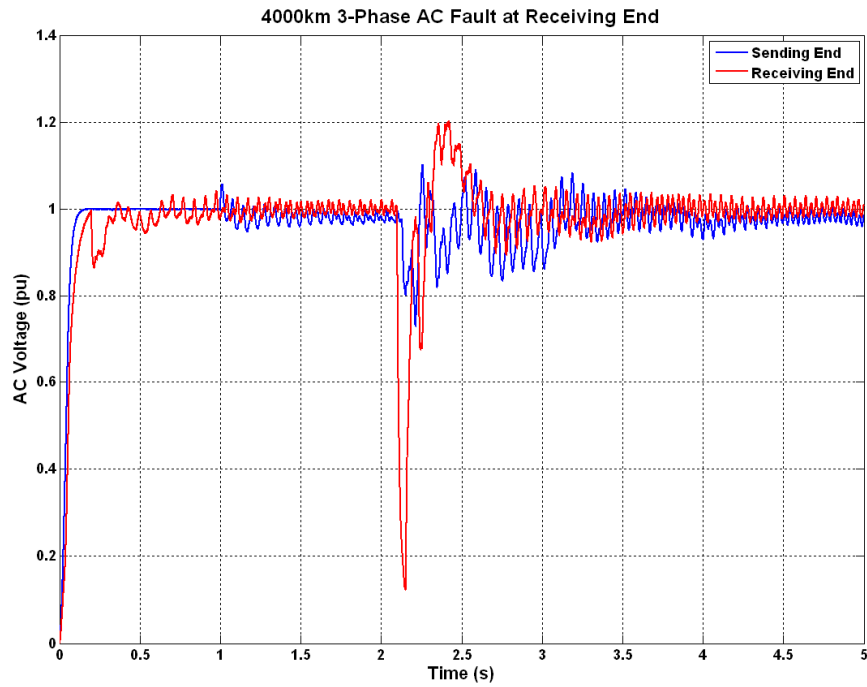


**Figure 6-44**  
4000km cable AC fault two voltage source converters, AC voltage

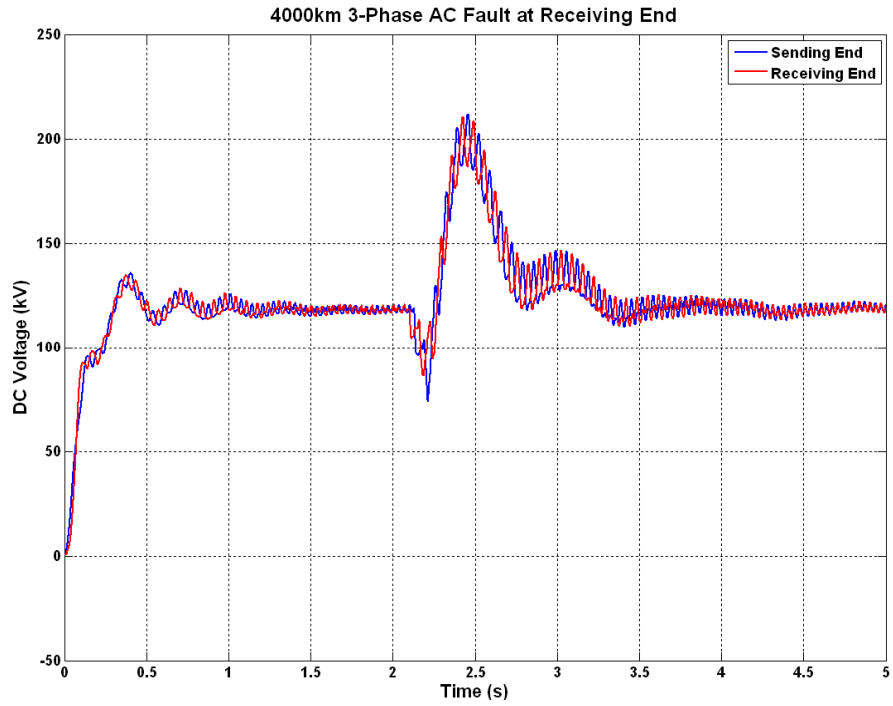


Figure 6-45  
4000km cable AC fault two voltage source converters, DC voltage

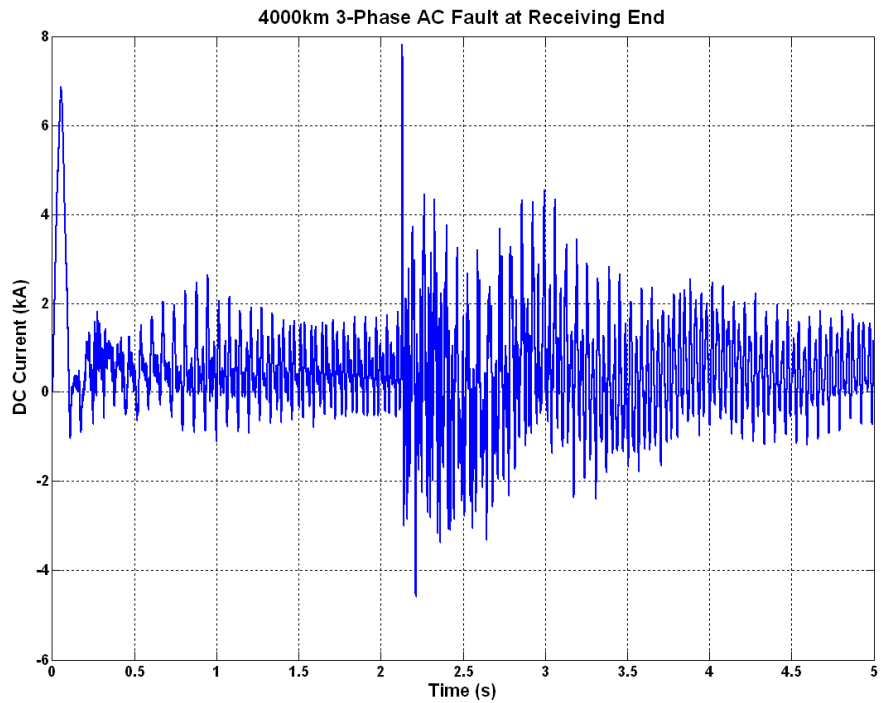
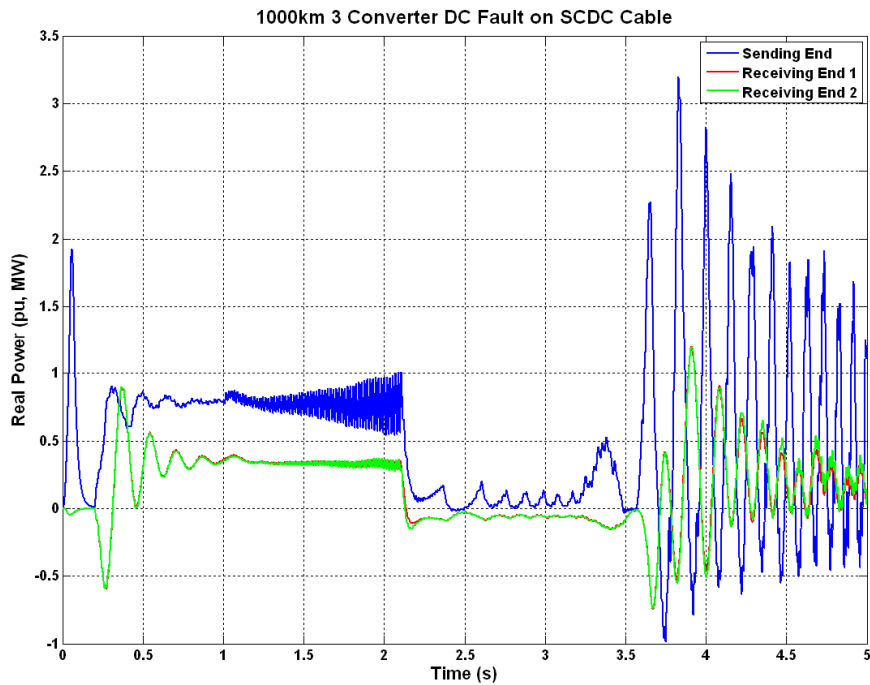


Figure 6-46  
4000km cable AC fault two voltage source converters, DC current

## Superconducting DC System Results – DC Fault with Three Voltage Source Converters

The following two sections show the electromagnetic transient study results for an superconducting dc transmission system with three voltage sourced converters (one rectifier and two inverters). In this section, each case was subjected to a fault on the cable at 2.1 seconds into the run. The simulation parameters for this set of cases are identical to that of the parameters in section 6.2, except that there is an additional voltage source converter. This multi-terminal superconducting dc transmission system model demonstrates extreme instability and severe transient oscillations. This section is presented without further comment, only to highlight that the low damping of superconducting dc cables indeed gives rise to serious transient conditions. These results also provide evidence that multi-terminal topology implementation will require special filtering and precise control systems optimization.



**Figure 6-47**  
1000km cable DC fault three voltage source converters, real power

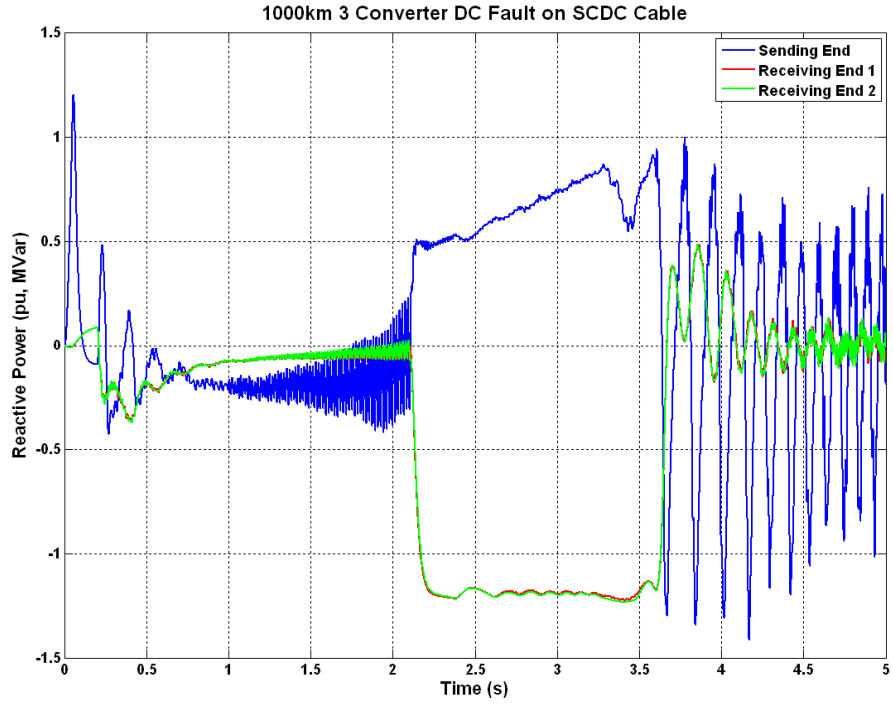


**Figure 6-48**  
1000km cable DC fault three voltage source converters, reactive power

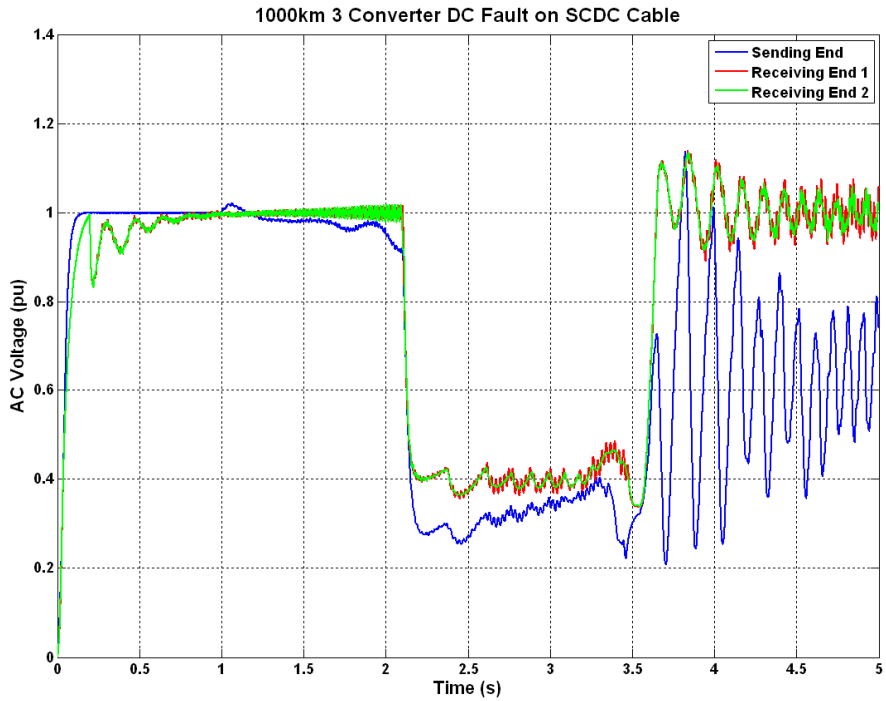


**Figure 6-49**  
1000km cable DC fault three voltage source converters, AC voltage

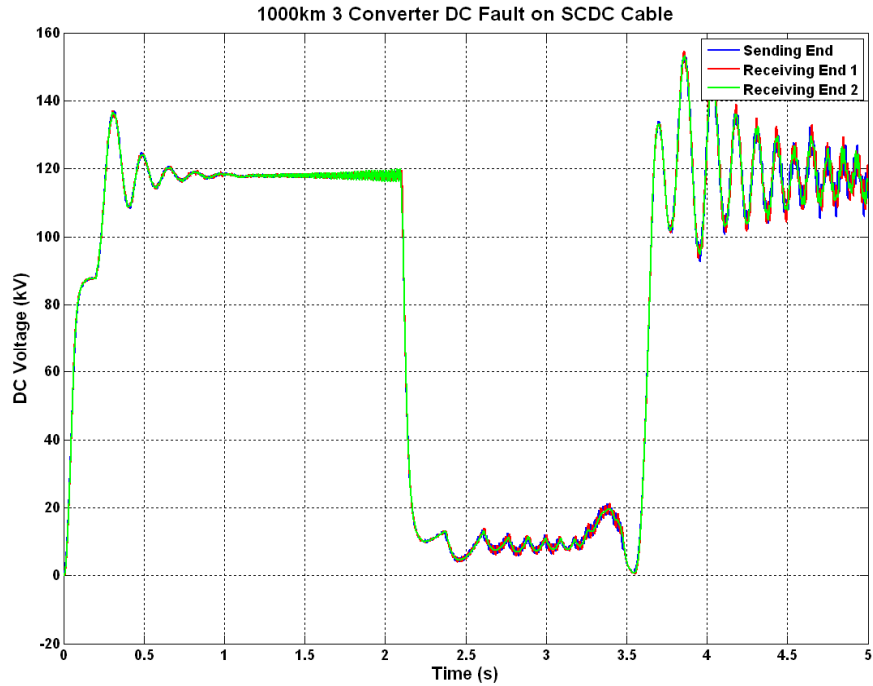


**Figure 6-50**  
1000km cable DC fault three voltage source converters, DC voltage

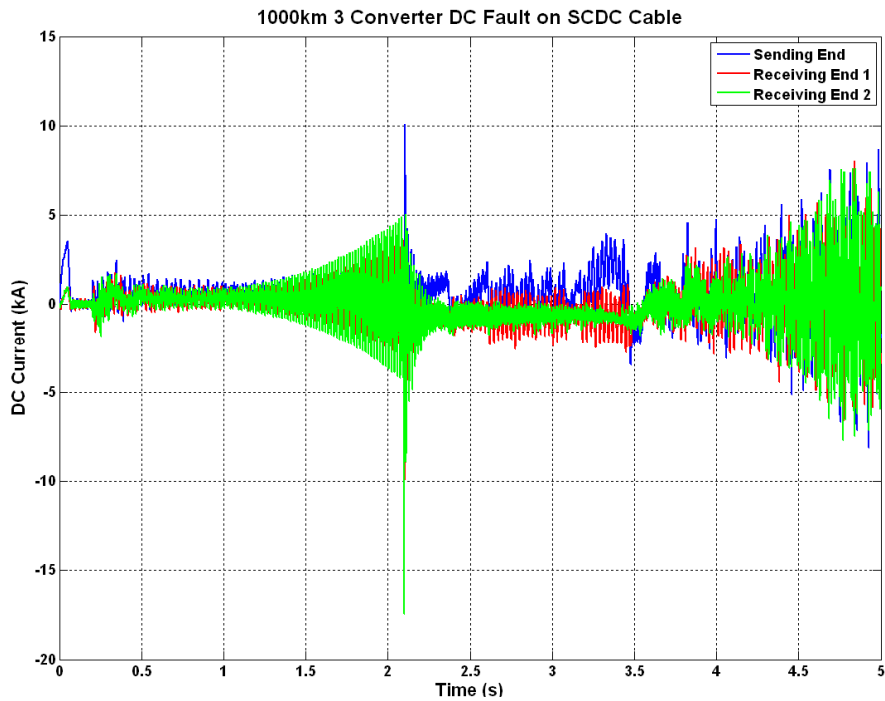


**Figure 6-51**  
1000km cable DC fault three voltage source converters, DC current

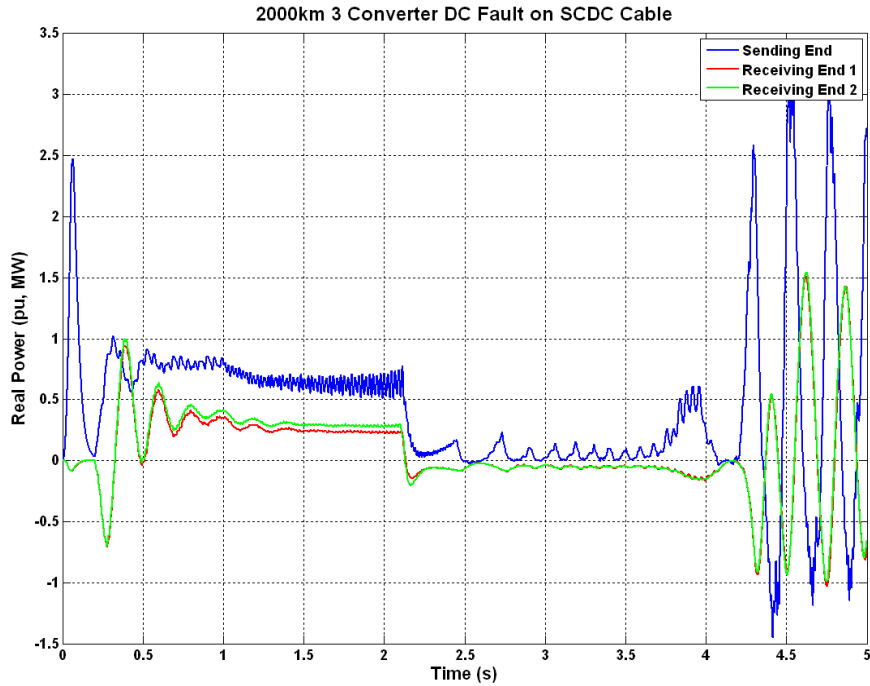


**Figure 6-52**  
2000km cable DC fault three voltage source converters, real power

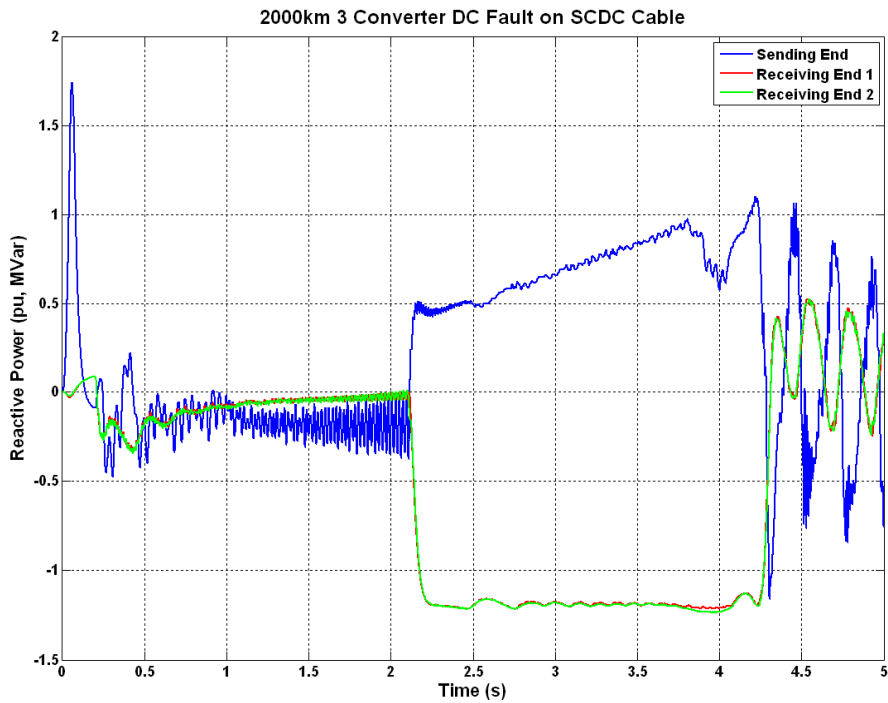


**Figure 6-53**  
2000km cable DC fault three voltage source converters, reactive power

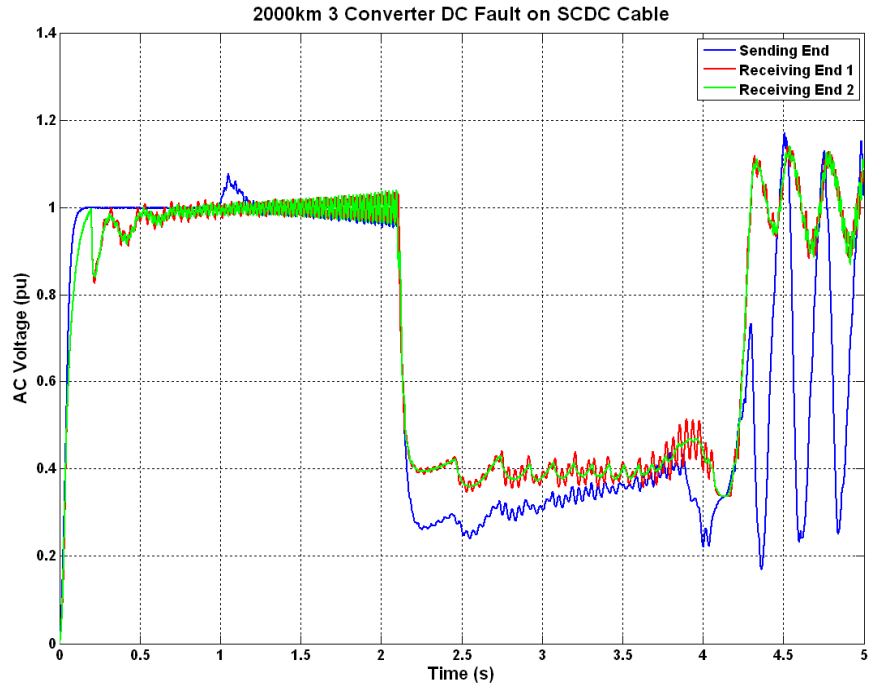


Figure 6-54  
2000km cable DC fault three voltage source converters, AC voltage

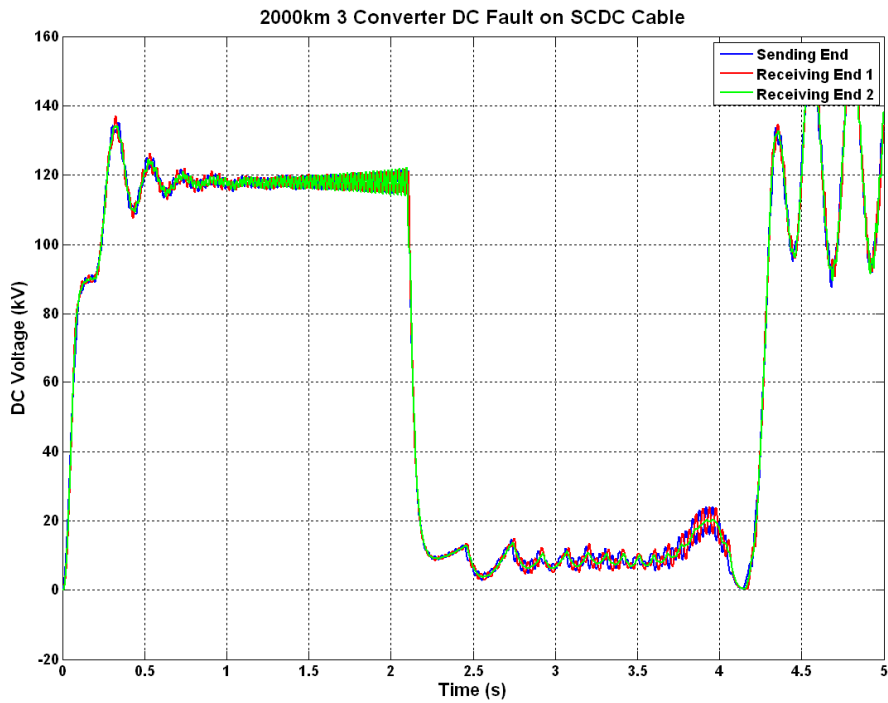


Figure 6-55  
2000km cable DC fault three voltage source converters, DC voltage

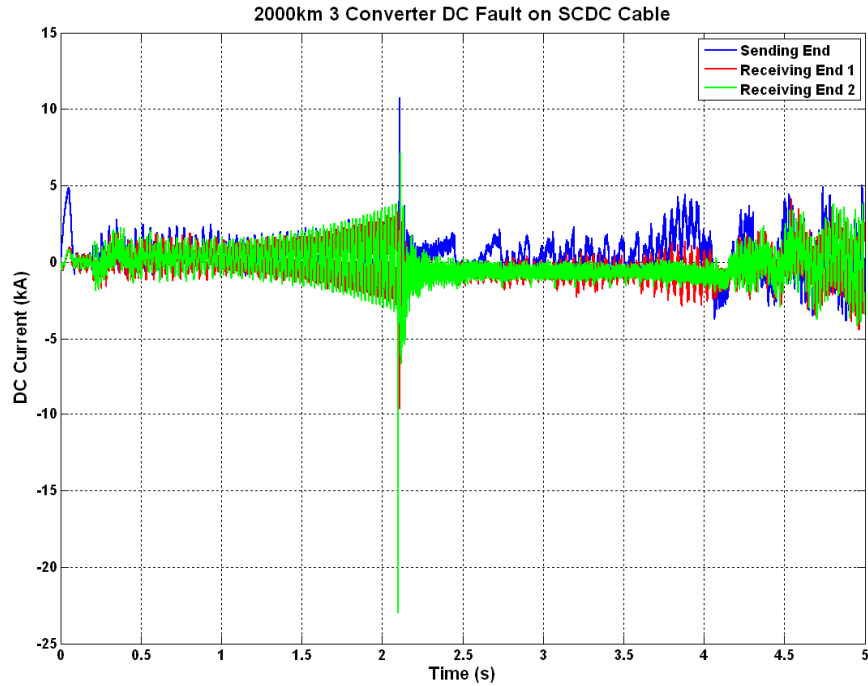


Figure 6-56  
2000km cable DC fault three voltage source converters, DC current

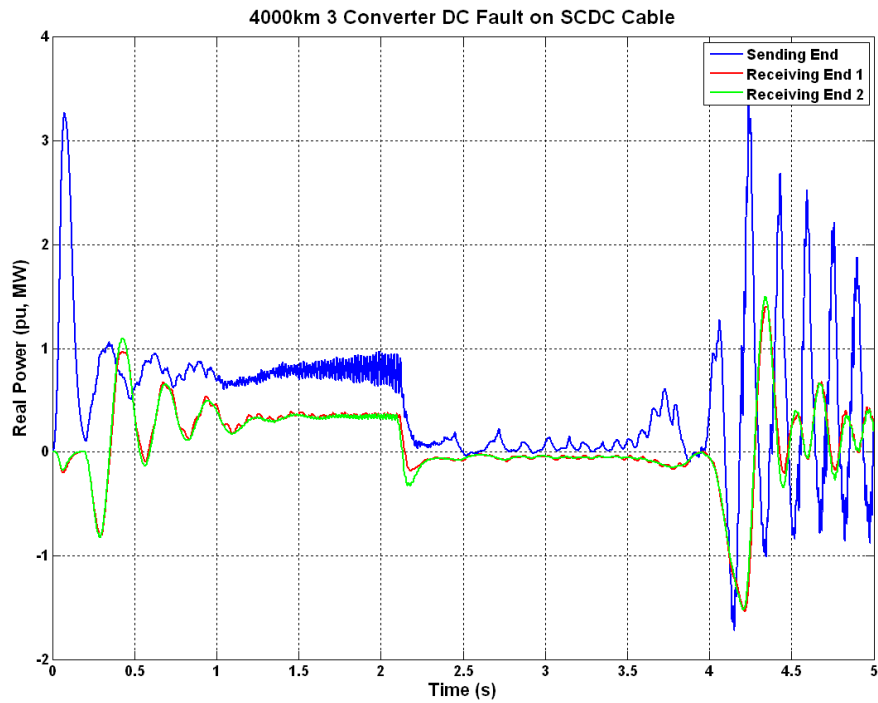


Figure 6-57  
4000km cable DC fault three voltage source converters, real power

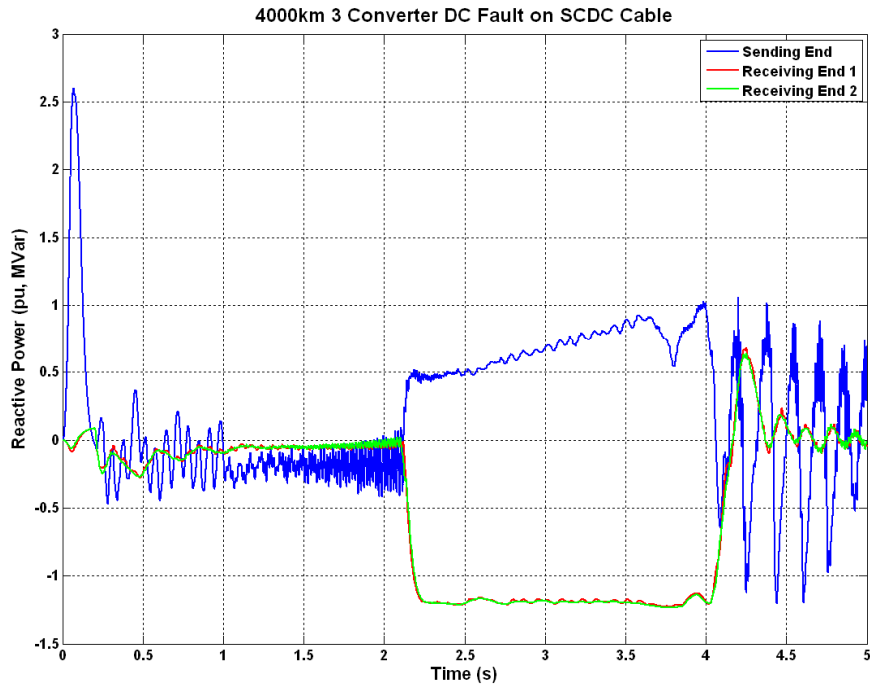


Figure 6-58  
4000km cable DC fault three voltage source converters, reactive power

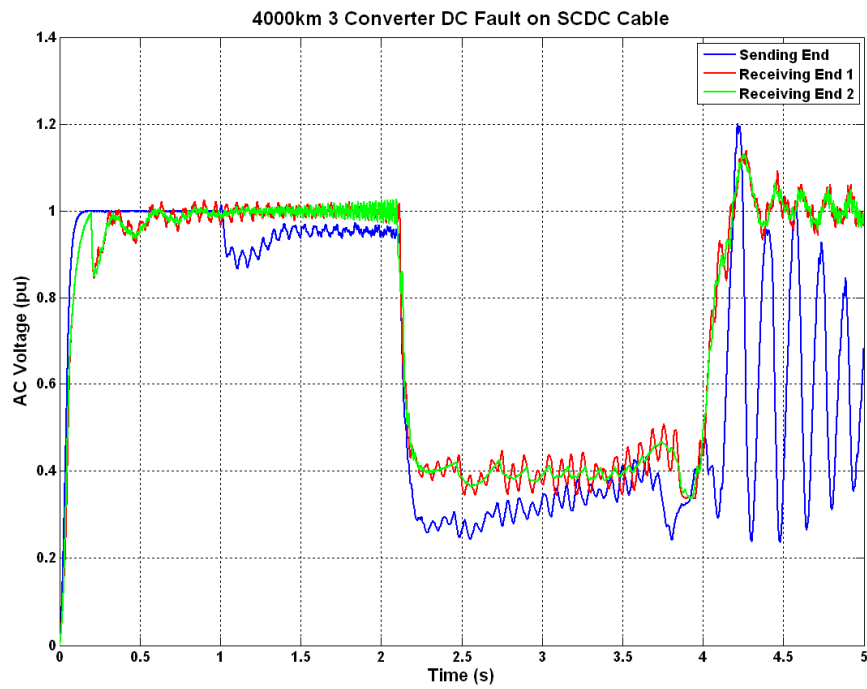


Figure 6-59  
4000km cable DC fault three voltage source converters, AC voltage

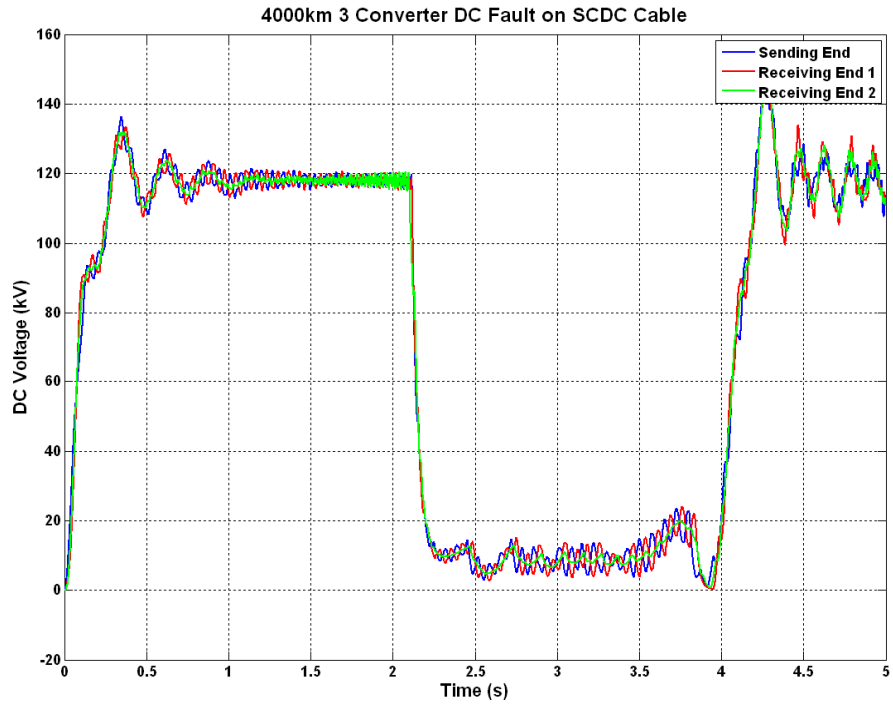


Figure 6-60  
4000km cable DC fault three voltage source converters, DC voltage

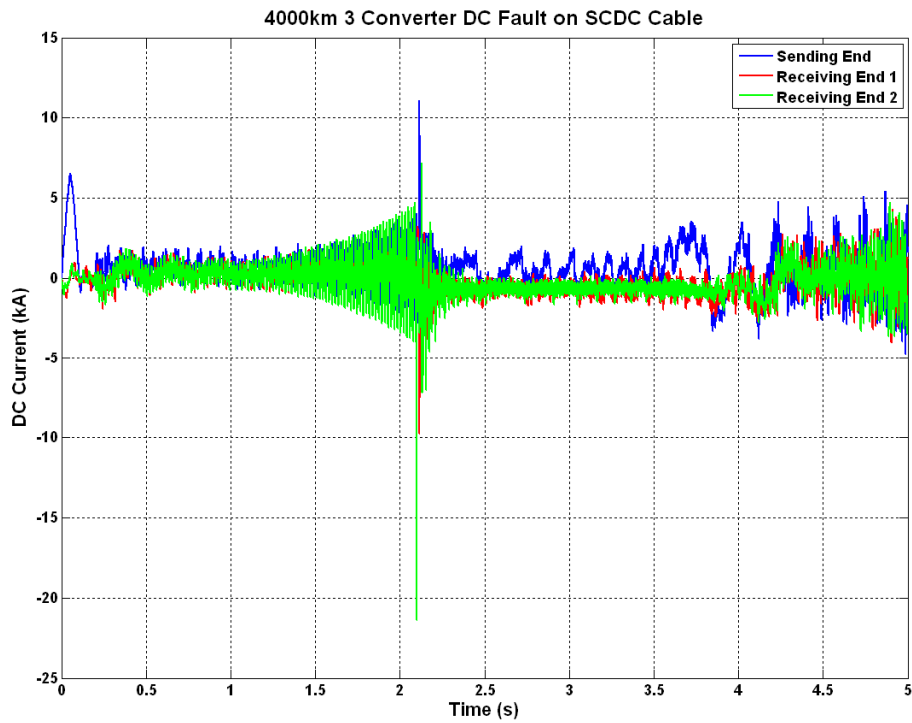
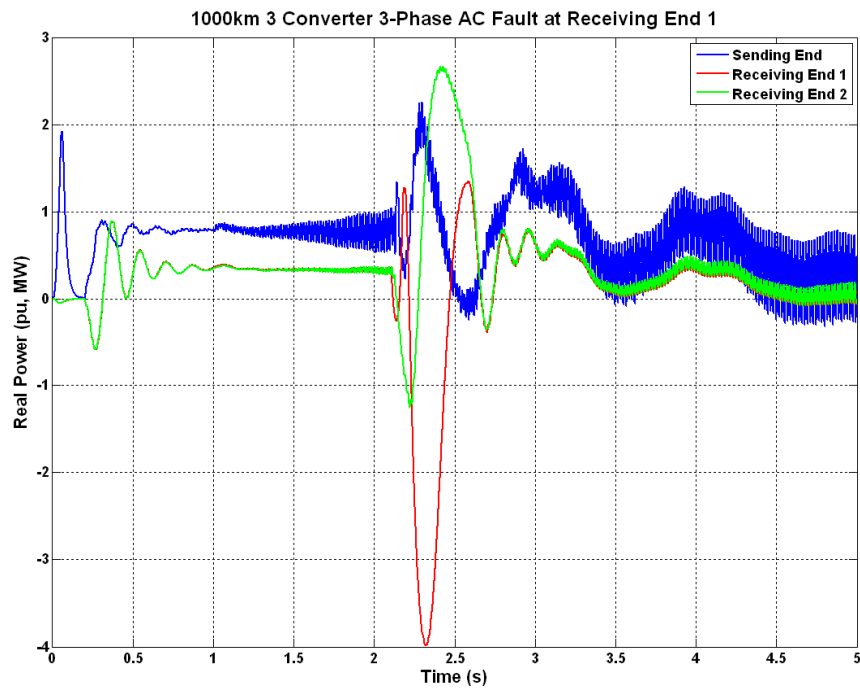


Figure 6-61  
4000km cable DC fault three voltage source converters, DC current

## Superconducting DC System Results – AC Fault with Three Voltage Source Converters

This final section presents the electromagnetic transient study results for a superconducting dc transmission system with three voltage sourced converters under an ac fault condition. The ac fault was applied at ‘Receiving End 1’ at 2.1 seconds into the run. The simulation parameters for this set of cases are identical to that of the parameters in section 6.3, except that there is an additional voltage source converter. This section is also presented without further comment, simply to show that the voltage and current transients on the superconducting dc line after an ac fault are extremely severe, and need to be dealt with using creative solutions to achieve stable operation.



**Figure 6-62**  
1000km cable AC fault three voltage source converters, real power

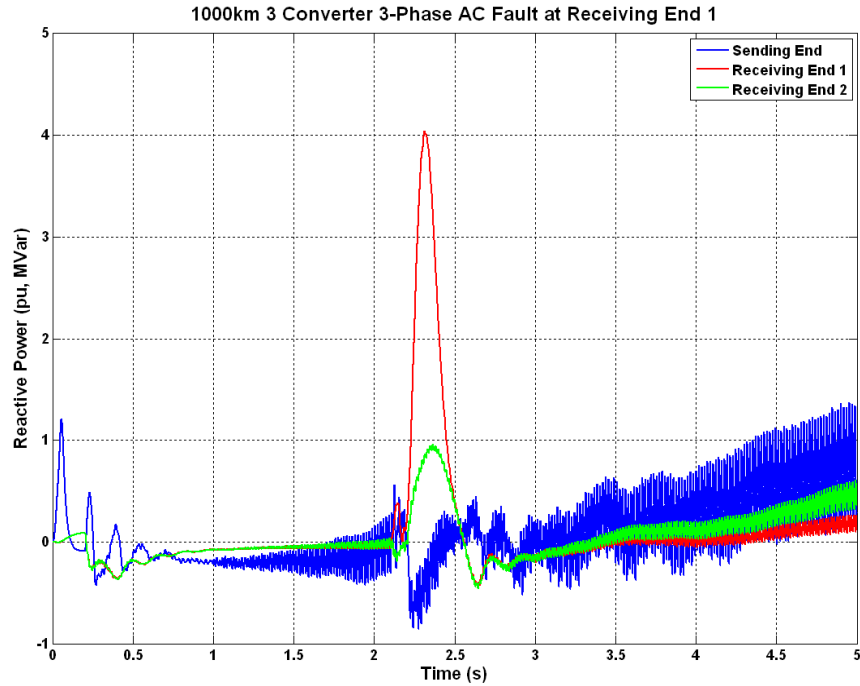


**Figure 6-63**  
1000km cable AC fault three voltage source converters, reactive power

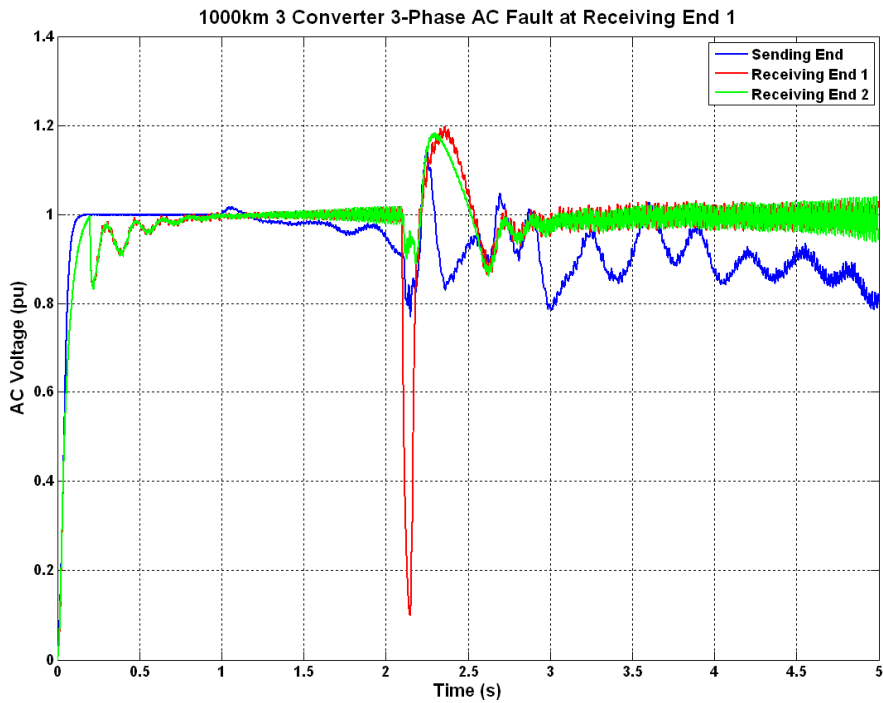


**Figure 6-64**  
1000km cable AC fault three voltage source converters, AC voltage

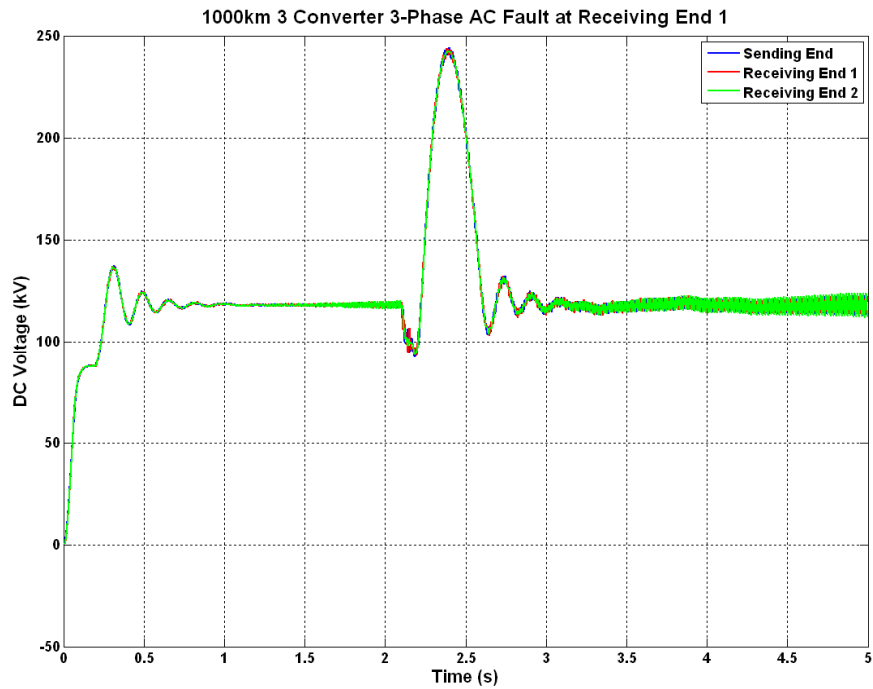


**Figure 6-65**  
1000km cable AC fault three voltage source converters, DC voltage

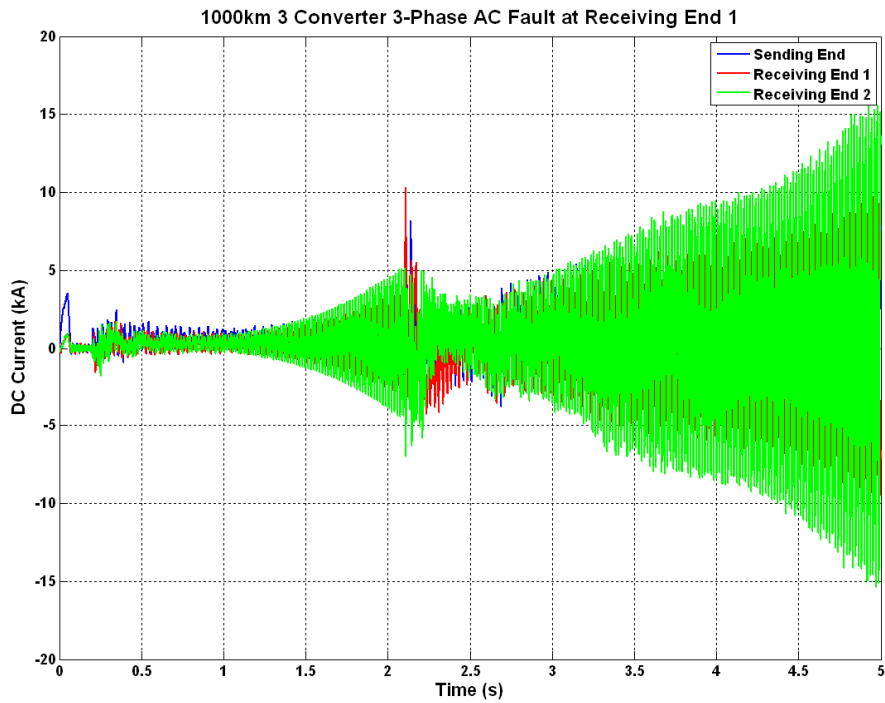


**Figure 6-66**  
1000km cable AC fault three voltage source converters, DC current

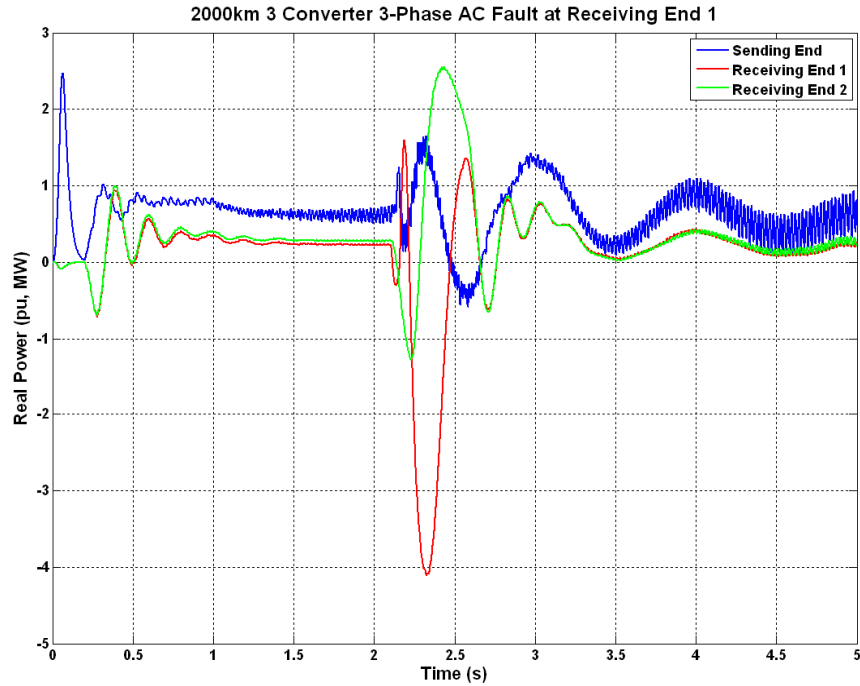


**Figure 6-67**  
2000km cable AC fault three voltage source converters, real power

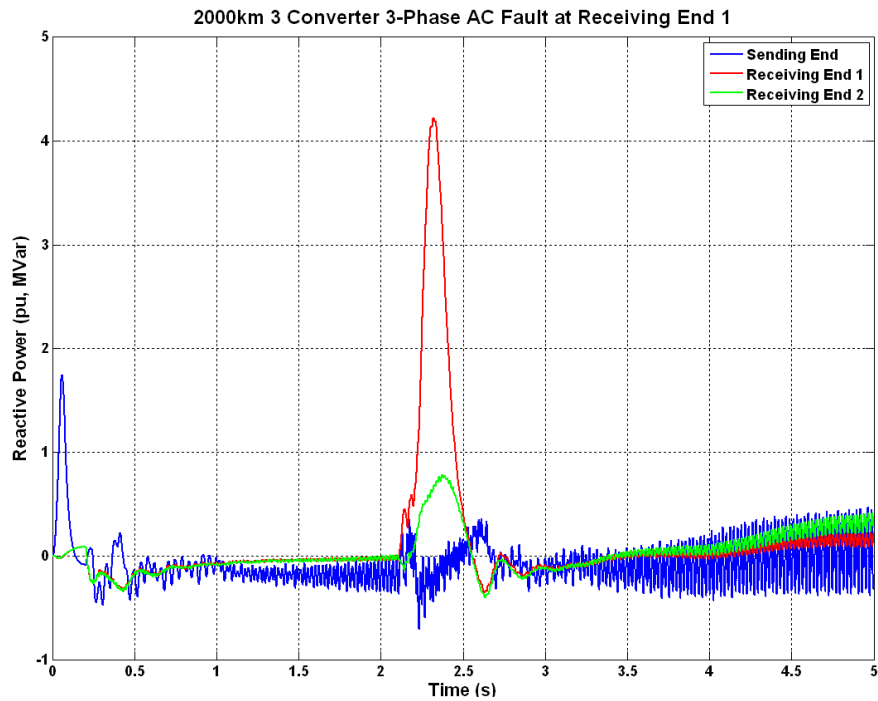


**Figure 6-68**  
2000km cable AC fault three voltage source converters, reactive power

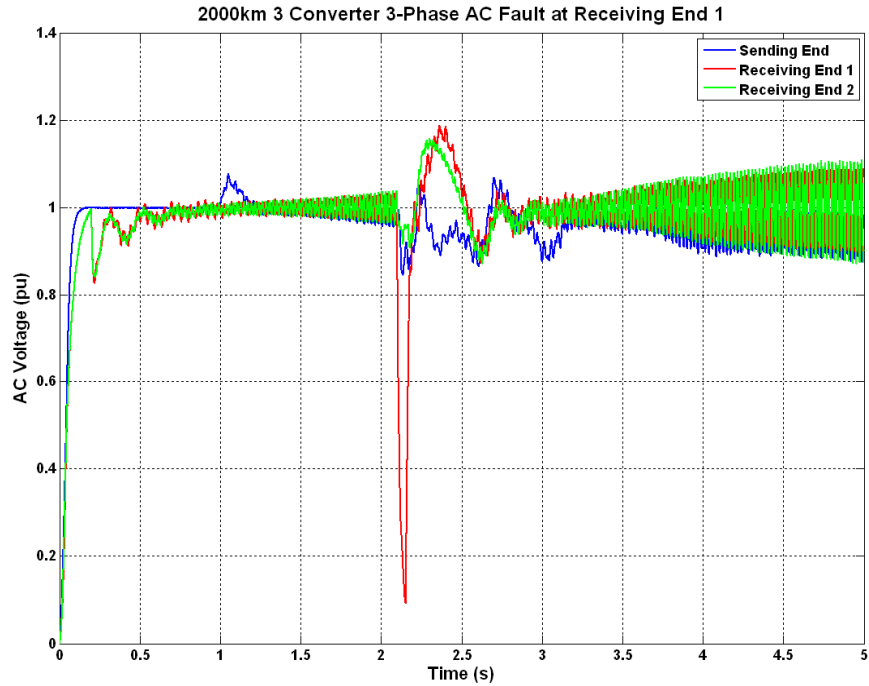


**Figure 6-69**  
2000km cable AC fault three voltage source converters, AC voltage

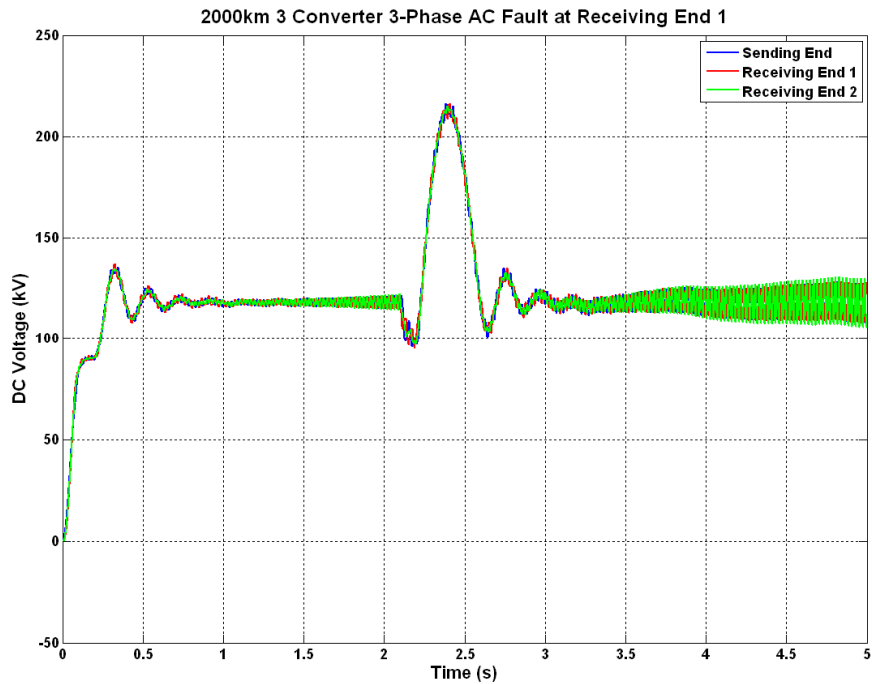


**Figure 6-70**  
2000km cable AC fault three voltage source converters, DC voltage

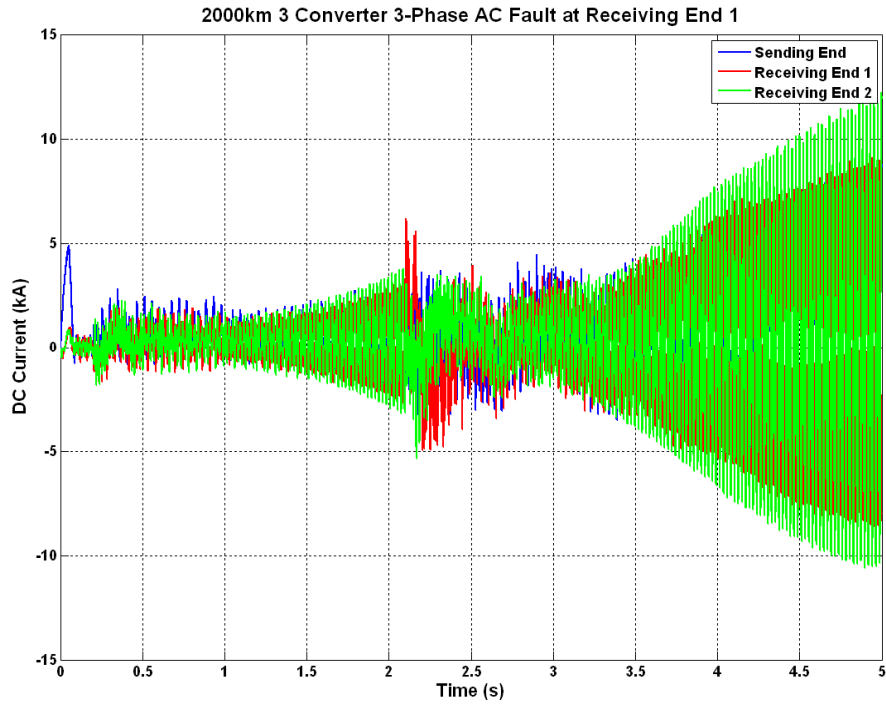


Figure 6-71  
2000km cable AC fault three voltage source converters, DC current

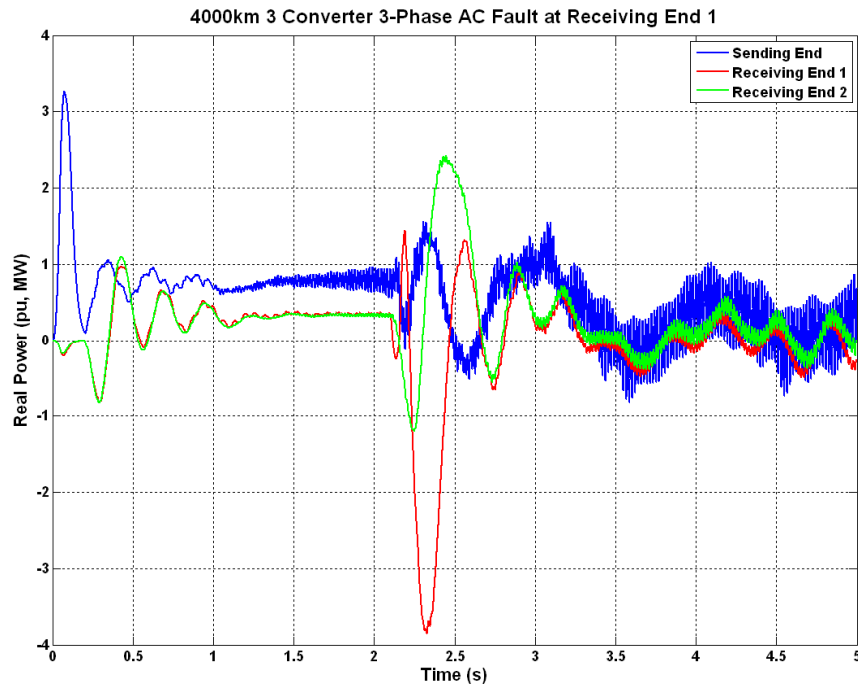
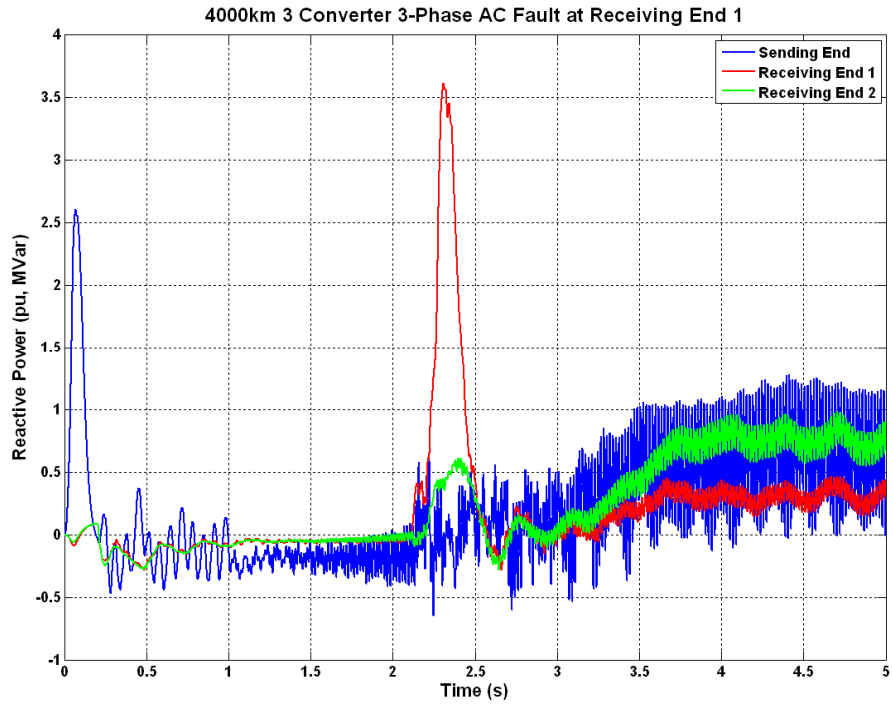
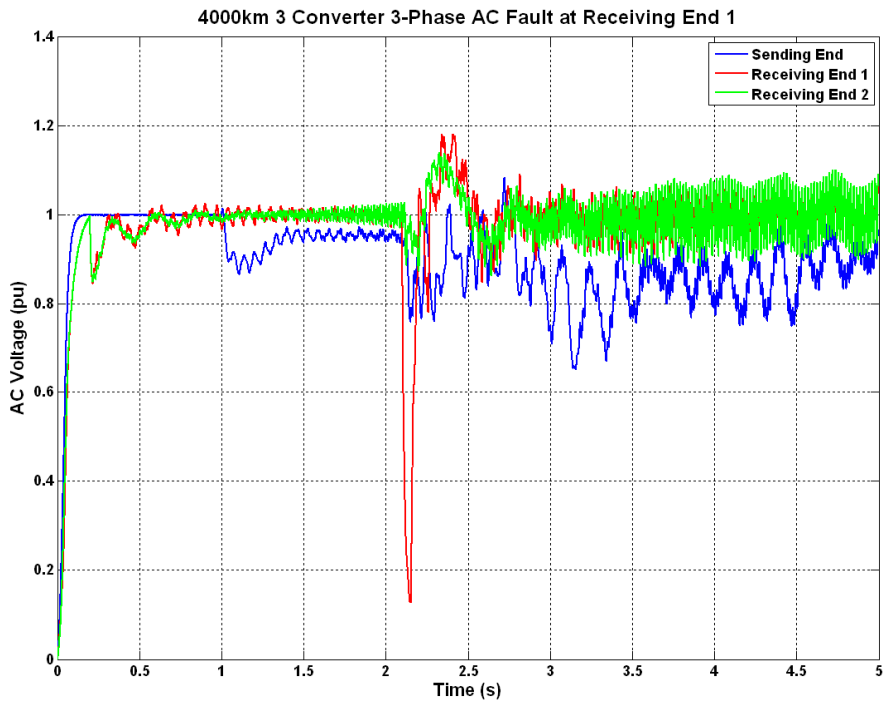


Figure 6-72  
4000km cable AC fault three voltage source converters, real power



**Figure 6-73**  
4000km cable AC fault three voltage source converters, reactive power



**Figure 6-74**  
4000km cable AC fault three voltage source converters, AC voltage

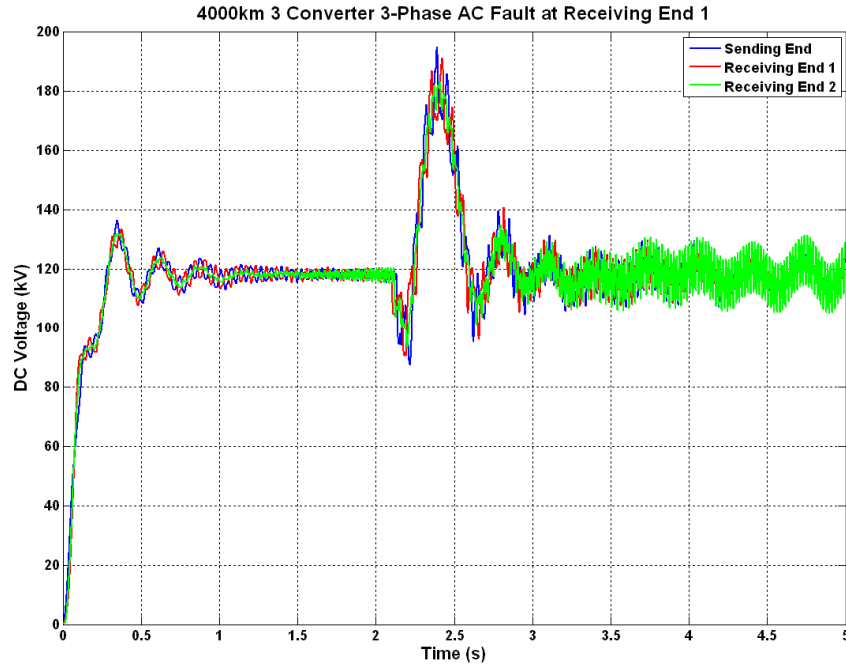


Figure 6-75  
4000km cable AC fault three voltage source converters, DC voltage

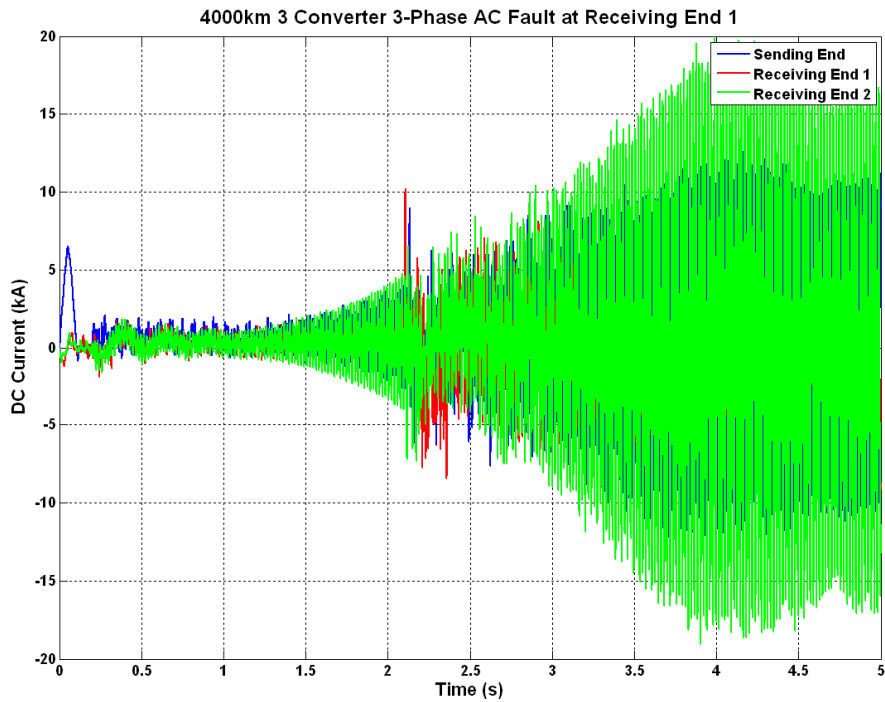


Figure 6-76  
4000km cable AC fault three voltage source converters, DC current



# 7

## VOLTAGE SOURCE CONVERTER – HIGH VOLTAGE DC CONTROLS

The principal characteristic of a high voltage dc (HVDC) station based on a voltage source converter (VSC) is its ability to independently control the reactive and real power flow at each of the ac systems. In contrast to line-commutated HVDC transmission, the polarity of the dc link voltage remains the same with the dc current being reversed to change the direction of power flow.

A typical VSC–HVDC station is shown in Figure 7-1. The HVDC station consists of a voltage source converter connected to dc cables. Today the maximum power handling of the system of at least 1000 MW at 300 kV dc is available from several vendors. The VSCs are three-phase, two-level, six-pulse bridges, employing insulated gate bi-polar (IGBT) power semiconductors. The relative ease with which an IGBT can be controlled, as well as its suitability for high frequency switching, make this device the better choice over gate-turn-off (GTO) and conventional thyristors. The converters are connected to phase reactors, which are connected to the ac system through conventional power transformers. The reactors are used for controlling the active and reactive power flow by regulating the current through them and for reducing the high frequency harmonic content of the ac line current caused by the switching of the VSCs. Tuned shunt filters are needed to reduce the high frequency switching ripple on the ac voltage and current. The transformers transform the ac system voltage to a value suitable for the converter. The dc capacitors provide an energy buffer to keep the power balance during transients and reduce voltage ripple on the dc side.

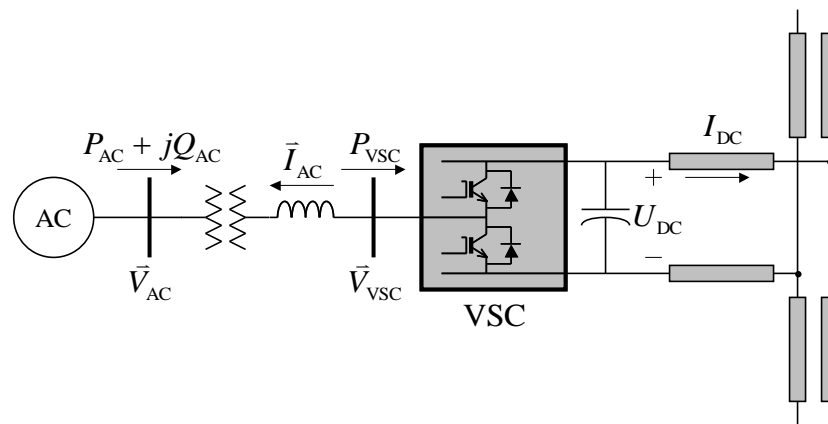


**Figure 7-1**  
**One-line diagram of a VSC-HVDC converter station**

The dc capacitor size is characterized as a time constant  $\tau$ , defined as the ratio between the stored energy at rated dc voltage and the rated apparent power of the converter.

$$\tau = \frac{0.5 C_{DC} U_{DC\_Nominal}^2}{S_{Nominal}} \quad \text{Equation 2}$$

where  $U$  denotes the nominal dc voltage and  $S$  is the nominal apparent power of the converter.

## Dynamic Model of the VSC-HVDC Converter Station

The converter and controls presented in this report are for dynamic/electro-mechanical transient analysis. The appropriate time step size for these models are in the range of 1 to 10 milliseconds. This work provides a simplified control model, which handles the higher level controls that solve for the ac terminal voltage phasor of the voltage-source converter. Algebraic equations map the dynamic voltage phasor to the active and reactive power flows on the ac side of the converter and the direct current and voltage on the other side.

The consequence of using a simplified model is primarily the elimination of lower level architecture such as the firing control. Details such as the phase-lock loops, dq-axis representation, and pulse width controls are condensed into equivalents.

A simplified one-line diagram of a VSC-HVDC converter station is shown in Figure 7-1. Its dynamic equivalent circuit is shown in Figure 7-2. At the system interface bus, voltage,  $V_{AC}$  is the fundamental-frequency phasor. On the secondary side of the transformer, the VSC's ac terminal bus has the output voltage phasor  $V_{VSC}$ .

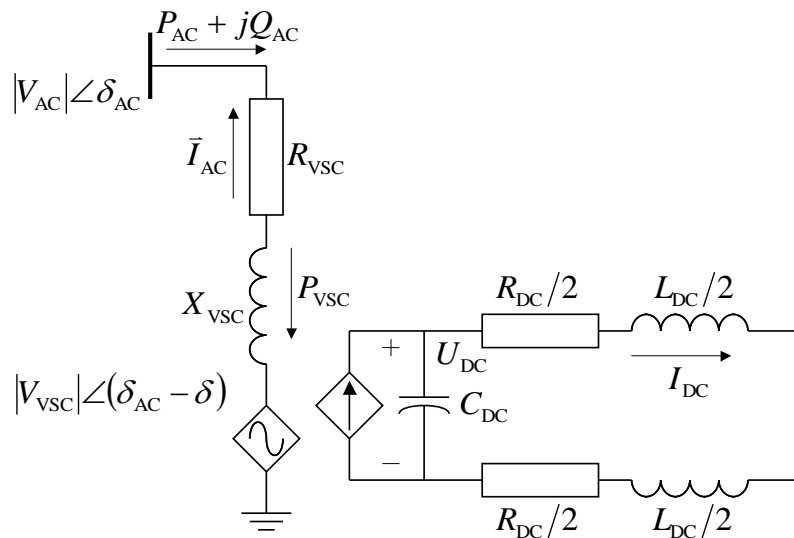


**Figure 7-2**  
Dynamic equivalent circuit of a VSC-HVDC converter station

$V_{VSC}$  is the fundamental phasor of the converter’s output voltage.  $\delta_{AC}$ , is the phase angle of voltage  $V_{AC}$ .  $\delta$  is the phase angle between  $V_{VSC}$  and  $V_{AC}$  (also denominated as the shift or power angle relative to  $V_{AC}$ ).  $P_{AC}$  and  $Q_{AC}$  are the active and reactive power absorbed from the ac side of the system by the converter.  $P_{DC}$  is the active power injected onto the dc side of the converter. Assuming no losses in the converter, it is equal to  $P_{VSC}$ .  $I_{AC}$  is the phasor current injecting from the converter to the ac system.  $R_{VSC}$  and  $X_{VSC}$  are the resistance and reactance of the interfacing transformer.  $C_{DC}$  is the capacitor on the dc side of the converter.  $R_{DC}$  and  $L_{DC}$  represent the resistor and inductor of the dc transmission line.

### Model of VSC-HVDC Control System

Based on the PWM control technology for conventional HVDC cable systems, the amplitude and phase angle of the VSC output voltage are regulated independently and rapidly by the modulation ratio  $M$  and the power angle  $\delta_{VSC}$ . With these two control variables, the VSC can control the active and reactive powers in all four quadrants.

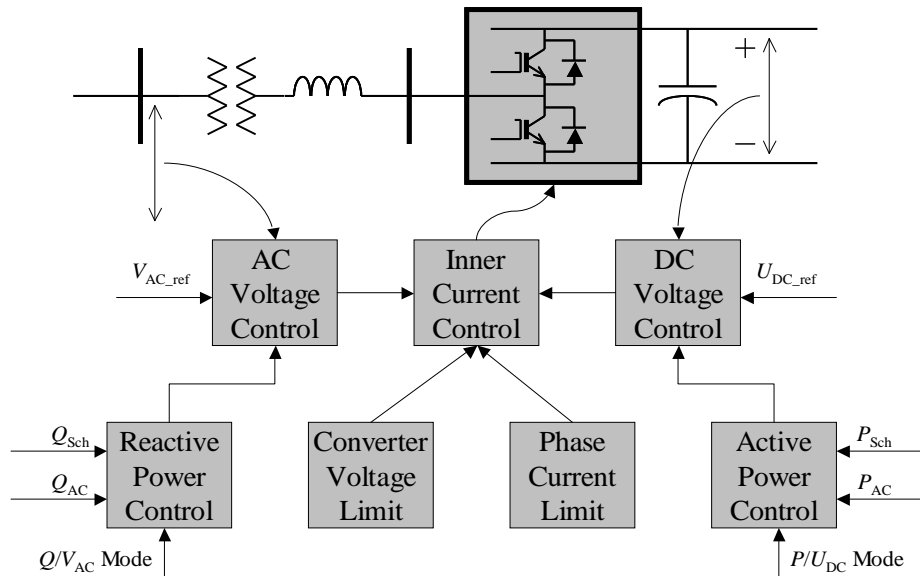


**Figure 7-3**  
Hierarchical control diagram for the VSC-HVDC converter

The output voltage,  $V_{VSC}$ , is dependent on the dc bus voltage,  $V_{DC}$ , and the timing of the sinusoidal PWM switching sequence. The following relationship models the ac output voltage of the converter.

$$V_{VSC} \angle \delta_{VSC} = \left| \frac{\mu M}{\sqrt{2}} V_{DC} \right| \angle (\delta_{AC} - \delta) \quad \text{Equation 3}$$

From the calculated converter voltage phasor, the ac system can be solved. The active power injection to the converter is mapped to the dc side of the converter. From the measured dc voltage, the dc current can be computed.

There are two sets of optional control objects for each VSC-HVDC converter station. They are (i) the active power,  $P_{AC}$ , or the dc bus voltage,  $U_{DC}$  and (ii) the reactive power,  $Q_{AC}$ , or the amplitude of the ac bus voltage  $V_{AC}$ . Under normal operation conditions, each converter can control its reactive power independent of the other converter stations. However, the active power injected into the VSC-HVDC inner dc system must be balanced. Active power flowing out from the dc network must equal the active power flowing into the dc network less any losses in the network. Any difference in flows will cause the dc voltage to increase or decrease. In order to achieve the active power balance automatically, one of the converters must select the dc-voltage mode as the control object. The other converters can control active power at any value within the capacity limits.

The transfer-function block diagram of the four primary controllers for the converter is based on the proportional integral (PI) regulator. These controllers are shown in Figure 7-4. Four measurements and four set points provide input to the controls. Measurements and their corresponding set points include:

- Active power flowing on the ac side and the scheduled power flow
- Reactive power flowing on the ac side and the scheduled power flow
- Voltage magnitude on the ac side and the reference ac voltage
- Voltage magnitude on the dc side and the reference dc voltage

For the primary control functions, there are four reference values,  $P_{Sch}$ ,  $Q_{Sch}$ ,  $U_{ref}$  and  $V_{ref}$ , for the corresponding control objects. Time constants,  $T_{Pmeas}$ ,  $T_{Qmeas}$ ,  $T_{Umeas}$  and  $T_{Vmeas}$ , model the time delays for the measurements. The PI controls use proportional factors:  $K_P$ ,  $K_Q$ ,  $K_U$ , and  $K_V$ , and integral time constants:  $T_P$ ,  $T_Q$ ,  $T_U$ , and  $T_V$ . The remaining parameters are associated with the active power damping during transient events, and are described next. Suggested values for the parameters are provided in Table 7-1, Table 7-2, and Table 7-3.

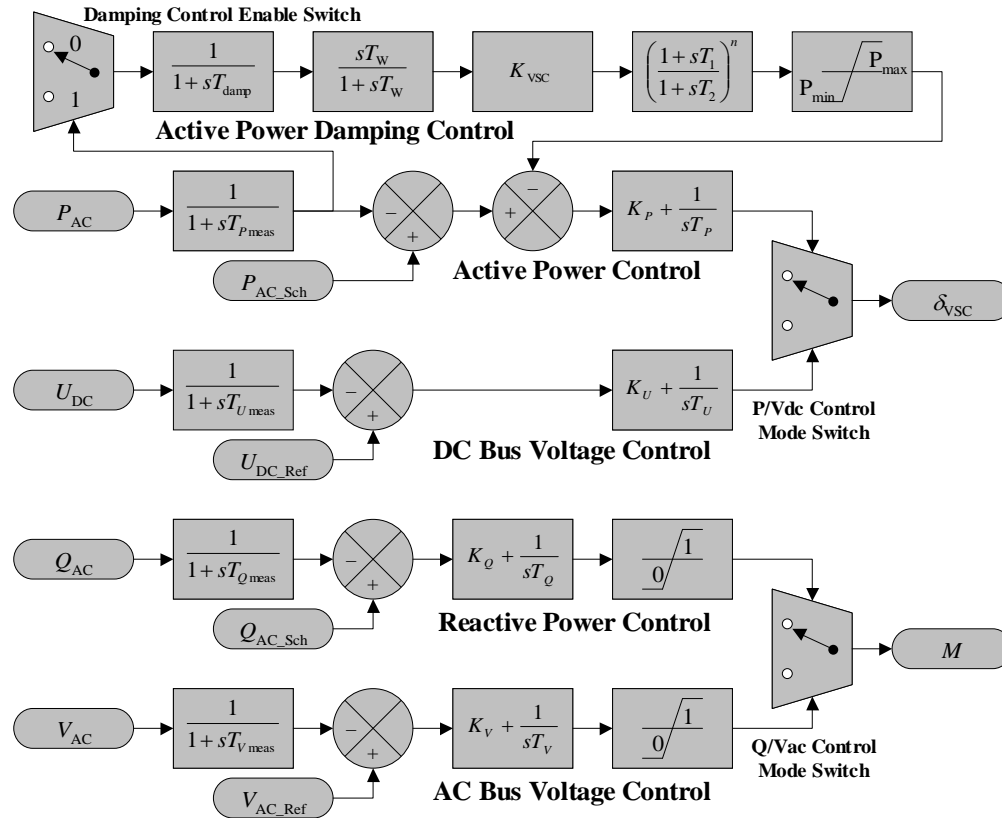


**Figure 7-4**  
Transfer-function block diagram of the simplified VSC-HVDC controls

### Transient Damping Control

In order to improve the damping characteristic on low frequency oscillations, it is necessary to add another damping controller to the VSC-HVDC. This control adjusts the active power transmitted by the VSC-HVDC during transient events. The active power of the ac line at one of the converter stations is selected to provide the damping control. The parameters of the damping controller are shown in Table 7-2.

**Table 7-1**  
Active power/DC bus voltage control parameters

Parameter	Value
$T_{P_{meas}}$	0.02
$K_P$	0.052
$T_P$	0.115
$T_{U_{meas}}$	0.005
$K_U$	0.5
$T_U$	0.04

**Table 7-2**  
**Active power damping control parameters**

Parameter	Value
$T_{damp}$	0.005
$T_w$	10.0
$K_{VSC}$	1.5E3
$T_1$	0.55
$n$	0.2
$T_2$	2
$P_{max}$	0.5
$P_{min}$	-0.5

**Table 7-3**  
**Reactive power/AC bus voltage control parameters**

Parameter	Value
$T_{Qmeas}$	0.02
$K_Q$	0.03
$T_Q$	0.20
$T_{Vmeas}$	0.01
$K_V$	0.03
$T_V$	0.20

## Operation Modes

The VSC-HVDC converter station can be operated in several modes; examples include:

1. *Reactive power control.* Each converter operates independent of each other. The reactive power order could be selected to best suit the ac system, or could be modulated with an auxiliary input from some external control.
2. *AC voltage control.* Each converter operates independent of each other. The ac voltage order is normally constant, but may also be modulated with an auxiliary input from some external control.
3. *Active power modulation.* One converter acts as an active damping control, frequency control etc.
4. *Passive net operation.* Operation on a passive system or at black start with no other voltage source present.

For the test cases of the superconducting dc cable project, the following initial operating modes have been defined. Both the  $\delta$  and M modes of operation are defined for each converter station. As needed one of the converter stations may be used for damping oscillations by activating the active damping controls.

**Table 7-4**  
**Control modes for the converters stations in the seven-node test system**

<b>Converter</b>	<b><math>\delta</math>-Mode</b>	<b>M-Mode</b>
Sub-system 1	V_DC	Q_AC
Sub-system 2	P_AC	Q_AC
Sub-system 3	P_AC	Q_AC
Sub-system 4	P_AC	Q_AC
Sub-system 5	P_AC	V_AC
Sub-system 6	P_AC	Q_AC
Sub-system 7	P_A	Q_AC

**Table 7-5**  
**Control modes for the converters stations in the six-node test system**

<b>Converter</b>	<b><math>\delta</math>-Mode</b>	<b>M-Mode</b>
Sub-system 1	V_DC	Q_AC
Sub-system 2	P_AC	Q_AC
Sub-system 3	P_AC	Q_AC
Sub-system 4	P_AC	V_AC
Sub-system 5	P_AC	V_AC
Sub-system 6	P_AC	Q_AC



# A

## VOLTAGE SOURCE CONVERTER FUNCTIONAL SPECIFICATIONS

---

### **Voltage Source Converter Functional Specifications for Superconducting DC Multi-Terminal Operation**

This appendix defines a typical document for specifying the performance and design requirements for a voltage source converter (VSC) power conversion system, as part of a multi-terminal superconducting dc cable system. The system is intended to transport, absorb, and deliver power at several points that will be interconnected with the ac transmission grid. The system will also provide continuous reactive power for utility network support.

This specification is intended to convey to those familiar with utility operations the unique requirements for operation of a VSC in the utility environment. However, the specification is not intended to convey all of the requirements for the VSC system. The VSC system supplier is responsible for the design of the VSC and is expected to do all that is necessary to ensure that the VSC is fit for its intended purposes. The control system and special active and passive filtering capability for the operation of multiple VSC connected together via superconducting cable will need a special feature of these converters.

### **Sample Document**

The VSC includes all components between the dc power terminals on the superconducting cable and the connections to a 3-phase, 60 Hz line. The VSC shall be self-commutated, and shall contain a voltage source ac-to-dc converter, ac filters, shorting switches and buses, internal wiring and buses, instrumentation, and a controller as specified herein.

The VSC shall provide independent four-quadrant (active and reactive) compensation for variations in the network voltage and frequency and superconducting dc cable power variations. The VSC shall measure the voltage, current, frequency, and frequency rate of change on the ac line, and shall compute appropriate levels of active and reactive power to inject or absorb from the line in each of several modes of operation.

Operator selection of VSC operating modes, and transmission of VSC operating status will be accomplished by discrete or analog signals transmitted between the VSC and the utility supervisory control and data acquisition (SCADA) system via a utility provided remote terminal unit.

The VSC shall be designed and constructed for integrated power utility operation and minimum life cycle cost. Life cycle cost shall include the costs of capital, operating inefficiency, downtime, and maintenance.

## **1. Applicable Codes and Standards**

The following codes and standards are part of this specification to the extent referenced herein.

### **1.1 Codes and Standards**

Unless otherwise specified, all VSC equipment, components, and services shall meet the design, test, system performance, and quality control requirements of this specification and applicable ANSI, IEEE, NEMA, NESC, NEC IEC, OSHA, ASTM, AEIC, ICEA, UL, ASME, EIA, FCC, and NFPA.

## **2 Requirements**

### **2.1 Item Definition**

The VSC includes the functions specified herein, interconnecting cables, wiring, and ancillary parts as required to meet the performance requirements when connected to the magnet, a utility provided SCADA remote terminal unit, and the utility power grid.

#### **2.1.1 Item Diagram**

The VSC shall contain the major elements shown on the electrical interconnection diagram (TBD).

#### **2.1.2 System Interfaces**

##### **2.1.2.1 Utility AC Line Interface**

- a. The VSC shall have a physical interface with the utility grid at the secondary side of a 230 kV (primary) / 115 kV (secondary) interface transformer. The utility interface transformer and breakers will be provided by the utility.
- b. Utility line characteristics and VSC performance shall be measured at a point of common coupling on the 230 kV side of the interface transformer provided by the utility. Current and potential measurement transformers will be provided by the utility.

##### **2.1.2.2 Auxiliary Power Interface**

- a. The utility shall supply auxiliary power for the converter at 4160 V, 480 V, 240 V, and 120 V.
- b. The VSC shall have an uninterruptible power supply (provided by VSC supplier) to allow for safe disconnect from the utility interface transformer and controls operational (for at least 45 minutes).
- c. The utility will also supply dc power for the trip mechanism of the ac breakers.

### **2.1.2.3 Command Interface**

The VSC controller shall interface to a utility provided SCADA remote terminal unit as a collection of signal discrete or analog. The remote terminal unit shall transmit operator initiated mode commands as a unique combination of dry contact switch closures. In turn, the VSC shall continuously indicate operating mode by a similar unique combination of signal discretely transmitted to the remote terminal unit interface.

### **2.1.2.4 Superconducting DC Cable Interfaces**

- a. The VSC shall include the dc buses and switchgear required to connect to the magnet dc terminals.
- b. Redundant signals shall be transmitted from the superconducting dc cable system to the VSC.
- c. The inductance of the cable will be TBD Henrys, and the maximum energy stored TBD MJ.

### **2.1.2.5 Site Interface**

- a. The location of VSC units shall be as shown on diagram TBD. The VSC dc buses, high-voltage switchgear and cooling units shall be located outdoors, and an indoor area shall be provided which accommodates the VSC components, their installation and subsequent maintainability.
- b. The environment provided within the VSC facility shall be within the limits to be defined. The VSC shall not require cooling fluids or special environmental control from the facility.
- c. The VSC grounding shall be integrated to the substation grounding grid.

### **2.1.2.6 Data Interface**

The VSC shall have a front panel connector for accessing a VSC generated data stream. The data stream shall consist of VSC measurements and status data.

### **2.1.2.7 Refrigeration System**

The VSC shall have an interface with the RS via a Warning signal discrete. The VSC shall automatically cancel active power interchange on receipt of the warning signal indicating excessive dewar pressure from the superconducting dc cable refrigeration system.

### **2.1.2.8 Cable Monitoring System**

The VSC shall have an interface with the cable monitoring system via an Emergency signal discrete.

## **2.2 Characteristics**

### **2.2.1 Performance**

#### **2.2.1.1 Rated Power**

The VSC shall be capable of continuously delivering to the utility grid, at nominal voltage, rated power of TBD MVA in a four-quadrant form. Due to large ratings of power injected or absorbed by the ac systems the VSC may be composed of several modules and divided into separate groups feeding the two separate cables.

#### **2.2.1.2 Efficiency**

- a. The VSC shall have a one-way efficiency of not less than 95% at rated active power during discharge or charge, including losses on both the VSC and auxiliary power systems.
- b. The VSC shall have a one-way efficiency of not less than TBD %.

#### **2.2.1.3 Utility AC Line Characteristics**

##### **2.2.1.3.1 Voltage**

The VSC shall be capable of continuous operation on the utility line (at reduced power) for voltage deviations between +10/-20% of nominal, and shall tolerate without disconnect a deviation of -50% for at least 150 cycles under transient conditions. It should be understood that the transient voltage conditions represent fault or switching events in the ac network, which can affect one, two or all three phases to a varying degree. These events are typically associated with significant voltage distortion. The VSC shall provide support to the ac network within the inverter allowable transient voltage and current limits. If the VSC operation ceases during the network transient, the VSC system must respond as required in 2.2.1.5.1 upon return of the voltages to within the +10 to -20% band as specified herein.

##### **2.2.1.3.2 Frequency**

- a. The VSC shall be capable of continuous operation on the utility line with frequency deviations of  $60 \pm \text{TBD}$  Hz. The VSC shall automatically synchronize to the utility line.
- b. The VSC shall be capable of continuous operation on the utility line with a frequency rate of change not exceeding TBD Hz/sec. Active power exchange will not occur if the rate of frequency change is greater than TBD Hz/sec. Note that the specified frequency changes represent the electromechanical modes of the power system. Fault and switching operations will cause sudden phase changes in the system voltages, which shall not be interpreted as a rate of change of frequency as specified in this subparagraph. Distorted voltage waveforms arising from geomagnetic induced currents, transformer energizations or other switching events shall not effect the frequency measurements.

### **2.2.1.3.3 Voltage/Current Harmonics, Unbalance, and Subsynchronous Oscillations**

- a. The total harmonic voltage and current distortion introduced by the VSC on the 230 kV (or above) line shall not exceed the recommendations of ANSI/IEEE 519. These limits shall be applied at the point of common coupling with the utility, for voltage unbalance up to 3%.
- b. The VSC shall be designed to preclude exciting subsynchronous resonance and/or oscillations in the utility system.
- c. Protection systems shall consider unbalances where may arise for many reasons including those created by geomagnetically induced currents. Also consideration to carrier frequency interference should be given.
- d. The VSC shall be capable of continuous operation on the utility line with voltage unbalances up to TBD %, and provide correction (within VSC capabilities) for unbalances.

### **2.2.1.3.4 AC Line Protection**

- a. The VSC shall include an ac circuit breaker capable of interrupting the maximum fault power at the utility line physical interface.
- b. Ground fault protection shall be provided by the utility on the high-voltage windings of the utility interface transformer.
- c. The utility interface transformer shall include sudden pressure, over-temperature, over-current, and differential relay sensors. Over-current and differential relay fault conditions shall cause a VSC shutdown.
- d. The VSC shall contain provisions to protect against transient voltage surges from switching, lightning, and similar causes. The utility interface transformer shall contain a grounded electrostatic shield between the high voltage and low voltage windings to prevent the capacitive let-through of steep waveforms caused by lightning and switching surges.
- e. The VSC shall detect a reverse phase sequence and disconnect or not connect if a reverse phase sequence is detected.

## **2.2.1.4 Superconducting DC Cable Characteristics**

### **2.2.1.4.1 Voltage, Current, and Grounding**

- a. The rated operational dc voltage across the magnet terminals shall be 100 kV. For insulation protection purposes an absolute maximum voltage of 250 kV or TBD. The operating voltage limit shall be software programmable at a level less than the rated level.

- b. The superconducting dc cable impedance has a number of resonances that can amplify harmonic voltages and currents. Due to the superconducting nature of the cable, the cable itself provides very little damping. Adequate dc filtering will be required. The component of the VSC voltage (at the resonance frequencies) applied to the superconducting dc cable should not exceed TBD V.
- c. The dc current shall not exceed TBD kA when the superconducting cable is fully loaded, or be less than TBD kA. The superconducting cable shall be considered fully loaded when the current is within TBD of the maximum current.
- d. The maximum allowable dc voltage at superconducting cable terminal to ground shall be TBD. The VSC shall include a sensor to monitor the coil potential with respect to ground.

#### **2.2.1.4.2 DC Isolation and Over-Current Protection**

- a. Two-pole un-fused no-load-break disconnect switches shall be provided for isolating the VSC from the superconducting dc cable and shorting switch for VSC maintenance. The isolation switches shall be operable manually or by the VSC controller.
- b. The design of the VSC shall ensure that the current in the superconducting dc cable does not exceed the maximum value.
- c. The VSC over-current protection device shall clear faults within the VSC, including commutation failures.
- d. The VSC dc link capacitor used in the VSC shall be a self-fusing type for protection and shall be capable of being rapidly charged and discharged as required when subject to the ac system voltage transients. The capability of the capacitors to survive a short circuit from the maximum dc voltage shall be demonstrated in a type test.

#### **2.2.1.4.3 Superconducting DC Cable Protection**

- a. The VSC shall contain a switch connected in series with an energy dump resistor. The switch shall be a normal-open fault-to-close type, with a reaction time of less than TBD seconds after receipt of a detection signal from the superconducting dc cable supervision system to damp the energy on the cable.
- b. The switch shall have a dc voltage rated more than TBD kV, and a life of more than 100 switching cycles.

## 2.2.1.5 Operating Modes

### 2.2.1.5.1 Mode Description

The VSC shall operate in the following modes in response to commands as specified in 2.2.1.7.2:

a. Mode 1 - Variable VAR Compensation (Operator Selected)

When this mode is selected, the VSC shall operate as a variable source of reactive power with no real power exchange (except for losses). The VSC shall calculate and apply reactive power, within its operating range, to minimize the voltage deviation from a preprogrammed voltage set point.

Alternatively, the set point at the VSC front panel can be a reactive power set point. These limits shall be user programmable parameters. The reactive power delivered by the VSC for voltages within the range for continuous operation (-20% to +10%) as defined in 2.2.1.3.1 shall be constrained only by the maximum and minimum voltage and current limits for inductive and capacitive reactive power operation.

For voltage deviations from -20% to -50% the VSC shall remain connected to the grid but will not respond to voltage deviations.

In this operating mode (variable var compensation), the VSC shall apply independent voltage control to each of the three phases to minimize any unbalance in the three phase voltages (minimize negative sequence components).

b. Mode 2 - Frequency Support (Automatic Mode, Operator Enabled/Disabled)

When this mode is enabled, the VSC shall automatically determine the need for frequency support in the event of a network disruption.

This mode of operation shall interrupt operation in Modes 1, 3, or 6. This mode shall terminate when spinning reserve is able to maintain the line frequency at a software programmable level.

The VSC shall initiate frequency support when system frequency falls below a threshold that is software programmable (but not less than TBD Hz) and the frequency rate of change is less than TBD Hz/sec. Power shall be supplied to the line at a level determined by the VSC until the frequency recovers to a value that is also software programmable (but not greater than TBD Hz).

The time to initiate frequency support after crossing the low-frequency threshold shall not exceed TBD milliseconds. Also, this response time shall be met after recovery of the ac system from disturbances in the ac network.

When the VSC active power output is less than maximum rated power, the VSC shall, while maintaining the active power transfer, use available capacity of the VSC for reactive power control as defined in variable VAR compensation mode.

The VSC shall inject or absorb power into the superconducting dc cable system at a TBD charging rate.

c. Mode 3 - Combined Operation (Operator Selected)

When this mode is selected, the VSC shall operate with independent control of active and reactive power in a four-quadrant form up to the rated apparent (MVA) power.

The VSC shall calculate and apply the real and reactive power levels required to stabilize the line frequency and voltage. The frequency deviation range and frequency rate of change for which the VSC will respond for frequency stabilization purposes shall be software programmable.

In order to stabilize the system frequency, the VSC shall inject or absorb real power in a steady or oscillatory form.

The VSC shall automatically switch to variable VAR compensation mode on receipt of a warning from the superconducting dc cable supervisory system.

d. Mode 4 - Disconnect / Reconnect (Automatic)

The VSC shall automatically disconnect from the utility bus (secondary side of the utility interface transformer) for voltage or frequency deviations in excess of TBD or from an internal fault. After the voltage or frequency returns to within specified limits, the VSC shall automatically reconnect to the line after a (which is software programmable within the limits of TBD seconds) to support the system in the mode that was selected before the power disconnect.

This mode of operation shall interrupt any mode, except Mode 9.

e. Mode 5 - Startup / Restart (Manually Selected from VSC Console)

When this mode is selected, the VSC shall connect to the secondary side of the utility interface transformer. The VSC shall inject power into the superconducting dc system.

f. Mode 6 - Standby (Operated Selected)

When this mode is selected, the VSC shall close the electronic shorting switch and remain connected to the utility line but shall not provide active or reactive power in response to system deviations.

g. Mode 7 - Manual Disconnect (Operated Selected)

When this mode is selected the VSC shall discharge all the energy on the superconducting dc cable system to the utility grid at a programmable power level, disconnect from the secondary side of the utility interface transformer when the maximum current is reached, discharge the dc capacitor, and close the mechanical coil shorting switch.

- h. Mode 8 - Manual Shutdown, Discharge (Manually Selected from VSC Console)  
When this mode is selected, the VSC shall discharge the superconducting dc cable and then shall close the mechanical shorting switch and disconnect from the utility line. The discharge shall be at an initial programmable constant power output.
- i. Mode 9 - Emergency Shutdown, Discharge (Automatic or Operator Selected)  
In response to a signal from the superconducting dc cable supervisory system, the VSC shall automatically activate the dumping of cable energy.

#### **2.2.1.5.2 Superconducting DC Cable Discharge Requirements**

- a. The VSC shall be capable of tracking the superconducting dc cable current and controlling the dc discharge voltage to produce a constant power output. The power level shall be variable up to the rated power.
- b. In case of operation in manual shutdown, discharge (Mode 8), the VSC shall calculate and apply discharge power profiles to minimize frequency and voltage deviations in the utility system. The VSC shall discharge the coil with a power level not to exceed TBD MW and with a droop characteristic between TBD % and TBD % that shall be software programmable.

#### **2.2.1.5.3 Superconducting DC Charge Requirements**

- a. During initial coil charging, the charging rate and the value of current at the end of a charging interval shall be programmable at the VSC front panel and limited to values specified in 2.2.1.4.1.
- b. During cable injection, the VSC controller shall automatically initiate and carry out the power transfer required. The charging rate and current shall be software programmable and limited to values specified in 2.2.1.4.1.

#### **2.2.1.5.4 Operating Mode Changes**

- a. The time to initiate any mode after selection, or to change from any selected mode to another selected mode, shall not exceed TBD seconds unless otherwise specified.
- b. The VSC shall sustain operation in the selected mode until a command is received to change to a new mode, or until initiation of frequency support, emergency shutdown, or an superconducting dc cable supervisory system.

#### **2.2.1.6 Auxiliary Power**

- a. Auxiliary power at required voltage levels will be supplied for VSC components such as fans and the control system. The power required to operate the VSC system at rated load shall not exceed TBD kW on a continuous basis as specified in the ICD. The VSC system shall not be damaged by loss of auxiliary power for an indefinite period.

- b. The VSC shall safely disconnect from the utility line in the event that auxiliary power is lost.

## **2.2.1.7 Control and Instrumentation**

### **2.2.1.7.1 General**

- a. Master control of the superconducting dc cable system facility will be implemented through the utility provided remote terminal unit, which is connected to the VSC. A slave capability for mode selection shall be provided at the VSC controller front panel.
- b. VSC-generated status discrete shall be transmitted to the remote terminal unit interface, and shall be accessible at the VSC controller front panel. VSC data displays shall be adequate to present system status and fault conditions, and to permit timely detection and isolation of problems and identification of faulty units at the lowest field-repairable level. The VSC front panel shall conform to IEEE Standards.
- c. The VSC controller shall prevent any commands from operating the VSC in a manner that is unsafe, or potentially damaging to the VSC, the superconducting dc cable system, or the utility.
- d. All superconducting dc cable operation and other parameter values necessary for verification of operation and performance shall be stored in non-volatile memory such that the VSC can resume operation without reloading data after a loss of line or auxiliary power, or after a shutdown due to a fault. Also logging the time and specific operator inputs shall be required for diagnostic and performance analysis.
- e. The design of the VSC (including wiring configuration) shall be such as to prevent power circuits from interfering with control and logic circuits. Logic or control printed circuit boards shall not contain high voltage or high current circuits. Wiring associated with logic functions shall be twisted pair(s) shielded cables.

### **2.2.1.7.2 Voltage Source Converter Controls**

- a. The VSC shall provide for manual selection of all modes. A key lockout of all front panel functions shall be provided.
- b. All control functions shall be entered with a keyboard at the VSC front panel. Operator initiated mode commands and variable var compensation (var or voltage levels) shall be received by way of the SCADA remote terminal unit interface.

### **2.2.1.7.3 Voltage Source Converter Instrumentation and Displays**

- a. The VSC shall measure the line voltage, current, frequency, and frequency rate of change with sufficient accuracy that superconducting dc cable system response to disruptions shall be capable of maintaining the line frequency and voltage within the programmable limits.

- b. The VSC shall measure, display on the VSC front panel and make accessible at least the following data:
  - 1) DC current at superconducting dc cable terminals
  - 2) Average dc voltage at superconducting dc cable terminals
  - 3) Average voltage across link capacitor
  - 4) AC voltages
  - 5) AC currents
- c. The VSC shall transmit the following:
  - 1) Current VSC operating mode discretetes
  - 2) Go/No Go (Pass / Fail) discrete
  - 3) AC and dc switchgear discretetes
- d. Overall resolution of measurement accuracy shall be TBD % of full scale reading. The time resolution and range of the measurements shall be consistent with transient and trend analysis, considering the expected time variations and parameter ranges.
- e. Digital meters shall be used to continuously display voltage and current at the storage coil terminals, and lights on the front panel shall be used to display the status of the ac and dc switchgear. Other status and diagnostic data shall be displayed on CRT screens that collect data of similar type and function. Operating mode and status data shall be available continuously on a single screen.
- f. All status indicator lights shall include a circuit to permit positive testing via a single front panel push-button.
- g. The instrumentation signals shall be accessible during operation to portable diagnostic test equipment (e.g., oscilloscope) without requiring bypass of the safety interlock system.
- h. All settable values shall be resettable from the front panel.
- i. All meters and sensors shall be easily accessible for calibration.
- j. Transient data necessary for VSC fault diagnostic and performance analysis shall be stored in a circulating memory and shall be accessible at the VSC front panel. After a fault event data collected shall be automatically downloaded to permanent storage.

#### 2.2.1.7.4 Fault Conditions

- a. The VSC shall enter Mode 4 and set the VSC fault discrete in the event of any of the following conditions:
  - 1) AC interface conditions out of tolerance
  - 2) AC or dc faults within the VSC, unless isolation of the failed module is possible, and then continued operation at reduced power operation is possible
  - 3) Reverse phase sequence
  - 4) Voltage source converter overtemperature or loss of cooling, unless overtemperature is limited to one module and isolation of the affected module is possible, then continued operation at reduced power operation is possible
  - 5) Loss of VSC auxiliary power for more than TBD seconds
  - 6) Opening of VSC cabinet doors or panels
  - 7) Loss of VSC controller function
- b. Emergency commands from either the magnet, the VSC front panel, or SCADA / remote terminal unit shall over-ride any mode of operation.
- c. The VSC shall not resume operation after a fault shutdown until the cause of the fault has been removed and manual reset has been performed. It shall be possible to lock out the manual reset capability by means of a keylock or padlock on the front panel.
- d. When enabled by software selection, the VSC shall automatically attempt one restart after an internal fault disconnect has occurred. The restart attempt shall occur following a software-programmable delay of TBD to TBD seconds. Additional restarts will require a manual VSC front panel reset as well as removal of the cause for the disconnect.
- e. In the event of disconnect or shutdown, the operation of all isolation switchgear on both the ac and dc connections to the VSC shall be independent of the VSC controller (i.e., implemented directly within the ac and dc switchgear). The displays of switchgear status on the VSC front panel shall also be independent of the VSC controller.

# B

## BIBLIOGRAPHY

---

- G. Venkataramanan and B. K. Johnson, "A superconducting DC transmission system based on Voltage Source Converter transmission technologies," *IEEE Trans. on Applied Superconductivity*, vol. 13, no. 2, pt. 2, June 2003, pp.: 1922–1925.
- B. K. Johnson, R. H. Lasseter, and R. Adapta, "Power control applications on a superconducting LVDC mesh," *IEEE Trans. on Power Delivery*, vol. 6, July 1991, pp.: 1282–1288.
- B. K. Johnson, R. H. Lasseter, F. L. Alvarado, and R. Adapta, "Expandable multiterminal DC systems based on voltage droop," *IEEE Trans. on Power Delivery*, vol. 8, Oct. 1993, pp.: 1926–1932.
- B. K. Johnson, R. H. Lasseter, F. L. Alvarado, D. M. Divan, H. Singh, M.C. Chandorkar, and R. Adapta, "High-temperature superconducting DC networks," *IEEE Trans. on Applied Superconductivity*, vol. 4, no. 3, Sept. 1994, pp.: 115–120.
- S. Gonzalez-Hernandez, E. Moreno-Goytia, and O. Anaya-Lara, "Analysis of wide area integration of dispersed wind farms using multiple Voltage Source Converter-HVDC links," 13<sup>th</sup> Power Electronics and Motion Control Conference (EPE-PEMC 2008), 1–3 Sept. 2008, pp.: 1784–1789.
- L. A. Lamont, D. Jovcic, and K. Abbott, "Voltage Source Converter transmission control under faults," 39th International Universities Power Engineering Conference (UPEC 2004) 6–8 Sept. 2004, vol. 2, pp.: 1209–1213.
- Hu Zhaoqing, Mao Chengxiong, Lu Jiming, "Improvement of transient stability in AC system by HVDC Light," 2005 Transmission and Distribution Conference and Exhibition: Asia and Pacific (IEEE/PES 2005), pp.: 1–5.
- X. F. Fuan and Shijie Cheng, "Performance analysis of a hybrid multi-terminal HVDC system," *Proceedings of the Eighth International Conference on Electrical Machines and Systems (ICEMS 2005)* 27–29 Sept. 2005, vol. 3, pp.: 2169v2174.



# C

## REFERENCES

---

1. IEEE Task Force on Load Representation for Dynamic Performance, “Standard Load Models for Power Flow and Dynamic Performance Simulation,” *IEEE Trans. on Power Systems*, vol. 10, Aug. 1995, pp. 1302–1313.
2. L. Pereira, D. Kosterev, M. Mackin, D. Davies, J. Undrill, and W. Zhu, “An Interim dynamic Induction Motor Model for Stability Studies in the WSCC,” *IEEE Trans. on Power Systems*, vol. 17, Nov. 2002, pp. 1108–1115.
3. J. A. Diaz de Leon II and B. Kehrli, “The Modeling Requirements for Short-Term Voltage Stability Studies,” Power Systems Conference and Exposition (PSCE), Atlanta, GA, Oct. 2006, pp. 582–588.
4. IEEE Task Force on Large Interconnected Power System Response, “Interconnected Power System Response to Generation Governing: Present Practice and Outstanding Concerns,” *IEEE Publication 07TP180*, May 2007.
5. R. P. Schultz, “Modeling of Governing Response in the Eastern Interconnection,” *Proc. Of the 1999 IEEE PES Winter Meeting*, New York, NY, Feb. 1999, pp. 561–566.
6. P. W. Sauer and M. A. Pai, *Power System Dynamics and Stability*, Prentice Hall, Upper Saddle River, NJ, 1998, (Chapter 7).
7. B. Kirby, J. Kueck, H. Leake, and M. Muhlheim, “Nuclear Generating Stations and Transmission Grid Reliability,” *Proc. of the 39<sup>th</sup> North American Power Symposium (NAPS)*, Las Cruces, NM, Oct. 2007, pp. 279–287.
8. L. Pereira, et. al., “New Thermal Governor Model Selection and Validation in the WECC,” *IEEE Trans. on Power Systems*, vol. 19, Feb. 2004, pp. 517–523.
9. W. Hassenzahl, et. al., *A Superconducting DC Cable*, “Chapter 7 – End Stations and Converters,” EPRI, Palo Alto, CA: 2009. 1020458.
10. T. Baldwin, et. al., “Issues Associated with a Superconducting DC Line Fed by a Multi-Terminal VSC System,” *Proceedings of the Eighth EPRI Superconductivity Conference*, EPRI, Palo Alto, CA: 2008. 1018498.
11. Nilsson S. and Daneshpooy A., *Transient Response of a Superconducting DC, Long Length Cable System Using Voltage Source Converters*, EPRI, Palo Alto, CA: 2009. 1020339.





**The Electric Power Research Institute Inc.,** (EPRI, [www.epri.com](http://www.epri.com)) conducts research and development relating to the generation, delivery and use of electricity for the benefit of the public. An independent, nonprofit organization, EPRI brings together its scientists and engineers as well as experts from academia and industry to help address challenges in electricity, including reliability, efficiency, health, safety and the environment. EPRI also provides technology, policy and economic analyses to drive long-range research and development planning, and supports research in emerging technologies. EPRI's members represent more than 90 percent of the electricity generated and delivered in the United States, and international participation extends to 40 countries. EPRI's principal offices and laboratories are located in Palo Alto, Calif.; Charlotte, N.C.; Knoxville, Tenn.; and Lenox, Mass.

Together...Shaping the Future of Electricity

***Programs:***

Technology Innovation

Increased Transmission Capacity

© 2009 Electric Power Research Institute (EPRI), Inc. All rights reserved. Electric Power Research Institute, EPRI, and TOGETHER...SHAPING THE FUTURE OF ELECTRICITY are registered service marks of the Electric Power Research Institute, Inc.

1020330

**Electric Power Research Institute**

3420 Hillview Avenue, Palo Alto, California 94304-1338 • PO Box 10412, Palo Alto, California 94303-0813 USA  
800.313.3774 • 650.855.2121 • [askepri@epri.com](mailto:askepri@epri.com) • [www.epri.com](http://www.epri.com)